ELECTRON TUBES

Volume I

(1935-1941)

ELECTRON TUBES

Volume I

(1935-1941)

Edited by

ALFRED N. GOLDSMITH
ARTHUR F. VAN DYCK
ROBERT S. BURNAP
EDWARD T. DICKEY
GEORGE M. K. BAKER

Published by
RCA REVIEW
RADIO CORPORATION OF AMERICA
RCA LABORATORIES DIVISION
Princeton, New Jersey

Printed in U.S.A.

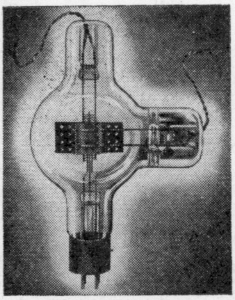

1920's

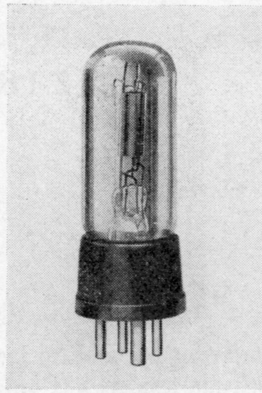

Early 1940's

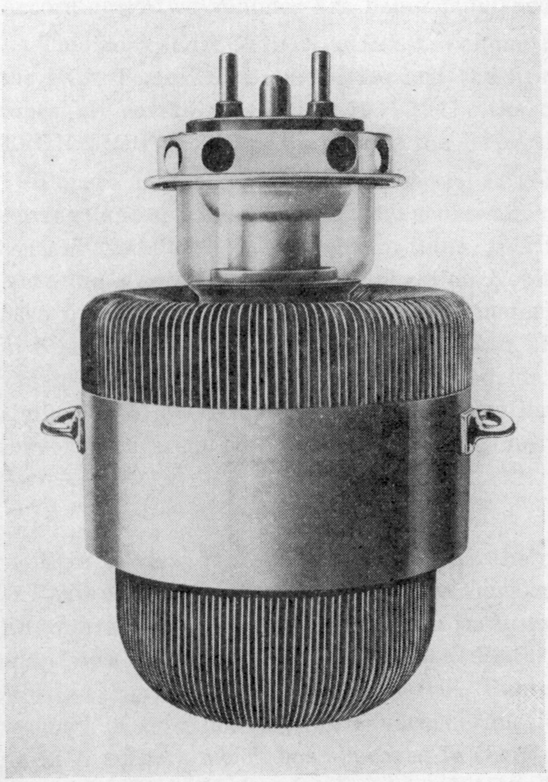

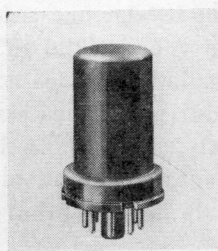

ELECTRON TUBES

Past and Recent

ELECTRON TUBES

Volume I

(1935-1941)

PREFACE

The wealth of material on the general subject of vacuum tubes and thermionics which was originally published during the years 1935-1948 has required more than one volume for its presentation even though a very stringent selection process has been followed by the editors. Accordingly, two volumes are being published at this time.

This book, ELECTRON TUBES, Volume I, is the ninth volume in the **RCA Technical Book Series** and the first devoted exclusively to tubes. It covers the period 1935-1941; the companion book, ELECTRON TUBES, Volume II, carries the series through 1948.

Papers are presented in four sections: general; transmitting; receiving; and special. As additional sources of reference, the appendices contain a bibliography on vacuum tubes, thermionics, and related subjects and a reference list of Application Notes. The bibliography has been included to insure that applicable material on tubes is available in this volume—at least in reference form. Papers concerning tubes which relate to specific applications or fields such as television, facsimile, UHF, or frequency modulation, are listed in the bibliography; they are covered, however, in other volumes of the Technical Book Series.

* * *

RCA Review gratefully acknowledges the courtesy of the Institute of Radio Engineers *(Proc. I.R.E.)*, the American Institute of Electrical Engineers *(Elec. Eng.)*, the American Institute of Physics *(Phys. Rev.* and *Physics)*, the Society of Motion Picture Engineers *(Jour.Soc. Mot.Pic.Eng.)* and the McGraw-Hill Publishing Company *(Electronics)* in granting to RCA Review permission to republish material by RCA authors which has appeared in their publications. The appreciation of RCA Review is also extended to all authors whose papers appear herein.

* * *

Since the days of the earliest discoveries of Fleming and De Forest, electron tubes have been one of the foundations upon which the entire structure of modern radio, electronics and television has been built. Progress in tube design and technique has often controlled the rate of advance in various applications in the communications, entertainment and industrial fields.

ELECTRON TUBES, Volume I, is, therefore, being published for scientists, engineers and others whose work involves the design of tubes or their application with the sincere hope that the material here assembled may serve as a useful background text and basic reference source to help speed new tube developments and thus advance the science and art of radio-electronics.

The Manager, RCA Review

RCA Laboratories,
Princeton, New Jersey
March 4, 1949

ELECTRON TUBES

Volume I

(1935-1941)

CONTENTS

THIN FILM FIELD EMISSION*†

By

Louis Malter

RCA Manufacturing Company, Inc.,
Camden, N. J.

Summary — *Aluminum, oxidized electrolytically, and subsequently treated with caesium and oxygen possesses new and interesting properties when subjected to electron bombardment in the presence of an adjacent collector electrode whose potential is held positive with respect to the aluminum. True secondary electron emission from the treated surface results in the establishment of a positive charge on the surface and a polarization of the oxide film. This positive charge acting through the thin oxide film produces a high gradient, resulting in the emission of electrons through the surface. The emission increases with collector voltage and beam currents, obeying power laws, but exhibits saturation tendencies. The removal of the primary beam does not result in the immediate cessation of the field emission, but rather in a slow decay which is due to the fact that the surface charge takes an appreciable time to leak away. Similar time lags are noticed when the beam is first applied, particularly if the collector voltage has been reversed while the beam impinges on the surface. The surfaces are also light sensitive, in that light causes a decrease in the field emission and a speeding up of decay. Attempts were made to demonstrate this effect for other surfaces, but, with a few exceptions, the results were negative.*

Introduction

THIS paper constitutes a more extended report of a letter published recently[1] under the title "Anamalous Secondary Electron Emission." Considerable criticism of this name for the phenomenon involved has arisen as not being descriptive of its apparent nature and, consequently, the above title suggested by Dr. J. A. Becker has been adopted.

In a search for a surface possessing a high secondary emission ratio, a considerable number of composite surfaces of various types were investigated. In the case of aluminum oxide treated with caesium and oxygen in a manner to be described below, it was found that a primary electron beam impinging upon the surface caused a current flow to a positive collector which, in certain cases, was several thousand times as great as the primary current. The phenomenon differed from that in the case of normal secondary emission in that the collector current

* Decimal Classification: R138.
† Reprinted from *Phys. Rev.*, July 1, 1936.
[1] Malter, *Phys. Rev.*, 49, 478 (1936)

was dependent upon the collector potential and primary current density. It exhibited very marked time lag characteristics and was also affected by light.

Experimental Procedure

A. Tube and circuit

A diagram of the tube employed, together with the accompanying circuit is shown in Fig. 1.

The cathode was of the barium oxide-strontium oxide type. The electron gun parts were made of tantalum. The electrodes on the walls of the tube were platinum formed by the reduction of Hanovia platinizing solution. The regions around the "side contacts" were coated with silver formed by the reduction of Hanovia silver paste.

The platinum film consisted of two portions, the first serving as the so-called "second anode" of the electron gun. The second portion served to collect the electrons emitted from the target. If a single

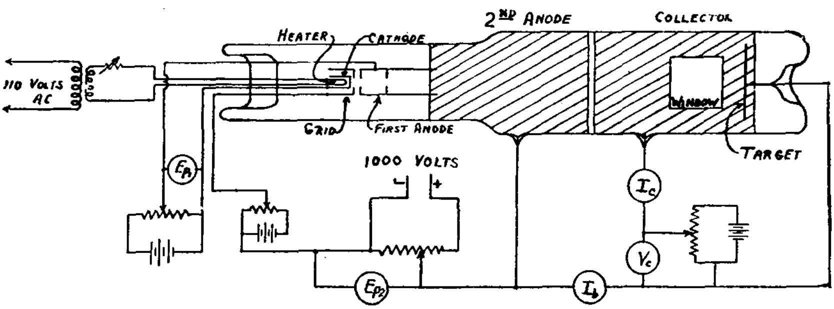

Fig. 1—Schematic diagram of apparatus.

film is used as both second anode and collector, a change in collector voltage (V_c) causes a much greater change in beam spot size than if two separate films are employed as shown. This precaution was necessary in view of the dependence of the collector current upon beam spot size.

The caesium was produced by exploding compressed pellets of powdered caesium chromate and zirconium in a side tube.

Two pairs of deflecting coils (not shown in Fig. 1), mounted just beyond the first anode (at right angles to each other), served to position the beam on the target.

B. Formation of the oxide film

The aluminum oxide was formed by making the aluminum the anode in a bath wherein the cathode was a platinum foil. Various composition baths were tried. Satisfactory results were obtained with a standard solution of borax and boric acid.

It has been shown[2] that for times of formation in excess of a few minutes the thickness of the oxide film formed is practically independent of the time and the bath employed. The thickness is given by the relation

$$D = 17.0V,$$

where D is the oxide thickness in A and V is the applied potential in volts. However, the resistance of the film does depend upon these factors. No real study of the effect of the nature of the bath upon the film properties appears to have been made.

If at any time during the oxidation process, the applied voltage is gradually reduced, it is found that plots of the logarithm of the applied voltage against the logarithm of the current through the film yield curves of the form shown in Fig. 2. It is seen that below a certain voltage the curve is linear. Güntherschulze and Betz[3] have shown that over this linear region the current is purely electronic, whereas above this point ions move through the oxide lattice and contribute to an increase in its thickness. The portion of the current lying below the extended linear portion of the curve is electronic, whereas that above is ionic.

The prepared aluminum foil was mounted on a nickel plate for support and its edges were painted with willemite in order to permit the position of the beam to be seen by the fluorescence excited. Equally spaced circles were scratched lightly on the willemite in order that it be possible to determine the size of the spot. For intense beams (in excess of 3 to 4 microamperes) a faint blue fluorescence appeared on the oxide surface, permitting of a direct determination of the position and diameter of the electron beam.

The tube was pumped and baked at 475°C until the pressure dropped below 10^{-5} mm of Hg. After cooling, the parts of the electron gun were outgassed by means of high frequency and the oxide cathode activated so as to be thermionically emissive.[4]

Caesium was now introduced into the tube and the tube then baked at 200°C for ten minutes. After cooling, oxygen was admitted into the tube to a pressure of 1 mm of Hg and pumped out after a few seconds. This treatment was sufficient to bring about the appearance of the thin film field emission, or enhance it in cases where it was present prior to any treatment.

---

[2] Güntherschulze and Betz, Zeits. f. Elektrochemie 37, 8-9 (1931).
[3] Güntherschulze and Betz, Zeits. f. Physik 92, 367 (1934).
[4] Dushman, Rev. Mod. Phys. 2, 381 (1930).

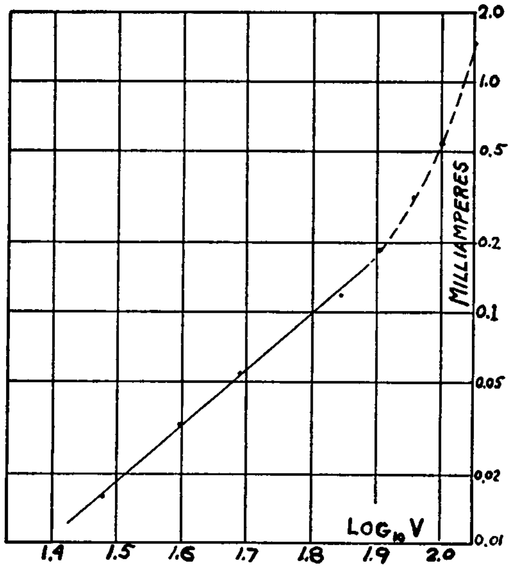

Fig. 2—Current voltage characteristic of aluminum oxide film after formation in saturated borax and boric acid bath for one hour.

It was found impossible to secure completely reproducible results. In an effort to determine the possible reason for this, all chemicals used were recrystallized and the water redistilled, and, in addition, the purest obtainable aluminum was secured from the Rheinische Blattmetall A.G.[5] However, their material was no better in this respect than the available commercial "electrolytic condenser" aluminum.

Experimental Results

Except where noted the measurement given were obtained from a tube having aluminum with an oxide thickness of 2000A. While the exact results obtained differ from those in other foils with the same oxide thickness, the essential conclusions and laws are the same, the actual magnitudes only being affected.

A. *Variation of collector voltage* (V_c)

If the beam current (I_b), second anode voltage (Ep_2) and spot size are held constant, the variation of the collector voltage (V_c) causes a rapid variation in the collector current (I_c).

The results for different values of I_b for the cases wherein ($Ep_2 =$ 500 volts, $Ep_1 = 48$ volts) and ($Ep_2 = 250$ volts, $Ep_1 = 26$ volts) have been plotted in logarithmic coordinates in Figs. 3 and 4. These combinations of Ep_1 and Ep_2 yield the same spot size.

In general, it is seen that:

$$I_c = B(V_c)^m. \qquad (1)$$

[5] Rheinische Blattmetall A. G. Grevenbroich (Niederrhein).

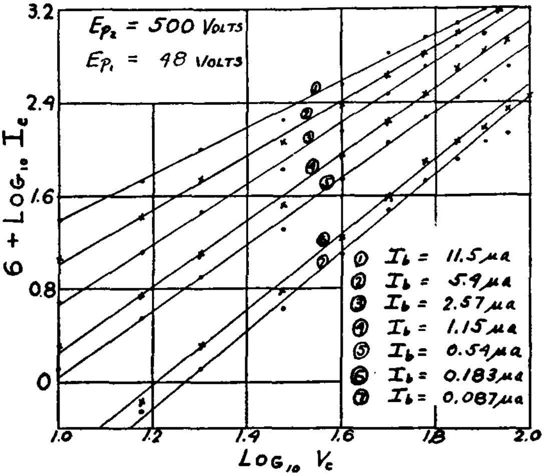

At this point, it should be made clear that the results apply to only one region of the target. The values of I_c obtained from different regions of this surface vary considerably. However, if one restricts oneself to a particular region and is careful not to alter the surface in the manner to be described below, the results are reproducible. In these measurements as well as in those that follow (except where noted) all the data were obtained at the spot on the surface which yielded largest collector currents.

B. Variation of beam current

A series of readings were taken, everything being held constant except I_b. The results for $Ep_2 = 500$ volts, $Ep_1 = 48$ volts, and different values of V_c are plotted in Fig. 5. All of these curves are "repeats." It is found that if I_b is increased in steps, and corresponding values of I_c obtained, a curve is obtained which does not repeat itself at low values of I_b. However, after the first run, all succeeding curves do repeat themselves. These stabilized I_b, I_c points, which are plotted in Fig. 5, and the curves obtained, are the "repeats" referred to above.

To illustrate the nature of this deviation for the initial run at low values of I_b, three successive runs are plotted in Fig. 6. The circles are the first run, the crosses and triangles the second and third, respectively. It is

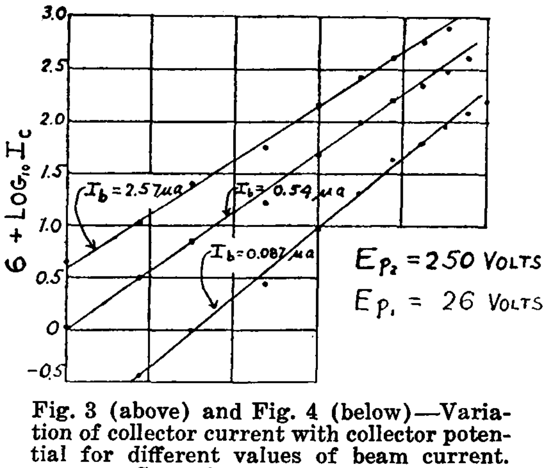

Fig. 3 (above) and Fig. 4 (below)—Variation of collector current with collector potential for different values of beam current. Spot size held constant.

seen that after the first run, the succeeding runs lie along the same line. The nature of the polarization and time lag effects which give rise to the deviations in the first run will receive more detailed consideration below.

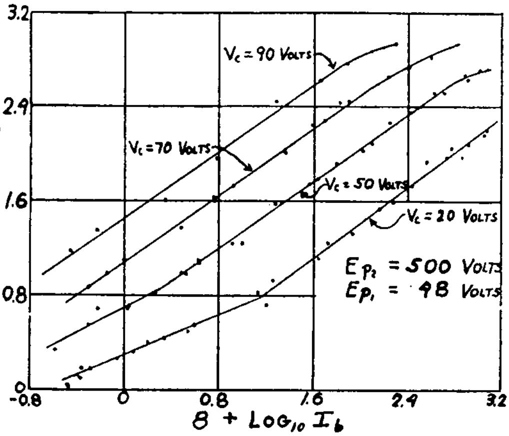

Fig. 5—Variation of collector current with beam current for different values of collector voltage. Spot size held constant.

Returning to a consideration of Fig. 5, it is seen that except for low values of V_c and I_b, the curves are all straight lines of the same slope. These results can be represented by:

$$I_c = PI_b^{0.71} \tag{2}$$

$\log_{10} P$ as a function of V_c is plotted in Fig. 7. If $V_c < 70$ volts,

$$P = 0.145 \times 10^{0.023V_c}. \tag{3}$$

By substituting (3) in (2), there results:

$$I_c = 0.145 \times 10^{0.23V_c}(I_b)^{0.71}. \tag{4}$$

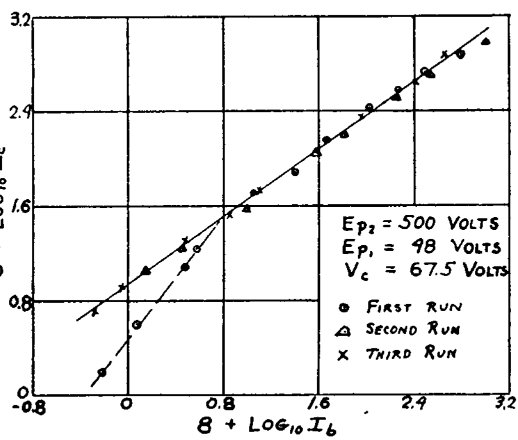

Fig. 6—Demonstration of variation between first and succeeding runs wherein beam current is varied.

This relation holds for all values of I_b and I_c except for those beyond the linear regions of the curves of Figs. 5 and 6.

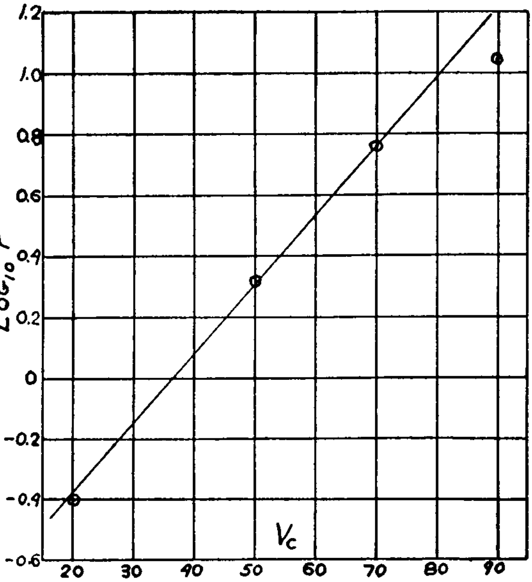

Fig. 7—Plot of intercepts of collector current—beam current characteristics as a function of collector voltage.

C. Variation of spot size

In order to see whether Eqs. (1) and (4) could be expressed in terms of current density, a series of runs were taken at different spot sizes, the spot sizes being determined by deflecting the spot onto the willemite. Because of a slight misalignment of the first anode, the spot was oval instead of circular. This made the determination of the spot size quite inaccurate, but it was felt that an approximation of the current density law could certainly be obtained.

In Fig. 8, the values of I_c/A and I_b/A for various values of I_b are plotted on logarithmic scale, where A is the spot size. When consideration is taken of the large error in the determination of A, it seems that the best representation of the results is a straight line drawn among the widely scattered points. We have thus:

$$\log 10^6 I_c/A = 1.92 + 0.73 \log 10^6 I_b/A. \tag{5}$$

The fact that the slope is practically the same as that for Eq. (4) indicates that the linear relationship expressed in Eq. (5) is a reasonable representation.

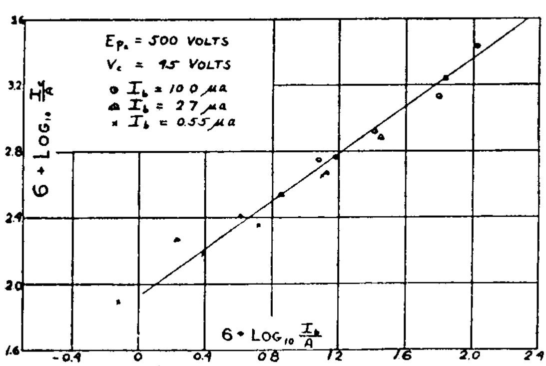

Fig. 8—Variation of collector current divided by spot size with beam current density.

The agreement between Eqs. (4) and (5) is very good and consequently Eq. (4) may be generalized into the form:

$$A(I_c/A) = 0.145(10)^{0.023V_c}A^{0.71}(I_b/A)^{0.71} \tag{6}$$

and since Eq. (4) was derived at $Ep_2 = 500$ volts, $Ep_1 = 48$ volts, for which values $A = 0.72$ cm^2; we can insert this value of A in Eq. (6) and obtain:

$$J_c = 0.160(10)^{0.023V_c}J_B{}^{0.71}, \tag{7}$$

where $$J_B = I_B/A \quad \text{and} \quad J_c = I_c/A.$$

Eq. (7) is the law representing the collector current as a function of beam current, spot size, and collector voltage for the oxide thickness employed and over the surface region investigated. In general, the law is of the form:

$$J_c = \alpha\epsilon^{\beta V_c}J_B{}^{\gamma}, \tag{8}$$

where α, β, and γ are functions of the oxide thickness and formation conditions. This law does not apply if V_c and I_c are above or below certain values. Possible reasons for this will be discussed below.

D. *Decay characteristics*

If I_b is suddenly reduced to zero by increasing the negative voltage on the grid of the electron gun, it is found that I_c does not immediately vanish but decreases rapidly at first, and then more slowly, and finally approaches a zero value asymptotically.

Samples of the decay characteristics for the same surface for which the preceding gain studies were made are shown in Fig. 9. Decay characteristics are extremely erratic in that small motions of the spot position cause large changes in the rate of decay. However, in general it is true that the greater the gain, the slower the absolute decay but the more rapid the relative decay. To show the extreme variability of the decay characteristics another curve is shown in Fig. 10. This is the decay characteristic for an entirely different surface, formed at the same voltage as the one previously described. The gains from this surface were slightly higher than from the one studied. Unfortunately, before further measurements could be made, this surface was destroyed by overheating with high frequency. The decay time for this surface was of an entirely different order of

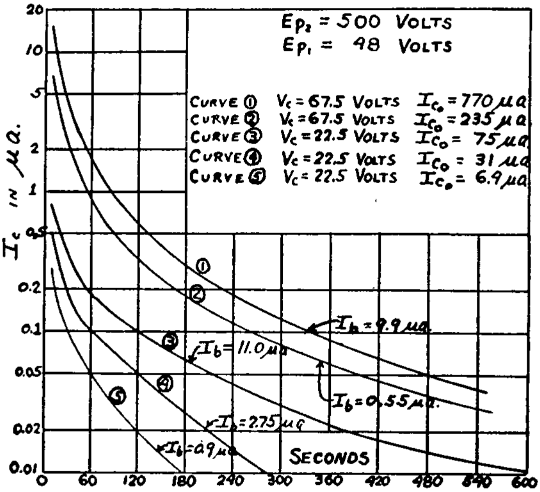

Fig. 9—Typical decay characteristic after removal of primary beam.

magnitude, being measured in minutes rather than seconds. Current to the collector could be detected after 24 hours.

It has been found that if log $[-\log(I_c/I_{c0})/T]$ is plotted against log I_c, a straight line is obtained. (T is the decay time). The case corresponding to Fig. 10 is shown in Fig. 11. The small numbers adjacent to the points represent the corresponding decay time in minutes. This linearity indicates that the neutralization of the surface charge is due primarily to the field emission itself.

If at any time during the decay the lead to the collector is opened momentarily, it is found on closing the circuit that I_c has dropped to practically zero. If V_c is reduced at any time during the decay, the rate of decrease of I_c is not affected unless V_c is reduced below some definite value, this value being lower the longer the decay period that has elapsed.

A more detailed consideration of the significance of decay characteristics will be given after the theory of the effect.

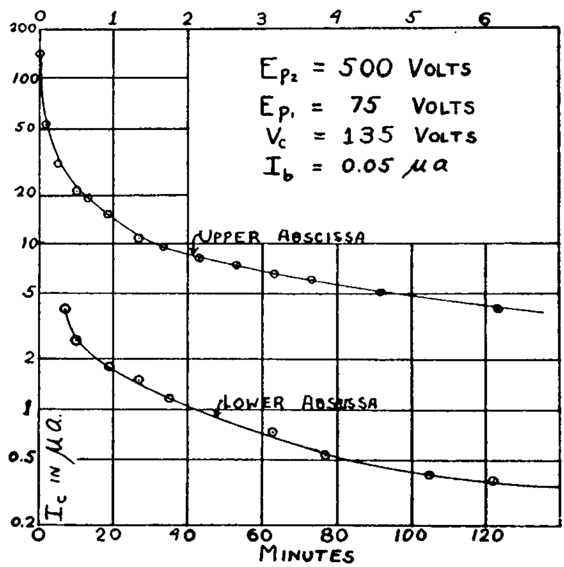

Fig. 10—Example of very slow decay.

E. *"Building-up" characteristics*

If, at any time, I_b is first cut off by an increase in the grid bias, and then after I_c has dropped to a negligible value, I_b is suddenly restored to its original value, I_c returns to its final value very rapidly. If, instead of biasing off I_b, V_c is reduced to zero and then restored to its original value, I_c also returns to its original value very rapidly.

If, however, instead of reducing V_c to zero with I_b unchanged, V_c is actually reversed in direction so that the collector is negative with respect to the target, upon restoring V_c to its original positive value, the building-up takes on new and interesting forms. Some of these results are shown in Fig. 12 for cases wherein $V_c = 22.5$ volts and 45 volts. It is seen that the lower the values of I_b and V_c, the slower the building up. A curious feature is the fact that I_c remains constant for a considerable time before beginning its rise, particularly for low values of I_b and V_c.

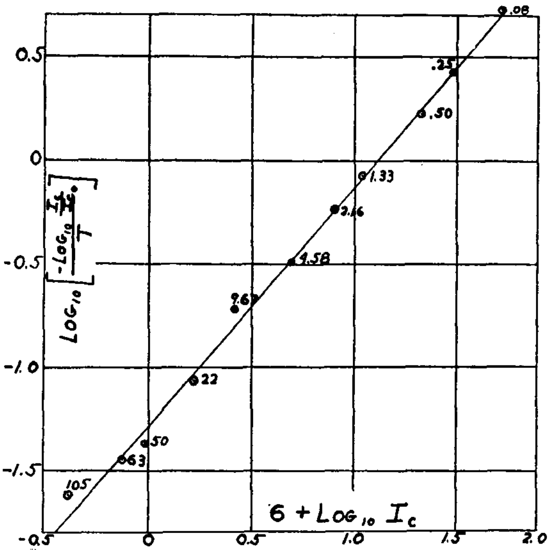

Fig. 11—Illustration of linear relation obeyed by persistent emission.

If, instead of reversing V_c, a negative voltage (V_R) different from V_c is applied to the collector and then the collector voltage is restored to its original V_c value, the building-up curves are altered. In Fig. 13 are plotted the building-up characteristics for $V_R = 0$, -22.5, -45 and -67.5 volts, for the case where $V_c = 67.5$ volts. As V_R is made smaller in absolute value, the building-up becomes more rapid. An interpretation of the various building-up curves will be given below.

F. *Scintillations and alteration of characteristics*

If V_c and I_b are increased beyond certain points, scintillations are observed on the aluminum oxide surface, their number and frequency increasing as V_c and I_b are raised. These scintillations alter the surface characteristics and, consequently, in the preceding experimental work, care was taken to keep them at a minimum. Their complete elimination is impossible except for very low values of V_c. Scintillations are undoubtedly due to momentary ruptures of the oxide film.

Continued scintillation causes a slow decrease in the gain characteristics, but a very rapid alteration in the decay characteristics. Continuous and rapid scintillations finally cause the complete disappearance of the thin film emission. A surface formed at 12 volts was run with $V_c = 90$ Volts. Under these conditions, the surface was covered with a uniformly dense distribution of pin-points of scintillation. After one-half hour these scintillations had completely disappeared, but so had the thin film emission.

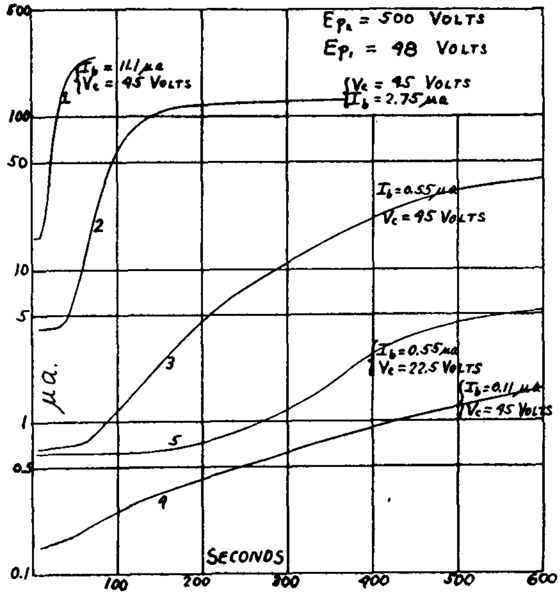

Fig. 12—Building-up curves obtained after reversal of collector potential with beam impinging on target.

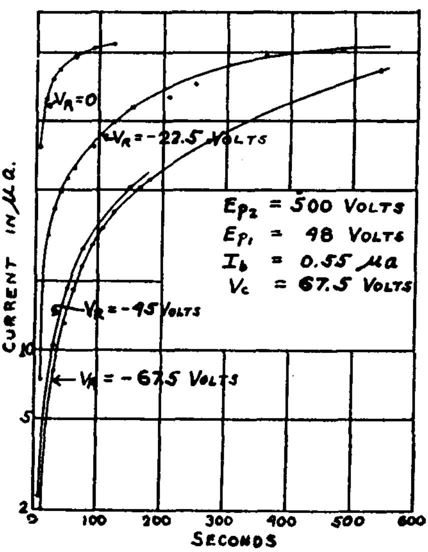

Fig. 13 — Building-up curves when collector potentials are reversed to different negative values and subsequently restored to same postiive value.

G. *Light effects*

It was noted that the shining of light upon the surface always causes a marked decrease in I_c. In addition, light causes a marked increase in the rate of decay after I_b is cut off. The effects upon gain and decay were most marked for tubes with the longest decay. In certain cases a decrease in I_c of

200 microamperes was observed when a flashlight was shone upon the surface. The same light impinging upon a caesiated silver oxide surface resulted in a current yield of only 10 microamperes. Thus when used in this way the device is many times more "photosensitive" than the best surface heretofore known.

Discussion of Experimental Results and Proposed Description of the Phenomenon

In the case of normal secondary electron emission, the primary electron reacts with the conduction electrons of the substance being bombarded in the presence of the force fields of the atoms or ions constituting the latter, resulting, in certain cases, in the transfer of sufficient backward momentum to conduction electrons to permit of their escape through the surface. The theory for the case of the uniform metallic lattice has been treated by Fröhlich.[6]

Thin film field emission appears to be due to an entirely different mechanism. The phenomenon appears to be closely related to one described by Güntherschulze[7] wherein extremely fine particles of aluminum oxide (among other substances) sprinkled on a semiconductor which serves as the cathode in a gas discharge, emit a copious stream of electrons with velocities corresponding to the cathode-anode difference of potential. In this case, according to Güntherschulze, positive ions lodge on the sides of the oxide particles away from the semiconductor and build up a positive charge thereon. If the gradient across any of the particles becomes sufficiently great, electrons will be extracted from the underlying semiconductor. The effect disappears after several hours, apparently due to the mechanical rupture of the oxide particles by the high fields and high current densities present, with a consequent destruction of their insulating structure.

In the case of the thin film field emission the primary electrons impinging upon the treated aluminum oxide surface cause the release of true (i.e., normal) secondary electrons therefrom, these being attracted to the collector electrode. If the secondary emission ratio is greater than unity, more electrons will leave the surface than impinge upon it. Because of the high resistance of the oxide film, a positive charge is built up on the surface, this charge ultimately causing the extraction of electrons from the aluminum and aluminum oxide because of the intense gradients established. Thus in this case the emitted true

---

[6] Fröhlich, Ann. d. Physik 13, 229 (1932).

[7] Güntherschulze, Zeits. f. Physik 86, 778 (1933).

secondary electrons take the place of the arriving positive ions in Güntherschulze's experiment.

Concomitant with the building up of the surface charge, the oxide becomes polarized, the polarization as well as the surface charge persisting after the removal of the primary beam. Evidence for the persistent polarization of aluminum oxide has been found by Güntherschulze and Betz.[8] In addition, space charges are established within the oxide, the sign of the charge depending upon the sign of the collector.

This picture enables the various manifestations of the phenomenon to be explained in a very convincing manner. These will be considered in turn.

1.

The reason for the special treatment required with caesium and oxygen is made clear. This treatment serves to form a thin, nonconducting film on the surface of the aluminum oxide whose true secondary emission ratio is considerably greater than unity, resulting in the rapid building up of the positive charge on the surface when bombarded with primary electrons. It is believed that the layer of caesium oxide is monomolecular. This belief is founded upon the following evidence:

(1) The amount of caesium beyond a certain minimum amount does not appear to affect the magnitude of the phenomenon.

(2) No change can be detected in the appearance of the oxide surface. In the case of silver oxide, on the other hand, the reduction of the oxide to appreciable depths by means of caesium is shown by the decided change in appearance.

(3) The heat of formation of aluminum oxide is so high that it cannot be reduced by metallic caesium. It is quite likely, however, that the heat of adsorption of caesium on aluminum oxide exceeds the heat of formation of the oxide.

The mere formation of the caesium layer on the surface, while it enhances the true secondary emission, does not by itself result in the appearance of the anomalous effect. This is due to the fact that the pure caesium film on the surfaces is conducting and thus prevents the positive charge from being established.

2.

The relation between collector current, beam current and collector voltage is expressed by Eqs. (1) and (4). It is of interest to note

[8] Güntherschulze and Betz, Zeits. f. Physik 73, 580 (1932).

that Eq. (1) is of the same form as the relation between voltage and current for the composition material "Thyrite."[9] For this material the current is given by:

$$I = BV^m, \tag{9}$$

where B and m are constants which depend upon the proportions and nature of the constituents. Thyrite is composed of particles of carborundum coated with silica imbedded in a highly resistive matrix. Güntherschulze has ascribed the non-ohmic characteristic to the establishment of high gradients across the particles with a resultant "cold emission" through the particles. This view is borne out by the fact that the "cold emission" through the oxide films in this experiment, i.e., the thin film field emission, obeys a law of the same type.

The identity in form of the Thyrite law, Eq. (9), and the thin film field emission law, Eq. (1), indicates that in the case of this effect, the potential of the front surface of the aluminum oxide surface with respect to the underlying aluminum (denoted by (V_s)) is proportional to V_c, i.e.,

$$V_S \propto V_c.$$

3.

The time lags which are a feature of this effect are immediately explained by this picture. If the beam is turned on or increased, it takes an appreciable length of time for the region being bombarded to come to equilibrium under the opposing actions of the charging due to the true secondary emission and discharging due to leakage through the film, as well as for the polarization of the oxide and internal space charge to assume equilibrium values.

The time lag of the space charge is apparently very much greater than that of the surface charge. This belief is borne out by the experiments in which V_c was reversed with the beam on. On restoring V_c to its original direction, the surface charge undoubtedly reassumes its original positive value in a time no greater than the building up required when V_c is not reversed, but merely reduced to zero. Yet, the reversal of V_c greatly increases the building-up time. This increase can be due only to the fact that the field effective in extracting the electrons is weakened by the presence of negative space charge produced while the collector potential was reversed.

The persistence of the surface charge when the beam is cut off is demonstrated by the slow decay of I_c. Only a small portion of the

[9] McEachron, U. S. Patent #1,822,742.

field emission serves to neutralize the surface charge. This is also borne out by the virtual disappearance of collector current after a momentary opening of the collector circuit.

4.

The scintillations which appear for intense beams and high collector voltages are due to a violent breakdown of the oxide film. It was thought at first that this rupture would occur only if the surface target potential exceeded the formation voltage of the film. However, it was soon found that scintillations occurred when the collector voltage was less than the formation voltage. It was then believed that scintillations should not occur if the target surface potential were less than the critical potential V_b in the formation curve. (See Fig. 3.) It would appear that if the surface potential exceeded V_b there would be a tendency for ions to move through the film. However, since there is no electrolytic bath to supply the loss of ions at the outer surface, a rupture would occur. However, it was found that scintillations occurred when the collector voltage was considerably less than V_b. Apparently the breakdown is due to there being weak spots in the oxide film. When the sample is in the bath, any tendency to breakdown is overcome by the oxidizing action of the bath. This cannot, of course, occur in the vacuum tube. It is probable that invisible breakdowns occur down to very small values of V_c. Recently, Zauscher[10] has established a relation between film thickness and breakdown voltage for a film in air. For small thicknesses ($<$ 4000A), the relationship is given by:

$$\text{Breakdown Voltage} = 8 \times 10^5 d,$$

where d, the film thickness, is measured in cm.

Thus for the 2000A film studied above, the breakdown voltage is 16 volts, whereas V_b is 78 volts and the formation voltage 116 volts.

The deviations from the laws as expressed in Eqs. (1) and (4) at high values of V_c may be due to Vs exceeding some definite value which may be the critical value of Zauscher's relation.

The fact that the deviation from linearity at the upper ends of Fig. 8 occur for approximately the same value of I_c and appear to be independent of V_c indicates that Vs is a function of I_c/A only.

5.

The sensitiveness of the treated surface to light appears to be explainable only by the ad hoc hypothesis that the aluminum oxide is

[10] Zauscher, Ann. d. Physik 23, 597 (1935).

photo-conductive. Light falling upon the oxide causes a decrease in its effective resistance. When the electron beam and light are simultaneously impinging upon the surface, the surface equilibrium potential will take on a smaller value than with the light absent. The light also causes an increase in decay rates by permitting the surface charge to leak away more rapidly through the lessened effective resistance of the oxide film.

THIN FILM FIELD EMISSION FROM OTHER SURFACES

Güntherschulze and Fricke[11] obtained field emission from a number of substances in a gas discharge where the positive surface charge was produced by positive ions. A set-up similar to theirs was employed in which finely powdered material was rubbed onto an aquadag surface. The tube was treated with caesium and oxygen in the same manner as for aluminum oxide surfaces. The materials were then bombarded by an electron beam with an adjacent collector highly positive with respect to the aquadag. Field emission would be demonstrated by the presence of scintillations. The following materials were tried in this way: Ta_2O_5, MgO, $CaCO_3$, Al_2O_3, Zn_2SiO_4, willemite, $BeCO_3$, SiO_2, ZrO_2, and ThO_2, all of these materials having yielded positive results in the experiments of Güntherschulze and Fricke. Scintillations were observed in the cases of Al_2O_3, SiO_2, MgO, and willemite. The non-occurrence of scintillations for the other materials does not indicate that field emission did not occur, but simply that the gradients established were not sufficient to cause breakdown. The coverage of the materials used was too small to enable the demonstration of any field effects as regards the collector current.

In addition, a number of other oxides were tried in tubes, but the results were generally negative. However, E. R. Piore, of the Electronic Research Laboratory of the RCA Manufacturing Company, obtained a pronounced field effect from Be oxidized in a glow discharge, then caesiated, and finally heated to dull redness inside the tube by means of high frequency induction. He has also observed the phenomenon with hot activated barium and strontium oxide cathodes.

The reason for the appearance of the phenomenon only in the case of a few out of a host of oxides tried can be accounted for on the basis of the possible chemical interactions between caesium and oxides. If an oxide is capable of reduction by the caesium, then the introduction of caesium into the tube will cause the destruction of the resistive

[11] Güntherschulze and Fricke, Zeits. f. Physik 86, 821 (1933).

properties of the oxide film. This will, of course, prevent the appearance of the field effect. In Table I, column one shows the oxide studied, column two its method of preparation, column three the heat of formation of the oxide *per unit atom* of oxygen, and column four the results achieved in an attempt to obtain field emission.

Table I. Field emission from various oxides.

1 OXIDE	2 MODE OF PREPARATION	3 HEAT OF FORMATION PER UNIT OXYGEN ATOM (Cal.)	4 RESULTS FOR ANOMALOUS EFFECT
Al_2O_3	Electrolytically in borax plus boric acid bath	126,700	Positive
BeO	Glow discharge in oxygen	?	"
CaO	" " " "	151,900	Negative
CbO	Electrolytically in . IN H_2SO_4	?	"
Ag_2O	Glow discharge in oxygen	7,000	"
CuO	" " " " and heating in air	37,000	"
NiO	Glow discharge in oxygen and heating in air	57,900	"
Ta_2O_5	Electrolytically in . IN H_2SO_4	60,300	"
WO_2	" " "	65,700	"
ZrO	" " "	86,800	"

Since the heat of formation of Cs_2O is 82,700 calories, only the oxides of Al, Ca, Mg, Si, and Zr in the above list should show the field effect. The result is believed to be negative in the case of Ca because of the low resistance of the oxide.

An attempt to evaporate SiO_2 from a carbon cup subjected to intense electron bombardment, as described by O'Brien,[12] failed because of the reduction of the SiO_2 by the carbon, with the consequent profuse evolution of CO resulting in a gas discharge. No further attempt was made to evaporate quartz. However, the previously described experiment with the quartz powder indicates that it should yield field emission.

The Zr yielded a negative result, although from the figures cited a positive result should have appeared. However, in heating the tube to 200°C to promote the distribution of the caesium, apparently the heat of formation of the zirconium oxide dropped below that of the caesium oxide. This is evidenced by the decided change in color of the zirconium oxide during caesiation.

This change in the appearance of the oxide upon caesiation occurred whenever field emission failed to occur. The aluminum oxide,

[12] O'Brien, Rev. Sci. Inst. 5, 125 (1934).

on the other hand, shows no change in appearance under the same conditions. This is evidence in favor of the belief that the caesium on the aluminum oxide is in the form of a monatomic layer.

ACKNOWLEDGMENTS

I wish to express my appreciation to Professor Lloyd P. Smith, under whose direction this work was carried out, for his constant advice and encouragement.

I also wish to express my gratitude to Dr. V. K. Zworykin, of the Electronic Research Laboratory of the RCA Manufacturing Company, for extending to me the facilities of the laboratories for this work, as well as to express my appreciation for his constant advice and encouragement.

I am particularly indebted to Dr. E. G. Ramberg for many valuable discussions and for his contributions to the explanation of the phenomenon.

I wish to express my thanks to Messrs. H. W. Leverenz and H. W. Rhoades for the care in preparing the various oxidizing baths employed.

EFFECTS OF SPACE CHARGE IN THE GRID-ANODE REGION OF VACUUM TUBES*†

BY

BERNARD SALZBERG AND A. V. HAEFF

RCA Manufacturing Company, Inc., RCA Radiotron Division,
Harrison, New Jersey

Summary—*The effects of space charge in the region between grid and anode of a vacuum tube, for the case where the planes of the grid and plate are parallel, are determined from the results of a simple analysis. The main effects of the space charge are (a) to introduce departures from the linear potential distribution of the electrostatic case; (b) to set an upper limit, under certain conditions, for the anode current; (c) to introduce instabilities and hysteresis phenomena in the behavior of the tube; and (d) to increase the electron transit time in this region.*

Four modes of potential distribution which may exist in this region are treated: (1) Neither potential minimum nor virtual cathode exist; (2) potential minimum exists; (3) space-charge-limited virtual cathode exists; and (4) temperature-limited virtual cathode exists (negative anode potentials). For each of the various states of operation, expressions are derived for the distribution of potential and electric intensity throughout the region; the time of flight of electrons from grid to anode, and from grid to the plane of zero potential; and the location and magnitude of the minimum potential. An expression is also derived for the dependence of the anode current on the space current, grid-anode distance, grid voltage, and anode voltage. Curves are plotted from these expressions, and it is shown how the behavior of a large variety of practical tubes can be predicted and explained with their aid. The assumptions which underlie the theory are stated, and the effects of the neglected phenomena are discussed qualitatively.

Anode-current vs. anode-voltage and anode-current vs. space-current curves representing observations made on a specially constructed tetrode are presented by way of experimental verification of the theoretical results.

For purposes of illustration, application is made of these results to elucidate the theory of the type of power-amplifier tube which employs a minimum potential, formed in front of the anode as a result of the space charge of the electrons, to minimize the passage of secondary electrons from anode to grid. In addition, it is shown how the decrease of anode current with increasing space current, which occurs when a space-charge-limited virtual cathode is formed in the grid-anode region, may be utilized to provide negative transconductance amplifiers and oscillators.

I. INTRODUCTION

THE effects of space charge in the region between grid and anode are of fundamental importance in any complete theory of vacuum-tube behavior. This is particularly true for the type of tube in which the anode is preceded by a grid electrode operated at a positive potential. Among such tubes, we may mention the Barkhausen-Kurz triode oscillator, in which the grid is operated at a high positive potential and the anode is either negative or only slightly positive; the common tetrode r-f and a-f amplifiers, in which the screen

* Decimal Classification: R138.1.

† Reprinted from *RCA Review*, January, 1938.

grid is operated at a relatively high positive potential, and the anode potential is caused to vary from a high positive potential to a smaller positive potential, which may be less than the screen-grid potential; and more recent types of power-amplifier tubes, such as the RCA 6L6, in which a minimum potential which occurs in the space between screen grid and anode at relatively low anode potentials is employed to minimize the passage of secondary electrons (liberated at the anode) to the screen grid.[1,2,3,4]

In this paper we wish to investigate theoretically, somewhat more completely than has been done hitherto, the properties of the grid-anode region.* The theory is also applicable, with suitable modifications, to the region between two grids, a problem which has also received some attention.[5] To this end, we postulate an idealized situation in which electrons pass through the interstices of a plane-accelerator grid, the effective potential of which is V_g, towards a parallel-plane anode separated a distance a from the grid and operated at a potential V_a. We assume that all of the electrons have been emitted from the cathode with zero velocity, and that they pass through the grid with a uniform velocity corresponding to the potential V_g. In general, we cannot assume that all of these electrons will pass on to the anode, for the potential distribution in the grid-anode region may be such that some, or even all of the electrons, will be turned back towards the grid at some intermediate point in this region. These returning electrons may be expected to execute excursions about the grid, a portion being absorbed on each passage through the grid.[6,7,8,9] In view of the uncertainty of the exact fractional absorption of the electrons by the grid on each complete passage, and to simplify matters, we shall assume that only two groups of electrons contribute to the space current: one group consists of the electrons which initially pass through the grid towards the anode, corresponding to a current I_0; and the second group consists of the electrons which may be turned back at an intermediate point in the grid-anode region, corresponding to a current I_0-I_A. Generally speaking, we are interested in the dependence of the anode current upon V_a, V_g, a, and I_0; the time of flight of the electrons; the distribution of potential and electric intensity throughout the region between the grid and anode; and the location and magnitude of the minimum potential which may occur in this region.

As stated above, the problem is only an approximation to the actual

[1,2,3,4, etc.] Numbers refer to bibliography.

* While we were preparing the results of our investigation for publication, our attention was called to four recent papers dealing with this subject. (Bibliography 13, 14, 15 and 16).

case. The complete treatment of the problem would require taking into account such things as the Maxwellian velocity distribution of emitted electrons; the tangential velocities of the electrons due to grid-wire deflections; the distribution of velocities of the electrons which pass through the grid, due to the variation of the potential in the plane of the grid; the presence of secondary electrons liberated at the anode and accelerator grid; multiple passages of electrons about the grid, etc. However, the solution of the problem set forth will ordinarily suffice for a first-order answer, since the effects of these neglected factors can frequently be inferred, at least, from the physics of the situation.

II. Theory

The equation which must be solved to determine the properties we seek is:

$$\frac{d^2V}{dx^2} = 4\pi\rho \qquad (\rho \text{ negative}) \tag{1}$$

together with

$$\tfrac{1}{2}\, mv^2 = eV \tag{2}$$

and

$$I = \rho v \tag{3}$$

In this problem we do not concern ourselves with the effects of variations of the potential with time. Consequently we may assume that both forward-moving and returning electrons always have the same velocity at any one point, and thus that the total space charge in the grid-anode region depends only upon the absolute values of the corresponding forward and return currents. For these reasons, we may define the quantities used in (1), (2) and (3) as

V = potential at any distance, x
x = distance from grid
ρ = charge density at x
e = electron charge
m = mass of electron
v = absolute value of velocity at x
I = sum of the absolute values of the current densities at x

Further on we shall have occasion to introduce the following additional symbols:

E = electric intensity at x
$H = 16\pi \left(\dfrac{m}{2e}\right)^{1/2} I_o$, where I_o is the current density corresponding to the forward-moving electrons
τ = transit time for an electron passing from grid to anode
τ' = transit time for an electron passing from grid to point of zero potential

$$P = \frac{3H^{1/2}x}{4V_g^{3/4}}$$

$$P_a = \frac{3H^{1/2}a}{4V_g^{3/4}}, \qquad \left\{ P_a = \frac{654\, I_o^{1/2} \left(\frac{\text{amp.}}{\text{cm}^2}\right)^{1/2} a\ (\text{cm})}{V_g^{3/4}\ (\text{volts})^{3/4}} \right\}$$

$$P_c = \frac{3H^{1/2}c}{4V_g^{3/4}} \qquad Q_g = \frac{E_g}{H^{1/2}\, V_g^{1/4}}$$

$$Q = \frac{E}{H^{1/2}\, V_g^{1/4}} \qquad Q_c = \frac{E_c}{H^{1/2}\, V_g^{1/4}}$$

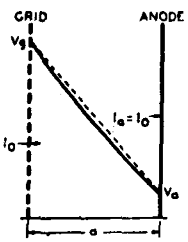

Fig. 1—Potential distribution between grid and anode typical of the case when neither potential minimum nor virtual cathode exist. All of the electrons which pass through the grid are collected at the anode.

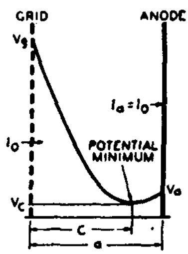

Fig. 2—Potential distribution illustrating the conditions which exist when a potential minimum is formed in the grid-anode region. All of the electrons which pass through the grid are collected at the anode.

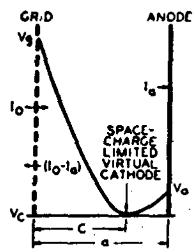

Fig. 3—This potential distribution represents the case when a space-charge-limited virtual cathode exists. Only part of the electrons which pass through the grid are collected at the anode; the others are returned towards the grid at the virtual cathode.

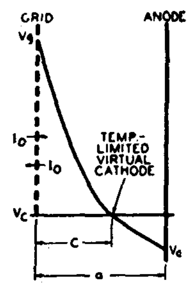

Fig. 4—This potential distribution illustrates the case when a temperature-limited virtual cathode exists. All of the electrons which pass through the grid are subsequently returned towards the grid at the virtual cathode.

The boundary conditions for the various states of operation are given in Figures 1, 2, 3, and 4, which depict typical potential distributions for these states of operation.

By combining (1), (2) and (3), and performing the first integration of (1) from any point x_1, to another point x, we get for the electric intensity at x,

$$\mathrm{E} = \pm \left[E_1^2 - HV_1^{1/2} + HV^{1/2}\right]^{1/2} \tag{4}$$

A second integration gives

$$\frac{3H^2}{4}(x-x_1)=\pm\,[E_1^2-HV_1^{1/2}+HV^{1/2}]^{1/2}\cdot[HV^{1/2}-2(E_1^2-HV_1^{1/2})]-$$
$$E_1\,[3HV_1^{1/2}-2E_1^2] \qquad (5)$$

The time of flight of an electron from x_1 to x is

$$\tau-\tau_1=\int_{x_1}^{x}\frac{dx}{v}=\left(\frac{m}{2e}\right)^{1/2}\cdot\int_{x_1}^{x}\frac{dx}{V^{1/2}} \qquad (6)$$

From (1), (2) and (3)

$$V^{-1/2}=\frac{1}{4\pi\left(\dfrac{m}{2e}\right)^{1/2}I}\cdot\frac{dE}{dx}$$

so that (6) becomes

$$\tau-\tau_1=\frac{1}{4\pi I}\int_{x_1}^{x}\frac{dE}{dx}\cdot dx=\frac{1}{4\pi I}\cdot(E-E_1) \qquad (7)$$

These general equations will now be applied to the various special states of operation.

1—*Neither Potential Minimum Nor Virtual Cathode Exist.*—This mode of operation is depicted in Figure 1. The situation is intermediate between the case when no electrons are present in the grid-anode region, for which condition the potential distribution is linear, and the case when enough electrons are present in this region so that the electric intensity is zero at the grid or anode. In this mode, all of the electrons which pass through the grid are collected at the anode.

Usually, I_o, a, V_g, and V_a are specified, and it is required to determine the distribution of the electric intensity and potential throughout the region and the time of flight of an electron from grid to anode. To start with, we must find E_g. This can be done by substituting the conditions that $V=V_a$ when $x=a$, and $E=E_g$ and $V=V_g$ when $x=0$ in (5). Thus,

$$\frac{3H^2a}{4}=\pm\,[E_g^2-H\,(V_g^{1/2}-V_a^{1/2})]^{1/2}\cdot[HV_a^{1/2}-2(E_g^2-HV_g^{1/2})]-$$
$$E_g\,[3HV_g^{1/2}-2E_g^2] \qquad (8)$$

This equation allows the determination of E_g in terms of I_o, a, V_g, and V_a. To put the equation into somewhat more convenient form for plotting, divide both sides by $H^{3/2}V_g^{3/4}$. We get an expression involving the dimensionless parameters, P_a and Q_g:

$$P_a = \pm \left[Q_g^2 - 1 + \left(\frac{V_a}{V_g} \right)^{½} \right]^{½} \left[\left(\frac{V_a}{V_g} \right)^{½} + 2 - 2Q_g^2 \right] - Q_g \left[3 - 2Q_g^2\right] \tag{8a}$$

A curve of P_a vs. $\frac{V_a}{V_g}$ for various values of Q_g may now be obtained very simply from (8a). This is shown in Figure 5.

For any given set of the four variables, Q_g can be located in Figure 5. For values of $\frac{V_a}{V_g}$ greater than unity, Q_g will range for this case, from zero to positive values; for values of $\frac{V_a}{V_g}$ which lie between unity and zero, Q_g will range from zero to negative values.

The potential distribution can now be determined by means of (5) by substituting the condition that $E_1 = E_g$ and $V_1 = V_g$ when $x_1 = 0$. Doing this, and rearranging, there results

$$P = \pm \left[Q_g^2 - 1 + \left(\frac{V}{V_g} \right)^{½} \right]^{½} \cdot \left[\left(\frac{V}{V_g} \right)^{½} + 2 - 2Q_g^2 \right] - Q_g \left[3 - Q_g^2\right] \tag{9}$$

This will be recognized as being similar to (8a) except that P replaces P_a, and V replaces V_a. Therefore, the same data can be utilized to study the variation of $\frac{V}{V_g}$ with P, (to which the distance from the grid, x, is proportional) for various values of Q_g. Figure 5 thus represents, also, generalized potential distribution curves.

The electric intensity at any point may be determined by means of (4) by substituting the condition that $E_1 = E_g$ when $V_1 = V_g$. This gives, after some rearrangement,

$$Q = \pm \left[Q_g^2 - 1 + \left(\frac{V}{V_g} \right)^{½} \right]^{½} \tag{10}$$

With the aid of (8a) and (9), (10) can be used to study the variation of Q (which is proportional to the electric intensity at any point, x) as a function of P, for various values of $\frac{V_a}{V_g}$.

The time of flight, τ, of an electron passing from grid to anode is, from (7)

$$\tau = \frac{1}{4\pi I_o} (E_a - E_g) \tag{7a}$$

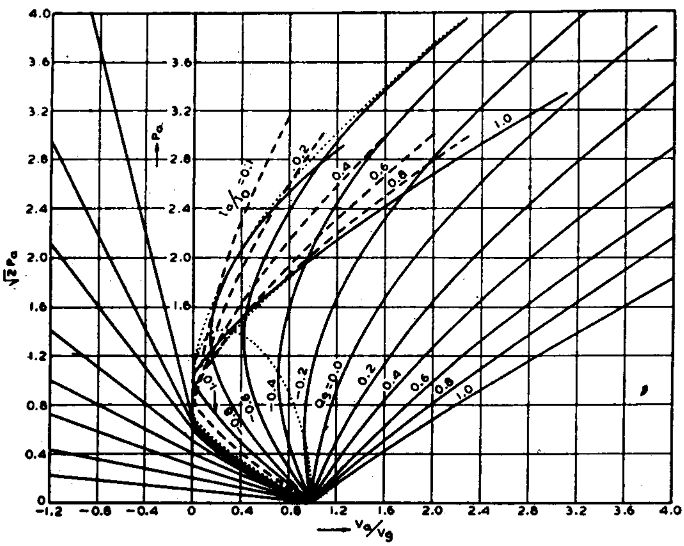

Fig. 5—Generalized potential distribution in the grid-anode region. This plot may be used to determine the particular mode in which the tube is operating, the anode current, and the electric intensity and potential distribution within the grid-anode region. Here,

$$P_a = 654 \cdot \frac{I_o^{1/2} \left(\frac{\text{amp.}}{\text{cm}^2}\right)^{1/2} \cdot a \text{ (cm)}}{V_g^{3/4} \text{ (volts)}^{3/4}}.$$

Equation (7a) can be put into more convenient form for plotting by making use of (4). After some rearrangement this gives

$$\tau = \frac{\tau_o}{P_a} \left\{ \pm \left[Q_g^2 - 1 + \left(\frac{V_a}{V_g} \right)^{1/2} \right]^{1/2} - Q_g \right\} \tag{11}$$

In (11) $\tau_o = \left(\frac{m}{2e} \right)^{1/2} \frac{3a}{V_g^{1/2}}$ represents the time of transit of an electron in a space-charge-limited diode, the electrodes of which coincide with the grid and anode, and for which the electric intensity at the cathode is zero and the anode voltage is V_g. The ratio $\frac{\tau}{\tau_o}$ is plotted in Figure 6, the necessary data for the curves being obtained from Figure 5.

It is of interest to note that when $I_o \rightarrow 0$, the limiting case for which the potential distribution is linear, (11) becomes

$$(\tau)_{I=o} = \left(\frac{m}{2e}\right)^{1/2} \cdot \frac{2a}{V_g^{1/2}} \cdot \frac{1}{\left(\frac{V_a}{V_g}\right)^{1/2} + 1} \tag{11a}$$

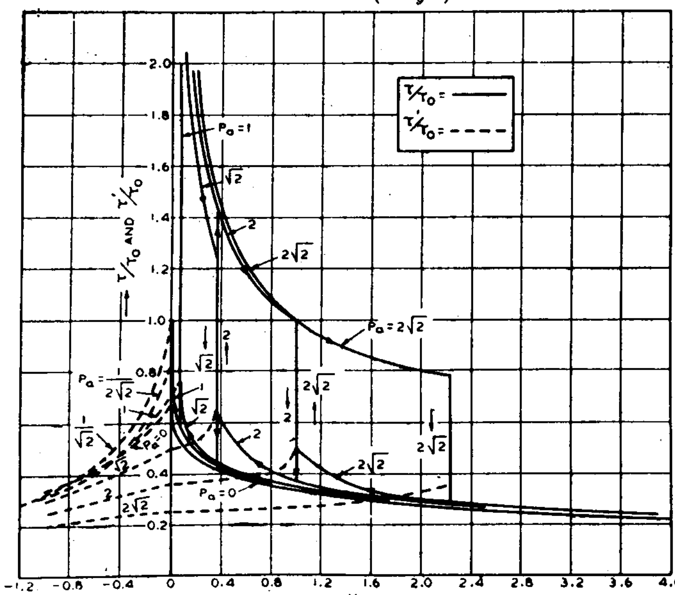

Fig. 6—Dependence of transit time upon anode voltage for various values of parameter P_a. τ is the transit time for electrons which travel from the grid to the anode. τ' is the electron transit time from grid to virtual cathode.

$\tau_o\ (\text{sec}) = \dfrac{3a\ (\text{cm})}{5.95 \cdot 10^7\ V_g^{1/2}\ (\text{volts})^{1/2}}$ is the electron transit time in a space-charge-limited diode.

The other limiting cases for the potential distributions under consideration here occur when $E_g = 0$, representing a potential minimum at the grid, or when $E_a = 0$, representing a potential minimum at the anode. In the first case

$$(\tau)_{Eg=o} = \left(\frac{m}{2e}\right)^{1/2} \frac{3a}{V_a^{1/2} + 2V_g^{1/2}} \tag{11b}$$

while in the second case

$$(\tau)_{E_a=0} = \left(\frac{m}{2e}\right)^{1/2} \cdot \frac{3a}{V_g^{1/2} + 2V_a^{1/2}} \tag{11c}$$

2—*Potential Minimum Exists.*—This mode of operation is shown in Figure 2. The situation existing here is intermediate between the case when enough space current flows through the grid so that the electric intensity is zero at the grid or anode, and the case when the conditions are such that the electric intensity *and* the potential are just zero at either electrode or in the intervening region. In this mode, also, all of the electrons which pass through the grid are collected by the anode.

Here again, I_0, a, V_g and V_a are usually specified, and it is required to find the distribution of the electric intensity and potential throughout the region, the time of flight of an electron from grid to anode, and the value and location of the minimum potential.

We start by substituting the condition that $V = V_g$ and $E = E_g$ when $x = 0$, and $V = V_a$ and $x = a$ in (5). This leads to an expression identical with (8a); the variation with $\frac{V_a}{V_g}$ of P_a for various values of Q_g is shown in Figure 5. For this mode Q_g ranges between 0 and -1 for all values of $\frac{V_a}{V_g}$, as shown in Figure 5. It is important to note that for one value of $\frac{V_a}{V_g}$ there can be two values of Q_g, corresponding to one value of P_a. We shall discuss this peculiarity further on.

In the same way, the expression for the potential distribution can be shown to be formally identical to (9), and the variation of $\frac{V}{V_g}$ with P for various values of Q_g can also be studied from Figure 5. For this mode of operation, $\frac{V}{V_g}$ passes through a minimum, representing the potential minimum.

The expression for the electric intensity is derivable, again, from (4); this is identical with (10). Now E is negative to the left of the potential minimum, zero at the potential minimum, and positive to the right of the potential minimum.

The time of flight, τ, of an electron from grid to anode is again given by (11), and the ratio $\dfrac{\tau}{\tau_0}$ is also plotted in Figure 6. It is of interest to note that for the limiting condition, when $V_c = 0$, (11) gives

$$\tau = \left(\frac{m}{2e}\right)^{1/2} \cdot \frac{3a}{V_g^{1/2}} \cdot \frac{1}{\left[1 - \left(\dfrac{V_a}{V_g}\right)^{1/4} + \left(\dfrac{V_a}{V_g}\right)^{1/2}\right]} \tag{11d}$$

The ratio of (11a) to (11d) gives us an estimate of the increase of the transit time for two important limiting cases which may be encountered. This is

$$\frac{(\tau)_{V_c=0}}{(\tau)_{I_0=0}} = \frac{2}{3} \cdot \left\{1 - \frac{1}{\left(\dfrac{V_a}{V_g}\right)^{1/4} + \left(\dfrac{V_g}{V_a}\right)^{1/4}}\right\} \tag{12}$$

Thus when $V_a = V_g$, the transit time for the case when a zero-potential minimum is just formed is three times larger than the transit time for very low values of anode current.

It is of considerable interest, in any consideration of this particular mode of operation, to determine the value and location of the minimum potential. This may be done indirectly by making use of Figure 5. Alternately, an implicit expression for the value of $\dfrac{V_c}{V_g}$ may be derived from (4) and (5). This is

$$P_a = \pm\left[1 - \left(\frac{V_c}{V_g}\right)^{1/2}\right]^{1/2} \cdot \left[1 + 2\left(\frac{V_c}{V_g}\right)^{1/2}\right] \pm \left[\left(\frac{V_a}{V_g}\right)^{1/2} - \left(\frac{V_c}{V_g}\right)^{1/2}\right]^{1/2} \cdot \left[\left(\frac{V_a}{V_g}\right)^{1/2} + 2\left(\frac{V_c}{V_g}\right)^{1/2}\right] \tag{13}$$

The variation of $\dfrac{V_c}{V_g}$ with $\dfrac{V_a}{V_g}$, for several values of P_a is shown in Figure 7.

In the same way, by making use of (4) and (5), the location of the minimum potential can be expressed in terms of $\frac{V_c}{V_g}$ and P_a, i.e.,

$$\frac{c}{a} = \frac{1}{P_a} \cdot \left[1 + 2 \left(\frac{V_c}{V_g} \right)^{1/2} \right] \cdot \left[1 - \left(\frac{V_c}{V_g} \right)^{1/2} \right]^{1/2} \tag{14}$$

The dependence of $\frac{c}{a}$ on $\frac{V_a}{V_g}$, for various values of P_a is shown in Figure 8.

Figures 7-11 are of the greatest importance in delineating the properties of the grid-anode region. We shall make extensive use of these curves in our discussion.

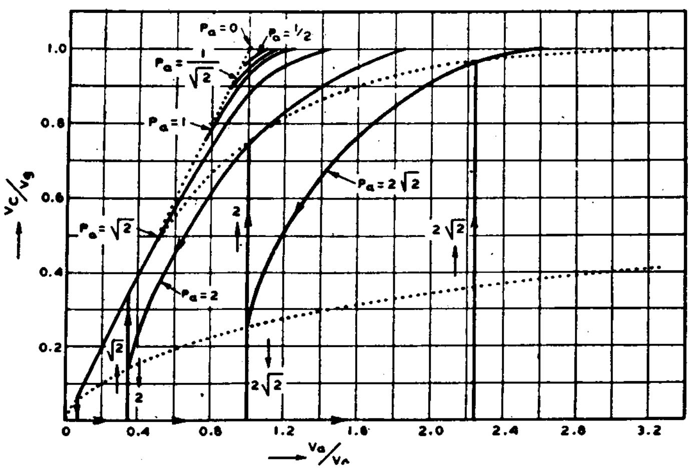

Fig. 7—Variation of the magnitude of the potential minimum with anode potential for several values of the parameter P_a.

Before proceeding to the next case, let us consider what happens when, with V_a, V_g, and a fixed, the current density I_0 is increased from zero until the potential minimum which is formed in the grid-anode region descends to the value zero. Figure 9, plotted from (13), shows the variation of $\frac{V_c}{V_g}$ with P_a^2 for various values of $\frac{V_a}{V_g}$. The rate of change of the minimum potential with respect to space current is given by the slope of these curves. Differentiating P_a in (13) with respect to $\left(\frac{V_c}{V_g} \right)^{1/2}$, considering $\left(\frac{V_a}{V_g} \right)^{1/2}$ fixed, and equating the derivative to zero tells us that $(P_a)_{\max}$ occurs when

$$\frac{V_c}{V_g} = \frac{\dfrac{V_a}{V_g}}{\left[1 + \left(\dfrac{V_a}{V_g}\right)^{1/2}\right]^2} \tag{15}$$

Substituting (15) in (13), we find that the maximum current (density) which can be passed is

$$(I_a)_{\max.} = \frac{1}{9\pi a^2} \cdot \left(\frac{2e}{m}\right)^{1/2} \cdot (V_g^{1/2} + V_a^{1/2})^3 \tag{13a}$$

The value of the potential minimum for this maximum current is given by (15). Equation (15) is plotted as a dotted line in Figure 7. Figure 11 is a plot of $\left(\dfrac{I_a}{I_o}\right) \cdot P_a^2$ vs. P_a^2 and shows the anode current increasing directly with the space current until the maximum value, given by (13a), is reached. At this point the potential minimum descends abruptly to zero, and a new state of operation sets in.

3—*Space-Charge-Limited Virtual Cathode Exists.*—This state of operation is shown in Figure 3. The situation existing here is such that at some plane in the region between the two electrodes, or possibly in the plane at either electrode, the electric intensity *and* the potential are zero. Such a point may be called a space-charge-limited virtual cathode, since it turns out that it behaves in many respects like a space-charge-limited thermionic cathode. It is pertinent to call attention to the difference between the virtual cathode of the present case and the potential minimum of the preceding case. In general, the potential minimum merely calls for a zero of electric intensity, but not of potential, since all of the electrons which flow through the grid are collected at the anode. However, when there is a point of zero potential in the region between the two electrodes, some of the electrons passing towards the anode may be turned back towards the grid at this point.

As a digression, we may study briefly the limiting case, when the anode current is exactly equal to the space current. We have, on putting

$\dfrac{V_c}{V_g} = 0$ in (13),

$$I_a = \frac{1}{9\pi a^2} \cdot \left(\frac{2e}{m}\right)^{1/2} \cdot (V_g^{3/4} + V_a^{3/4})^2 \tag{13b}$$

This is smaller than the current predicted by (13a), the ratio of (13a) to (13b) being

$$\frac{\left[1+\left(\dfrac{V_a}{V_g}\right)^{1/2}\right]^3}{\left[1+\left(\dfrac{V_a}{V_g}\right)^{3/4}\right]^2},$$

the maximum value of this ratio occurring when $\dfrac{V_a}{V_g}=1$. The ratio is equal to unity when $\dfrac{V_a}{V_g}=0$ or ∞. The difference between (13a) and (13b) is the basis of the hysteresis phenomena characteristic of the curves shown in Figures 5-11, and will be discussed further on.

We return now to the general case, for which some of the electrons are turned back towards the grid, and assume for simplicity that such electrons never again re-enter the grid-anode region.* The anode current is then, in view of (1), (2), (3), and the requisite boundary conditions, given by

$$I_a=\frac{1}{9\pi}\cdot\left(\frac{2e}{m}\right)^{1/2}\cdot\frac{V_a^{3/2}}{(a\text{-}c)^2} \tag{16}$$

The total space charge in the region between the grid and the virtual cathode depends upon both the forward-moving and returning electrons, and since these electrons have the same velocity at any one point, we may write

$$2I_o-I_a=\frac{1}{9\pi}\cdot\left(\frac{2e}{m}\right)^{1/2}\cdot\frac{V_g^{3/2}}{c^2} \tag{17}$$

If we divide (17) by I_o, and put $H=16\pi\left(\dfrac{m}{2e}\right)^{1/2}\cdot I_o$ and $P_a=\dfrac{3H^{1/2}a}{4V_g^{3/4}}$ as before, we get, on rearranging,

$$\frac{c}{a}=\frac{1}{P_a\left(2-\dfrac{I_a}{I_o}\right)^{1/2}} \tag{18}$$

It is of interest to note that when $I_a=0$, (18) becomes $\dfrac{c}{a}=\dfrac{1}{2^{1/2}P_a}$.

---

* The ensuing treatment can easily be generalized to include the multiple-passage case. See, for example, 7, 9 of Bibliography.

That is, when $V_a = 0$, the virtual cathode (if one exists) is at a distance $c = \dfrac{a}{2^{1/2} P_a}$ cm from the grid.

In order to use (18) to plot the location of the virtual cathode as a function of I_o, a, V_g and V_a, we must first derive an expression for $\dfrac{I_a}{I_o}$ as a function of $\dfrac{V_a}{V_g}$ and P_a. This can be done by dividing (17) by (16) and making use of (18). There results

$$\left(\frac{V_a}{V_g}\right)^{3/4} = \left(\frac{I_a}{I_o}\right)^{1/2} \cdot \left[P_a - \frac{1}{\left(2 - \dfrac{I_a}{I_o}\right)^{1/2}}\right] \tag{19}$$

Equation (19) is used (a) to plot P_a vs. $\dfrac{V_a}{V_g}$ for various values of $\dfrac{I_a}{I_o}$, as shown in Figure 5; (b) to plot $\dfrac{I_a}{I_o}$ vs. $\dfrac{V_a}{V_g}$ for various values of P_a, as shown in Figure 10;* and (c) to plot $\left(\dfrac{I_a}{I_o}\right) \cdot P_a^2$ vs. P_a^2 for various values of $\dfrac{V_a}{V_g}$, as shown in Figure 11. In addition, by making use in (18) of the data furnished by Figure 10, we are enabled to plot $\dfrac{c}{a}$ vs. $\dfrac{V_a}{V_g}$ for various values of P_a, as shown in Figure 8.

The potential distribution within the grid-anode region corresponding to any particular value of c is $\dfrac{V}{V_g} = \left(\dfrac{c-x}{c}\right)^{4/3}$ to the left of c, and $\dfrac{V}{V_a} = \left(\dfrac{x-c}{a-c}\right)^{4/3}$ to the right of c. The corresponding electric intensities are $E = -\dfrac{4}{3} \cdot \dfrac{V}{c-x}$, and $E = +\dfrac{4}{3} \cdot \dfrac{V}{a-c}$, respectively.

---

* Curves similar to those given in Figure 10 have been given by Tonks[7]; his curves however, are restricted to the virtual-cathode case and do not portray the important hysteresis-effects characteristic of the minimum-potential case.

The time of flight of an electron which travels from the grid to the virtual cathode is simply

$$\tau' = \left(\frac{m}{2e}\right)^{1/2} \cdot \frac{3c}{V_g^{1/2}} = \frac{c}{a} \cdot \tau_0 \qquad (20)$$

The time of flight of an electron which travels from grid to anode is

$$\tau = \left(\frac{m}{2e}\right)^{1/2} \cdot \left[\frac{3c}{V_g^{1/2}} + \frac{3\,(a-c)}{V_a^{1/2}}\right]$$

$$= \tau_0 \cdot \left\{\left(\frac{V_g}{V_a}\right)^{1/2} + \frac{c}{a} \cdot \left[1 - \left(\frac{V_g}{V_a}\right)^{1/2}\right]\right\} \qquad (21)$$

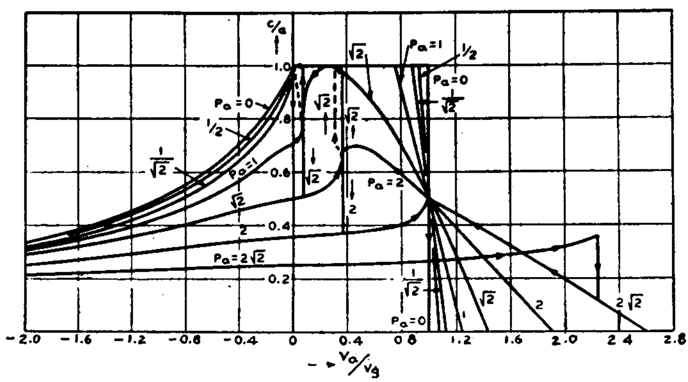

Fig. 8—Position of the potential minimum and virtual cathode as a function of the anode potential for various values of the parameter P_a.

The time of flight for each class of electrons can be plotted with the aid of (18), as shown in Figure 6.

4—*Temperature-Limited Virtual Cathode Exists (Negative Anode Potentials).*—This state of operation is illustrated in Figure 4. The situation now is such that the electric intensity is negative throughout the region between the two electrodes, and at some intermediate plane the potential is zero. The electrons which move through the interstices of the grid towards the plane of zero potential are gradually decelerated, and finally turned back at this plane toward the grid. Since the electric intensity at this plane is always finite, the potential distribution between *c* and *o* resembles that of a temperature-limited diode. It turns out, moreover, that the properties of the plane of zero potential are in many respects identical to that of the temperature-limited cathode. Accordingly, we shall designate this plane as a "temperature-limited virtual cathode", by analogy with the "space-charge-limited virtual cathode".

Here I_o, a, V_g, and V_a are specified and it is required to determine the distribution of the electric intensity and potential throughout this region, the position of the virtual cathode, and the time of flight of an electron from the grid to the virtual cathode. We shall not attempt a rigorous treatment, but instead we shall base our analysis on the same assumptions as we have made for the preceding cases.

Since the anode is negative, no electrons will be collected. (This is a consequence of our assumptions regarding the initial velocities of the electrons emerging from the grid plane: in actuality there is always a very small anode current as a result of a distribution of initial veloci-

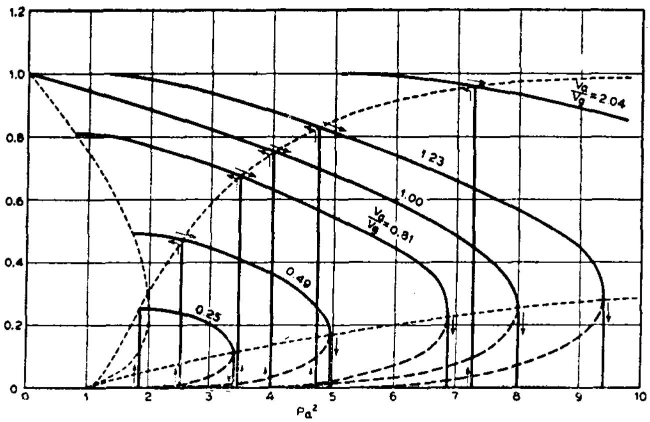

Fig. 9—Variation of the magnitude of the potential minimum with P_a^2 (to which the space current is proportional) for several values of $\frac{V_a}{V_g}$.

ties.) Furthermore, since the electric intensity must be continuous, and since there is no charge in the region $c < x < a$, the electric intensity, E_c, at the virtual cathode (and also to the right of this plane) will be equal to $\frac{V_a}{a\text{-}c}$.

We now make use of (4) and (5), subject to the appropriate boundary conditions. In (4) we put $E_1 = E_c$, $E = E_g$, $V_1 = 0$, $V = V_g$, and $I = 2I_o$. There results

$$E_g = -\,[E_c^2 + 2HV_g^{1/2}]^{1/2} \tag{22}$$

In (5) we put $x = c$, $x_1 = 0$, $E_1 = E_g$, $V_1 = V_g$, and $V = 0$ getting, with the aid of (22)

$$\frac{3H^2c}{2} = \mp\,[E_c^3 + (E_c^2 - HV_g^{1/2}).\,(E_c^2 + 2HV_g^{1/2})^{1/2}] \tag{23}$$

Dividing through by $2H^{3/2}. V_g^{3/4}$ and making use of our abbreviated symbolism, we get

$$P_c = \mp \frac{Q_c^3 + (Q_c^2 - 1).(Q_c^2 + 2)^{1/2}}{2} \tag{23a}$$

Now,

$$P_c\,Q_c = \frac{3H^{1/2}c}{4V_g^{3/4}} \cdot \frac{V_a}{(a\text{-}c)\;H^{1/2}\;V_g^{1/4}} = \frac{3}{4} \cdot \left(\frac{V_a}{V_g}\right) . \frac{\dfrac{c}{a}}{1 - \dfrac{c}{a}} = P_a \,.\, Q_c \frac{c}{a}$$

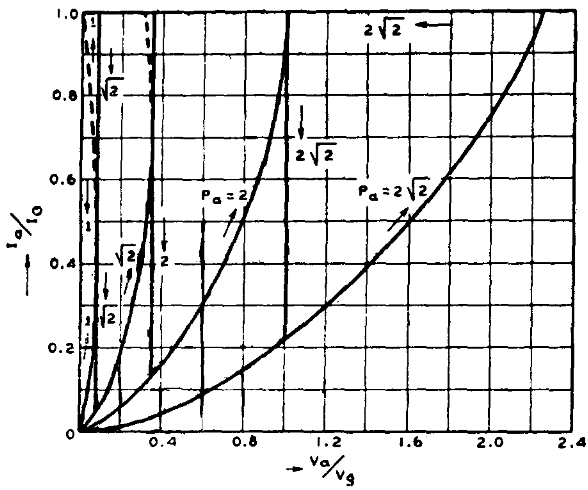

Fig. 10—Dependence of anode current upon anode potential for various values of the parameter P_a.

so that

$$\frac{c}{a} = \frac{P_c}{P_a} = 1 - \frac{3}{4} \cdot \frac{\left(\dfrac{V_a}{V_g}\right)}{P_a \cdot Q_c} \tag{24}$$

and

$$P_a = P_c + \frac{3}{4} \cdot \frac{1}{Q_c} \cdot \left(\frac{V_a}{V_g}\right) \tag{24a}$$

We may now plot P_c as a function of Q_c by means of (23a). The corresponding value of P_a for any given value of $\dfrac{V_a}{V_g}$ may then be found from (24a). This gives us sufficient information to plot $\frac{c}{a}$ as a function of $\frac{V_a}{V_g}$ for various values of P_a: such curves are included in Figure 8. We are also enabled to plot, from this information, P_a vs. $\frac{V_a}{V_g}$ for various values of Q_g: this is shown in Figure 5, which may be used again as a generalized potential distribution plot.

The electric intensity at any point is given by

$$Q = -\left[Q_g^2 + 2 \left(\frac{V}{V_g} \right)^{½} - 2 \right]^{½} \qquad (25)$$

The time of transit of electrons from grid to virtual cathode is, from (7) and (25),

$$\tau' = \frac{\tau_o}{2P_a} \cdot [Q_g + (Q_g - 2)^{½}] \qquad (26)$$

The ratio $\frac{\tau'}{\tau_o}$ vs. $\frac{V_a}{V_g}$ for various values of P_a is shown in Figure 6. The limiting case, $I_o \rightarrow o$, of (26) is

$$\tau' = \tau_o \cdot \frac{2}{3} \cdot \frac{1}{1 - \left(\frac{V_a}{V_g} \right)} \qquad (26a)$$

III. Discussion of Theoretical Results

We now proceed to interpret the results of the foregoing analysis. In the interests of clarity we shall lead up to the general discussion of Figures 5-11 by providing a preliminary verbal description of the results of varying first the space current and then the anode voltage for several representative cases of interest.

A—*Preliminary Discussion of Several Particular Situations*—

1. Effects of Varying I_o, when $\frac{V_a}{V_g} = 1$.

To begin with, let us suppose that the effective grid voltage, V_g, the anode voltage, V_a, and the grid-anode distance, a, are fixed, and that it is required to determine the effects of increasing the space current, I_0. This situation corresponds, for example, to the case of a tetrode, the screen-grid voltage and the anode voltage of which are fixed, and the control-grid voltage of which is varied. To fix ideas, we choose $\frac{V_a}{V_g} = 1$: a similar interpretation will hold for any other ratio.

When the control-grid bias is adjusted to cut off the cathode current, the potential distribution is linear, as shown by (*a*) of Figure 12. Decreasing the bias causes electrons to flow into the grid-anode region,

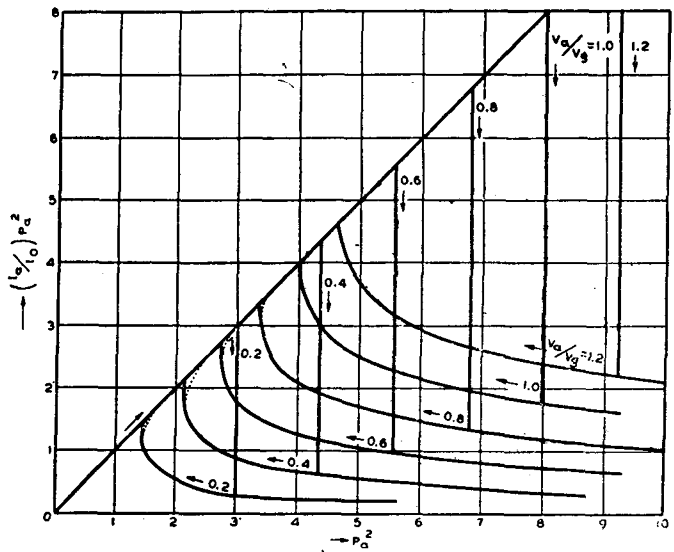

Fig. 11—Variation of the anode current with space current for several values of $\frac{V_a}{V_g}$.

and the potential is depressed, as shown by (*b*). A potential minimum is formed mid-way between the grid and anode. As the space current is increased, the potential minimum gradually descends until it reaches a value equal to 0.25 times the grid voltage, as shown in Figure 9. Up to this point the anode current increases directly with the space current, as shown in Figure 11. All of the electrons coming through the grid are collected at the anode. If, now, any additional electrons are permitted to pass into the grid-anode region, the potential minimum drops abruptly to zero, mid-way between the grid and anode. This is shown in Figure 9, the rate of change of the minimum potential with space current being infinite at this point. Since the minimum is now zero, some of the electrons are returned towards the grid, thus decreasing the space charge between the potential minimum and the anode, and increasing the space charge between the grid and the potential minimum. This causes an alteration of the potential distribution, the minimum (now a virtual cathode) shifting abruptly towards the grid until it reaches a distance from the grid equal to 0.265 times the grid-anode distance, shown by (*d*) of Figure 12. Thereafter, as the space current is increased, the anode current decreases gradually, in accordance with Figure 11, and the virtual cathode retreats toward the grid. The effect of increasing the space current on the time of flight of an

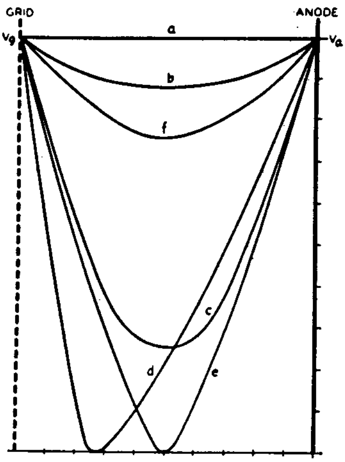

Fig. 12—Potential distribution for several values of space current. $\frac{V_a}{V_g} = 1$.

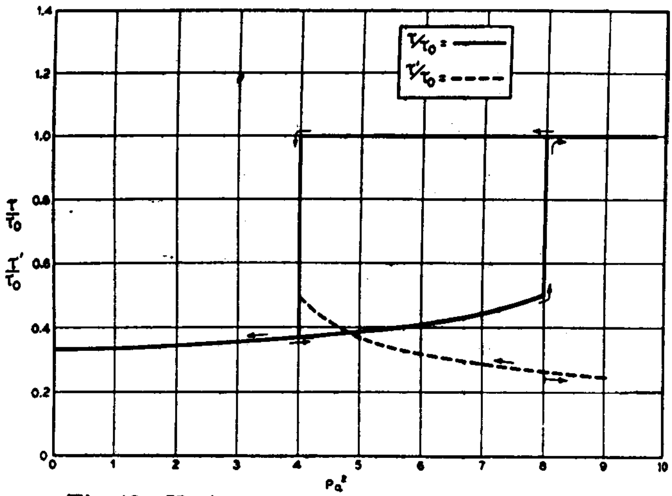

Fig. 13—Variation of electron transit time with space current. $\frac{V_a}{V_g} = 1$.

electron from grid to anode, and from grid to virtual cathode, is shown in Figure 13.

It will be observed that the transit time is initially one-third that of a space-charge-limited diode, the electrodes of which coincide with the grid and anode and for which the anode voltage is $V_g = V_a$. With increasing space current the transit time rises slowly until a current corresponding to $P_a^2 = 8$ is reached. At this point a virtual cathode is formed, and the transit time rises abruptly from $\tau = 0.500\tau_0$ to $\tau = \tau_0$. It remains constant thereafter at this value with further increase of space current. The transit time for the electrons which return toward the grid when a virtual cathode is formed is initially $\tau' = 0.265\tau_0$, and decreases slowly with increasing space current, since the virtual cathode retreats toward the grid. The time of flight of electrons from grid to virtual cathode and back to grid is twice τ'.

If the space current is now gradually decreased, the anode current will be found to increase, as shown in Figure 11. The operation now, however, does not take place entirely along the original curve. This is due to the fact that, originally, operation began with a potential minimum; now it takes place with a virtual cathode. When the space current reaches a value equal to one-half of the current at the transition value, where the potential minimum had previously shifted abruptly into a virtual cathode, the anode current becomes equal to the space current. The virtual cathode is now saturated. At this point the virtual cathode is mid-way between the grid and the anode, as shown by (*e*) of Figure 12. The slightest further reduction of space current causes the virtual cathode to shift abruptly into a potential minimum, the value of which is 0.75 times the grid voltage, as shown by (*f*) of Figure 12. Any further reduction of space current is accompanied by a proportionate decrease of anode current, the potential minimum gradually approaching (*a*) of Figure 12. The effect of decreasing the space current on the time of flight of an electron from grid to anode, and from grid to virtual cathode, is also shown in Figure 13.

The time of flight for electrons moving from grid to anode remains constant until the virtual cathode disappears; this occurs when the space current is decreased to a value corresponding to $P_a{}^2 = 4$. At this point the transit time drops abruptly to a value $\tau = 0.366\tau_o$. With further decrease of space current the transit time decreases slowly until the limiting value $\tau = 0.333\tau_o$ is reached for $P_a{}^2 \rightarrow 0$. The time of flight for the electrons which return from the virtual cathode increases slowly with decreasing space current, because the virtual cathode moves out slowly towards the anode. When $P_a{}^2 = 4$, the virtual cathode disappears and the transit time for the electrons which have been returning for space currents slightly greater than this value, is $\tau' = 0.500\tau_o$.

2. Effects of Varying I_o, when $\dfrac{V_a}{V_g} = 0.20$.

In the foregoing we have described in detail what occurs when the space current between the grid and anode is first increased, and then decreased. But this description was for the particular case when the grid and the anode voltages were equal. Similar phenomena, however, occur for any other ratio of $\dfrac{V_a}{V_g}$, with only slight differences. For example, suppose $\dfrac{V_a}{V_g} = 0.20$. Beginning with $I_o = 0$, the potential distribution is linear. As I_0 is increased, the behavior of the grid-anode region is initially characteristic of the first mode of operation, i.e., neither potential minimum nor virtual cathode exist. Further increase of I_0 finally causes a potential minimum to occur at the anode, the value of this potential minimum being equal to the anode potential. The corresponding value of P_a is given by equation (13) as $P_a = 1.41$, the equivalent space-current density being $I_0 = 4.62 \times 10^{-6} \times \dfrac{V_g^{3/2}}{a^2} \dfrac{\text{amp.}}{\text{cm}^2}$.

Reference to Figure 11 tells us that the anode current will increase directly with space current until the space-current density reaches a value

$I_0 = 7.00 \times 10^{-6} \dfrac{V_g^{3/2}}{a^2} \dfrac{\text{amp.}}{\text{cm}^2}$, corresponding to a value of $P_a^2 = 3.00$.

This is the maximum anode-current density which can be passed: at this point the potential minimum, which has decreased to a value 0.0956 times the grid voltage, drops abruptly to zero and becomes a virtual cathode. The potential minimum, which had initially been formed at the anode, gradually recedes toward the grid until it reaches a distance equal to 0.776 times the grid-anode distance, given by equation (14). At this point it becomes a virtual cathode, and enables some of the electrons to return toward the grid. The resulting re-distribution of space charge causes the virtual cathode to shift abruptly until it reaches a distance equal to 0.418 times the grid-anode distance, given by equation (18). Any further increase of I_0 results in a decreased anode current, as shown in Figure 11, the virtual cathode retreating still further toward the grid. If the space current is then decreased, the anode current will increase, as shown in Figure 11, and the virtual cathode will move back toward the anode. This behavior will continue until the space-current density reaches a value

$I_0 = 3.38 \times 10^{-6} \times \dfrac{V_g^{3/2}}{a^2} \dfrac{\text{amp.}}{\text{cm}^2}$, corresponding to a value of $P_a^2 = 1.45$.

At this point the virtual cathode is at a distance equal to 0.719 times the grid-anode distance, as given by equation (18). The slightest further reduction of space current permits enough electrons to pass abruptly through the virtual-cathode barrier toward the anode so that the space-charge distribution is radically altered, the virtual cathode disappears, and the anode current rises abruptly to the full value of space current. (An interesting observation about this example is that at this unstable point the virtual cathode does not become a potential minimum, but disappears.) From this point on, any further reduction of space current results in a proportionate reduction of anode current, as shown in Figure 11, and the potential distribution becomes more and more linear.

3. Effects of Varying V_a, when $P_a = 1.0$.

Let us now suppose that the grid-anode distance, a, the effective grid voltage, V_g, and the space-current density, I_o, are fixed, and that it is required to determine the effects of varying the anode voltage, V_a. This situation corresponds, for example, to the case of a tetrode, the screen-grid voltage and the control-grid voltage of which are fixed, and the anode voltage of which is varied.

To begin with, we assume that the control-grid voltage is set at a value which provides a space-current density corresponding to a value of $P_a = 1.0$. When the anode voltage is negative, the anode current is zero, and all of the electrons are returned toward the grid at the temperature-limited virtual cathode. The potential distribution for $\dfrac{V_a}{V_g} = -0.2$ is shown by (a) of Figure 14. The position of the virtual cathode is given by Figure 8 as $c = 0.645\ a$. When $V_a = 0$, then $I_a = 0$, and $c = 0.707\ a$, as shown by (b) of Figure 14. As V_a is made more positive, the anode current rises as shown in Figure 10 and the space-charge-limited virtual cathode moves toward the anode. (If there had been no movement of the virtual cathode, the anode current would rise as $V_a^{3/2}$.) This continues until $V_a = 0.068\ V_g$, while the anode current density rises to $I_a = 0.413\ I_o$, and the virtual cathode moves to $c = 0.793\ a$, as shown by (c) of Figure 14. The slightest further increase of anode voltage results in an abrupt saturation of anode current, the rate of change of anode current with anode voltage being infinite at this point, as shown by Figure 10. The virtual cathode disappears at this point, and the potential distribution is of the form shown by (c') of Figure 14, characteristic of the mode for which neither potential minimum nor virtual cathode exist. Further increase of anode voltage leaves the anode current, which is now equal to the space current, unaffected. However, when V_a reaches $0.75\ V_g$, a potential minimum appears at the anode, as shown by (d) of Figure 14. With increasing anode voltage this minimum recedes toward the grid, approaches V_g in value, and finally disappears, as shown in Figures 7 and 8.

If the anode voltage is now decreased, the anode current remains at saturation value until $V_a = 0$, as shown in Figure 10. The potential minimum re-appears at the grid when $V_a = 1.23\ V_g$, moves toward the anode as V_a is decreased, and reaches the anode when $V_a = 0.75\ V_g$, as before At this point the minimum disappears. When $V_a = 0$, the potential distribution is abruptly altered, and a virtual cathode is formed at a distance $c = 0.707\,a$, as shown by (f), (f') of Figure 14.

The time of flight of an electron moving from grid to anode, and from grid to virtual cathode, is shown for increasing and decreasing anode voltages in Figure 6.

4. Effects of Varying V_a, when $P_a = \sqrt{2}$, $P_a = 2\sqrt{2}$.

Similar interpretations hold for any other value of the parameter P_a. As a matter of interest, the various forms of the potential distribution for the particular cases $P_a = \sqrt{2}$ and $P_a = 2\sqrt{2}$ are shown in Figures 15 and 16. For the first of these, as the anode voltage is increased from a negative value, the potential distribution

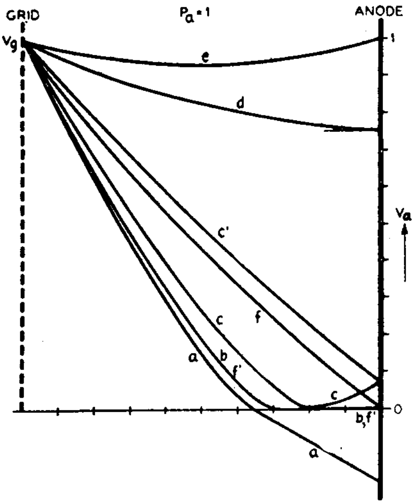

Fig. 14—Potential distribution for various values of anode voltage. $P_a = 1$.

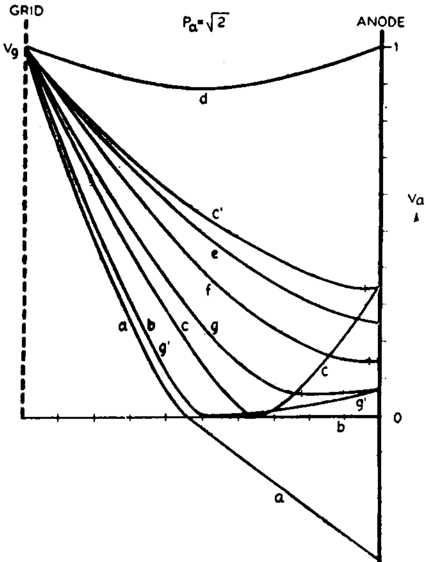

Fig. 15—Potential distribution for various values of anode voltage. $P_a = \sqrt{2}$.

passes from the state described by Case 4, which is characterized by a temperature-limited virtual cathode, (a), to that described by Case 3—the space-charge-limited virtual cathode case, (b), (c); thence abruptly to that described by Case 2, for which a potential minimum is formed, (c'), (d); and then finally to that described by Case 1, for which neither potential minimum nor virtual cathode exist. The behavior for decreasing anode voltage is successively illustrated by (d), (c'), (e), (f), (g), (g'), (a) of Figure 15. The abrupt decrease in anode current again occurs at a lower value of V_a than that required for the abrupt rise, as shown in Figure 10.

B—*General Discussion of Curves.*—The four distinct modes of potential distribution which are treated in the foregoing analysis represent a somewhat arbitrary and simplified division of the potential distributions which may occur in the grid-anode region. This simplification is made possible by the original assumptions that the electrons have all been initially emitted from the cathode with zero velocity and that no velocity distribution has been introduced during the passage of the electrons through the structure. In the rigorous treatment of this problem the separate analyses of the four modes of potential distribution would merge into a single general analysis. However, such a treatment would be considerably more involved, and the main results at least can probably be anticipated by combining the various results found here for the individual states of operation on common graphs. This has been done in Figures 5-11.

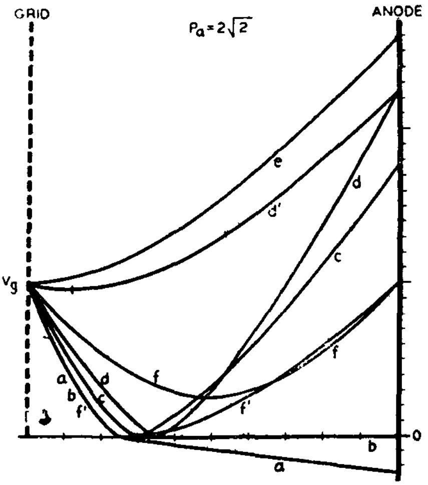

Fig. 16—Potential distribution for various values of anode voltage. $P_a = 2\sqrt{2}$.

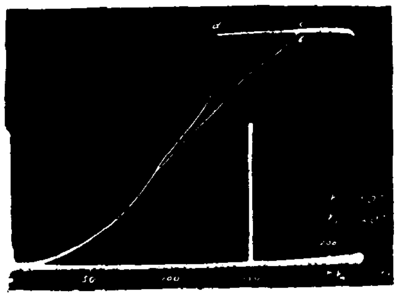

Fig. 17—Anode-characteristic oscillogram of special pentode showing the hysteresis and instability phenomena similar to curve marked $P_a = 2\sqrt{2}$ in Figure 10.

Figure 5 is a plot of P_a vs. $\dfrac{V_a}{V_g}$, for various values of Q_g. If I_o, V_a, V_g, and a are given, this plot enables one to determine the electric intensity at the grid, since P_a is proportional to $\dfrac{a I_o^{1/2}}{V_g^{3/4}}$ and Q_g is proportional to $\dfrac{E_g}{I_o^{1/2} V_g^{1/4}}$. As was pointed out in the analysis, these curves also represent a generalized potential distribution plot if P_a is replaced by P, which is proportional to $\frac{x I_o^{1/2}}{V_g^{3/4}}$, and $\frac{V_a}{V_g}$ is replaced by $\frac{V}{V_g}$. For the temperature-limited virtual cathode case (negative anode potentials) the scale of ordinates represents $\sqrt{2}\, P_a$ instead of P_a. This results from the fact that all the electrons which pass through the grid toward the anode are turned back toward the grid at the virtual cathode, and the space charge corresponds to a space current of $2\, I_o$ instead of I_o. The parameter Q_g is replaced by $\frac{I_a}{I_o}$ in the space-charge-limited virtual cathode case because this quantity is of greater practical significance. However, if the electric intensity at the grid is required for this case, it can be found very quickly from the relation

$$Q_g = -\left(2 - \frac{I_a}{I_o}\right)^{1/2}$$

It will be observed that there occurs a curious overlapping of the various possible states of operation in different regions of the plot. For example, for $0 \leqq \frac{V_a}{V_g} \leqq 1$ and $\frac{1}{\sqrt{2}} \leqq P_a \leqq \sqrt{2}$, there may be a virtual cathode, a potential minimum, or neither potential minimum nor virtual cathode. Again, for $\frac{V_a}{V_g} \geqq 0$ and $P_a \geqq \sqrt{2}$, there may be a virtual cathode or a potential minimum. To put it in another way, the potential at any point in the region, for certain values of I_o, V_a, V_g and a, is multi-valued. This is a typical hysteresis phenomenon, and in order to determine which of the values of potential is the correct one it is necessary to know, as in all cases of hysteresis, the previous history of the region. This point will be discussed in further detail in connection with the other figures.

Figure 9 is a plot of $\frac{V_c}{V_g}$ vs. P_a^2, for various values of $\frac{V_a}{V_g}$. The curves shown in this plot indicate how the minimum potential varies with space current, since P_a^2 is proportional to I_o. The section of the plot which lies to the left of the lightly-dashed line connecting the points $\left(\frac{V_c}{V_g} = 1,\ P_a^2 = 0\right)$ and $\left(\frac{V_c}{V_g} = 0,\ P_a^2 = 1\right)$ delineates the operating region in which neither potential minimum nor virtual cathode occur. The lightly-dashed line which starts at the point $\left(\dfrac{V_c}{V_g}=0,\ P_a{}^2=1\right)$ and passes through the point $\left(\dfrac{V_c}{V_g}=0.25,\ P_a{}^2=8\right)$ is a parametric line which indicates the points at which the rate of change of the potential minimum with (increasing) space current is infinite. If the grid and anode potentials of a given tube are fixed and the space current is increased from zero, the potential minimum shifts abruptly at these points into a virtual cathode. The lightly-dashed line which starts at the point $\left(\dfrac{V_c}{V_g}=0,\ P_a{}^2=1\right)$ and becomes asymptotic to $\dfrac{V_c}{V_g}=1$ for very large values of $P_a{}^2$ is a parametric line which indicates the points at which the virtual cathode shifts abruptly, with decreasing space current, into a potential minimum. The heavily-dashed continuations of the individual curves represent mathematical solutions of equation (13) which are probably unrealizable, at least in the steady-state or low-frequency operation of the tube.

These curves exhibit the instabilities and hysteresis phenomena which are characteristic of the grid-anode region, and again illustrate the necessity for a knowledge of the previous history of the operation of the tube in order to predict its future behavior.

Figure 11 is a plot of $\left(\dfrac{I_a}{I_o}\right)\cdot P_a{}^2$ vs. $P_a{}^2$ for various values of $\dfrac{V_a}{V_g}$. These curves illustrate the variation of the anode current with space current for several particular values of the ratio of anode potential to grid potential. It will be observed that if the space current is increased from zero, the anode current bears a linear relation to the space current until a maximum value, given by equation (13a), is reached. At this point a virtual cathode is formed and the anode current is abruptly reduced. Thereafter, the anode current decreases continuously with increasing space current. If the space current is now decreased, the anode current will increase until the virtual cathode disappears. At this point the anode current becomes exactly equal to the space current, the phenomenon being an abrupt one for values of $\dfrac{V_a}{V_g}\leqq 1$. For $\dfrac{V_a}{V_g}\geqq 1$ this discontinuous phenomenon does not occur.

Further decrease of space current causes the anode current to decrease linearly with space current. The portions of these curves in which the anode current decreases with increasing space current are intimately associated with the presence of a virtual cathode, and can be utilized to provide a negative-transconductance amplifier or oscillator. This matter will be elaborated upon in section *D* of this discussion.

The dotted appendages of the individual curves in this graph represent mathematical solutions of equation (19) which are probably unrealizable in the steady-state or low-frequency operation of the tube. The terminations of these dotted sections upon the linear portion of unit slope, common to all of the curves, are given by equation (13b). On occasion these values have been assumed, incorrectly, as giving the maximum anode-current density which can be obtained.[7]

Figure 7 is a plot of $\frac{V_c}{V_g}$ vs. $\frac{V_a}{V_g}$ for various values of P_a. The curves shown in this plot illustrate the variation of the minimum potential with anode potential for several values of space current. The dotted line connecting the points $\left(\frac{V_c}{V_g}=0, \frac{V_a}{V_g}=0\right)$ and $\left(\frac{V_c}{V_g}=1, \frac{V_a}{V_g}=1\right)$ passes through the points on the individual curves at which a potential minimum is suddenly formed when the anode potential is increasing. The dotted line which becomes asymptotic to the value $\frac{V_c}{V_g}=1$ passes through the points on the individual curves at which the virtual cathode is abruptly transformed into a potential minimum when the anode potential is increasing. The third dotted line, which starts at the point $\left(\frac{V_c}{V_g}=0, \frac{V_a}{V_g}=0\right)$ and passes through the point $\left(\frac{V_c}{V_g}=0.25, \frac{V_a}{V_g}=1\right)$, is a parametric line which indicates the points on the individual curves at which the potential minimum shifts abruptly, with decreasing anode potential, into a virtual cathode.

The curve which represents the case $P_a=0$ degenerates into a point located at $\left(\frac{V_c}{V_g}=1, \frac{V_a}{V_g}=1\right)$, since this is the only value of the ratio $\frac{V_a}{V_g}$ for which the electric intensity can be zero in the absence of space current. The curves which represent the case $P_a = 1$ consist of two discontinuous sections, the first being a portion of the axis of abscissas (this corresponding to the virtual cathode), and the second being the curved portion which begins on the first dotted line, which represents the potential minimum. For this case, when the anode potential is increased from negative values, a virtual cathode is first formed which presently disappears abruptly, and then for some greater value of anode potential, a potential minimum is formed. For values of $P_a \leq \frac{1}{\sqrt{2}}$, neither potential minimum nor virtual cathode is formed with increasing anode voltage until $\frac{V_a}{V_g} \geqq 0.888$. Then a potential minimum is formed.

Figure 8 is a plot of $\frac{c}{a}$ vs. $\frac{V_a}{V_g}$ for various values of P_a. These curves show the position of the virtual cathode and potential minimum for several values of space current plotted against different anode potentials. The sections of the various curves which lie to the left of the axis of ordinates reveal the location of the temperature-limited virtual cathode. The sections of the same curves which lie to the right of the axis of ordinates indicate the location of the space-charge-limited virtual cathode and potential minimum. The dashed-line portions of the curves for $P_a = 1$ and $\sqrt{2}$ are mathematical solutions of equation (18) which are probably unrealizable in the ordinary operation of the tube. Figures 7 and 8 together give the location and magnitude of the potential minimum under various operating conditions. This information is of considerable value to a proper understanding of the operation of the tube.

Figure 10 is a plot of $\frac{I_a}{I_o}$ vs. $\frac{V_a}{V_g}$ for various values of P_a. These curves show the variation of the anode current with anode potential for several particular values of space current. It will be observed that as the anode potential is increased from zero, the anode current increases from zero relatively slowly at first and then more rapidly. This rapidity of increase of anode current is more pronounced for the smaller values of space current. The initial variation of anode current with anode potential is approximately a $\frac{3}{2}$-power law, such as obtains in the case of an idealized diode. As the anode potential increases, however, the returning current (corresponding to the electrons which return toward the grid from the virtual cathode) decreases because the anode current increases. This results in a movement of the virtual cathode toward the anode, and thus causes a further increase in the anode current. The net result is similar to that which would exist if the cathode of the idealized diode moved toward the anode with increasing anode potential, i.e., the current would increase more rapidly than predicted by the $\frac{3}{2}$-power law. It will be observed further that for the curves which represent the cases $P_a = 1$ and $\sqrt{2}$, the anode current saturates abruptly with increasing anode potential. This action indicates an instability in the plate characteristic for relatively low values of space current. For values of P_a greater than 2, the saturation of anode current occurs at a finite rate, i.e., the saturation is a stable phenomenon. If the anode potential is decreased toward zero, after the saturated condition has been attained, the anode current does not vary with anode potential entirely as before. For example, in the case $P_a = 2\sqrt{2}$, the anode current saturates with increasing anode potential at the value $\frac{V_a}{V_g} = 2.24$. With decreasing anode potential, the anode current remains saturated until the value $\frac{V_a}{V_g} = 1.0$ is reached, and thereafter follows the same law of variation as occurred for increasing anode potential. This "overhang" of anode current illustrates the hysteresis phenomena which occurs in the plate characteristic.

The dashed-line portions of the curves for $P_a = 1$ and $\sqrt{2}$, which indicate a negative-resistance anode characteristic, represent mathematical solutions of equation (19) which are probably unrealizable in the steady-state or low-frequency operation of the tube. The existence of such solutions has been used, unjustifiably, to form the basis of a negative-resistance explanation of Barkhausen-Kurz oscillations.[7] Such oscillations can be explained more satisfactorily by an analysis which takes into account, at the start, the effect of the transit time of the electrons.

Before leaving the discussion of Figure 10, it should be pointed out that curves representing values of P_a less than 1 have been omitted from this plot, since the analysis indicates the physically unrealizable phenomenon of a saturation current "overhang" into the negative region of $\frac{V_a}{V_g}$. The value $P_a = \frac{1}{\sqrt{2}}$ represents the limiting case for which, with increasing anode voltage, the anode current rises gradually. For values of $P_a \leq \frac{1}{\sqrt{2}}$, the anode current saturates abruptly at $\frac{V_a}{V_g} = 0$.

Figure 6 is a plot of $\frac{\tau}{\tau_0}$ and $\frac{\tau'}{\tau_0}$ vs. $\frac{V_a}{V_g}$ for various values of P_a. These curves show the variation with anode potential of the transit time, τ, for the electrons which travel from the plane of the grid to the anode, and of the transit time, τ', for the electrons which travel from the plane of the grid to the virtual cathode. The curves illustrate the magnitude of the effect on the transit time of the electrons which can occur in the presence of space charge.

IV. Experimental Verification

To obtain experimental verification, at least of a qualitative nature, of the main features of the theoretical results, a special pentode was constructed. The tube consisted of an indirectly-heated cathode having an area of 6.3 sq cm; a control grid, the potential of which was varied to alter the space current between the screen grid and anode; and a screen grid spaced 1.5 cm from a suppressor grid located in front of, and very close to an anode having an area of 9 sq cm. The suppressor grid was connected to the anode to prevent any secondary electrons, which might have been emitted from the anode, from seriously disturbing the space-charge conditions in the region between screen grid and anode. The electrodes were made slightly concave to minimize spreading of the electron stream, and large enough in area to minimize edge effects.

Oscillograms of the anode and transfer characteristics of this tube were taken on a special cathode-ray curve tracer built by Mr. O. H. Schade, of this laboratory.* The characteristics were determined in this way because the heavy currents would have damaged the tube if the tube performance had been observed by the usual point-by-point method.

Figure 17 is an oscillogram record of the variation of anode current with anode voltage, the control-grid voltage being 150 volts and the

* This device was described by Mr. Schade before the Rochester Convention of the I.R.E. on November 20, 1935.

screen-grid voltage being 120 volts. It will be observed that the anode current increases uniformly, as the anode voltage is increased from zero, until the point marked "*c*" where saturation is reached, and thereafter changes very slowly with further increase of anode voltage. When the anode voltage is decreased, the anode current remains virtually constant until the point "*d*" is reached, at which point the anode voltage is considerably less than at the point "*c*". With further decrease of anode voltage, the anode current drops discontinuously and then decreases uniformly on the same curve as obtained with increasing anode voltage. This behavior is qualitatively similar to the theoretical curve marked $P_a = 2\sqrt{2}$ of Figure 10.

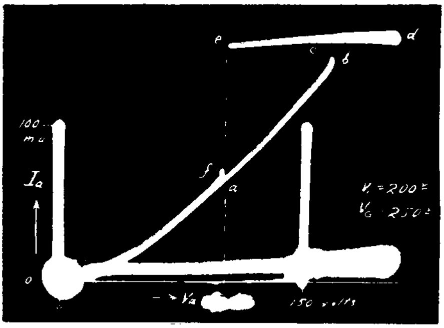

Fig. 18—Anode-characteristic oscillogram of special pentode showing the hysteresis and instabilities similar to curve marked $P_a = \sqrt{2}$ in Figure 10.

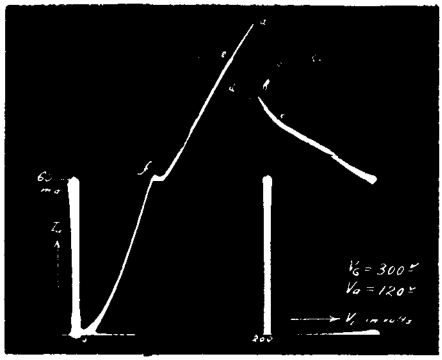

Fig. 19 — Transfer-characteristic oscillogram of special pentode showing the hysteresis and instabilities characteristic of the curve marked $\dfrac{V_a}{V_g} = 0.4$ of Figure 11.

Figure 18 is a similar oscillogram record, the control grid now being at 200 volts and the screen grid at 250 volts. This characteristic shows an abrupt increase of the anode current at the point "*b*" when the anode voltage is increasing, and an abrupt decrease of the anode current at the point "*e*" when the anode voltage is decreasing. This behavior is qualitatively similar to the theoretical curve marked $P_a = \sqrt{2}$ of Figure 10. The faint irregular traces which are present at the abrupt changes of anode current are probably mainly due to the unavoidable reactance of the tube connecting leads.

Figure 19 is an oscillogram record of the variation of anode current with control-grid voltage, to which the space current is proportional. The screen grid was maintained at 300 volts and the anode at 120 volts. This record is in qualitative agreement with the curve for $\frac{V_a}{V_g} = 0.4$ of Figure 11. It will be observed that the anode current increases uniformly, except at the point "*f*", with increasing space current until a virtual cathode is almost formed at the value corresponding to the point "*a*". Further increase of space current causes the formation of a virtual cathode between screen grid and anode, with an attendant sudden decrease of anode current, as indicated by the point "*b*". Still further increase of space current is accompanied by a uniform decrease of anode current. (The negative slope of the I_a vs. V_1 characteristic in this region represents a negative transconductance and can be utilized to form the basis of a novel type of amplifier and oscillator.) If the space current is now decreased, the anode current increases until the point "*d*" is reached, at which point an abrupt increase of anode current takes place. The point "*d*" corresponds to a lower value of space current than the point "*a*", in accordance with theoretical expectations, and marks the sudden disappearance of the virtual cathode and the formation of a potential minimum. Further decrease of space current is accompanied by a decrease of anode current, the same path now being followed as for increasing space current.

The curious kink in the early portion of the curve, indicated by the point "*f*", may be accounted for as follows: Since the control grid was operated at positive potentials in order to obtain sufficient space current for the experiment, it is to be expected that the possibility of primary and secondary emission from this grid is great. At relatively low values of control-grid voltage, corresponding to relatively low values of space current, these electrons contribute to the anode current. As the control-grid voltage is increased, the space current increases sufficiently so that the value of the potential minimum which has been formed in the region between screen grid and anode becomes less than that of the control grid. As a result the electrons emitted from the control grid are confronted by a potential barrier which they are unable to penetrate and consequently they execute excursions about the screen grid until captured. The slope of the I_a vs. V_1 curve is greater for values of V_1 corresponding to the range between zero and the point "*f*" than for the range above "*f*". This is accounted for by the explanation given above, because for values of V_1 less than those corresponding to "*f*" the electrons which are emitted from the control grid contribute to the anode current. Beyond this point these electrons do not contribute to the anode current, but instead because of their multiple excursions about the screen grid, they increase the value of space current and actually cause the anode current to increase at a lower rate with control-grid voltage than before. Approximate calculations which have been made support this explanation, but their reproduction at this point would be out of place.

V. Illustrative Applications

The theoretical results which have been presented in the foregoing treatment are applicable to a wide variety of vacuum-tube problems. For purposes of illustration, we will now discuss two such problems, both of considerable practical interest.

1—*The Type 6L6 Beam Power Tube.*—This tube is a quasi-pentode power amplifier which employs a minimum potential, deliberately formed in front of the anode by utilizing the space charge of the electrons, to minimize the passage of secondary electrons from anode to screen grid. The existence, under certain conditions, of a potential minimum or virtual cathode in the region between screen grid and anode has been known for some time,[6,7,8] and the applicability of the phenomenon to the minimization of the (undesired) passage of secondary electrons from the anode to the grid has also been recognized for some time.[1,5,6,7] Recently, however, the subject has received considerable attention,[2,3,4,10,11] and it appears to us that a number of misconceptions which have arisen concerning the theory of operation of such a tube can be cleared up by means of the foregoing theory with certain modifications, of a quantitative nature, introduced by the factors which we explicitly neglected at the start.

The objectives which were sought in the development of this tube were improvements over a-f power output tubes then available with regard to power output, efficiency, power sensitivity, and distortion. These objectives could best be attained by a high-transconductance tube having an anode characteristic as close as possible to that of an ideal pentode.[4] Although the usual pentode anode characteristic exhibits no trace of the secondary-emission phenomena typical of the conventional tetrode, it is invariably marked by a relatively slow initial rise of anode current with anode voltage and by a rather gradual saturation of the anode current. These undesirable features can be charged mainly to the presence of the suppressor grid, and therefore it was decided to dispense with this grid and replace it, at least as far as its effect on preventing the flow of secondary electrons from the anode to the screen grid was concerned, by a potential minimum. The ultimate result of this development was the 6L6, the anode characteristic of which is reproduced in Figure 20.

In general, the main features of the curves shown in this figure agree qualitatively with those of the idealized curves shown in Figure

10. For example, the curves corresponding to the largest values of space current, i.e., highest values of control-grid voltage, tend to saturate at higher values of anode voltage and also exhibit the abrupt type of saturation predicted by the theory for values of P_a less than 2. The smooth type of saturation shown in Figure 10 for larger values of P_a, which was verified experimentally in Figure 17, is also evident in Figure 20. However, there are several discrepancies between the theoretical results for the idealized parallel-plane tube and the curves of Figure 20. One of these lies in the fact that none of the curves saturate immediately, whereas the theory indicates that for P_a less than $\frac{1}{\sqrt{2}}$ the anode current should rise to saturation value for the smallest positive anode potential. This lack of agreement can be attributed in small part to the Maxwellian distribution of velocities of electron emission, and in much greater part to the angular deflection of the electrons which occurs because of the wire grid structure.[9] This effect is most pronounced at the very lowest values of space current: at the higher space currents, where a virtual cathode is formed, this effect is entirely overshadowed by the behavior predicted by the theory. Another discrepancy is to be observed in the curve for $E_{c1} = -30$ volts, which exhibits negative anode conductance for anode voltages between 25 and 75 volts. This can doubtless be explained by the existence of a potential minimum, the value of which is too high to provide a suitable retarding field for the proper suppression of secondary electrons which are emitted from the anode. A further discrepancy is to be observed in the fact that all of the curves have a finite slope in the saturation region. This is probably due in main part, to the penetration of the anode field through the screen grid, and perhaps also to the slight contribution to the anode current of primary and secondary electrons from the screen grid. A more serious discrepancy, from an academic point of view, is the relatively narrow area of the hysteresis loops which are to be observed in the curves for $E_{c1} = +10$ volts and $E_{c1} = +15$ volts. This may be due to the edge effects introduced by the zero potential "beam-forming" plates.

It may be well to point out here that the behavior of the initial portions of all of the theoretical curves of Figure 10 and also the corresponding portions of the experimental curves of Figures 17, 18, and 20, is at variance with that deduced by J. H. O. Harries,[3] shown in his Figure 9 as curve *G A D E*. Harries invokes the electron-velocity spread at the grid to explain the actual curvature of the rising portion of the anode characteristic, but it appears from the theoretical results that the curvature can be present even in the absence of a well-defined distribution of velocities of the electrons which pass through the grid. Nor is the suggestion of S. Rodda[11] that the work of Below and Schulze indicates that this curvature is due primarily to the angular deflection of electrons in the neighborhood of the screen grid valid, except (as we have mentioned above) for very low values of space current. As Harries pointed out,[11] this is because Below explicitly neglected the possibility of the formation of a virtual cathode.[9] The suggestion of Bell[10] that the "detailed mechanism" of the anode characteristic of tubes, ostensibly utilizing a potential minimum to mini-

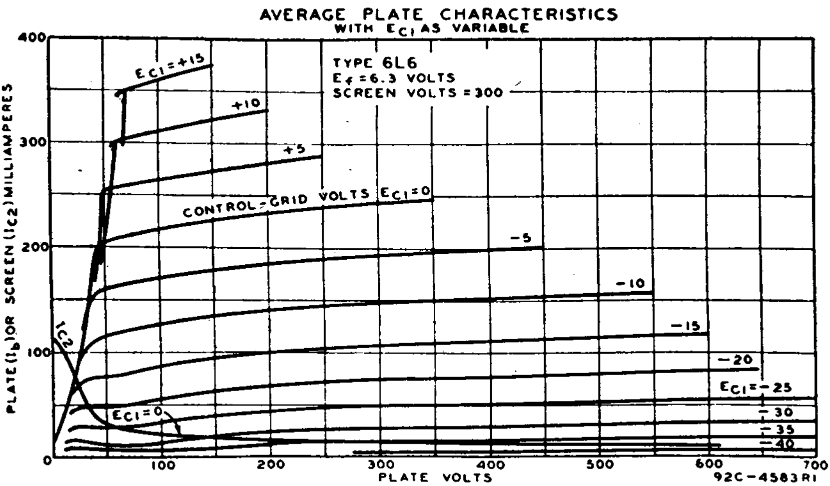

Fig. 20—Anode characteristic of RCA-6L6.

mize the passage of secondary electrons from the anode to the screen grid, may be due largely to the inherently steep initial rise of the tetrode plus the somewhat reduced secondary emission of electrons from the anode is interesting, but hardly satisfying as a complete theory. Finally, in passing, we wish to call attention to the possibilities of obtaining misleading results when using long glass tubes such as that of the "sliding-anode" tube employed by Harries.[2,3] This has been pointed out by I. Langmuir[12], in a discussion of Lilienfeld's work.

2—*Negative-Transconductance Amplifiers and Oscillators.*—To illustrate the application of the negative-transconductance features of Figure 11, in which the anode current decreases with increasing space current[6], a special pentode capable of operation with negative control voltage was constructed. The relative spacings of the electrodes were K-G_1: G_1-G_2: G_2-G_3: G_3-$A = 0.6$: 0.6: 1.0: 8. The first grid was used as a negative-control electrode, the second grid as a positive-accelerator electrode, the third grid as a positive electrode for controlling the velocity of the electrons entering the G_3-A region where a virtual cathode was formed, and the anode was used as the output electrode. The tube could be used as an amplifier and as an oscillator having several unique properties.

For an oscillator application, a typical circuit is shown in Figure 21. The control grid is coupled to the plate circuit by means of a large blocking condenser, C_{AG1}, the negative bias being supplied to the grid through a high resistance R_g. The grid excitation is adjusted by sliding

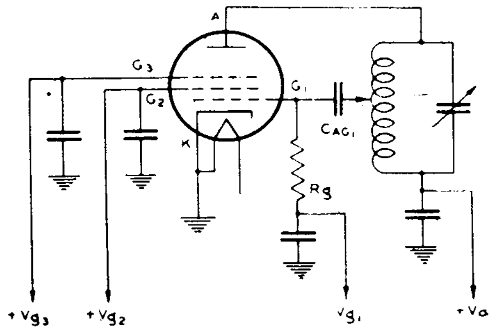

Fig. 21—Schematic circuit of negative-transconductance oscillator.

the tap along the plate inductance. In this circuit the grid voltage is essentially in phase with the anode voltage, so that the tube oscillates only when the transconductance is negative. The condition for oscillation requires that the negative transconductance be greater than the sum of the internal anode conductance and the external circuit conductance, which includes the anode circuit proper and the reflected conductance of the grid resistor. Typical operating conditions were: $g_m = -2500$ μmhos, $g_p = 500$ μmhos, $g_c = 200$ μmhos, $V_a = 210$ volts, $I_a = 55$ ma, $V_3 = 200$ volts, $I_3 = 25$ ma, $V_2 = 200$ volts, $I_2 = 25$ ma, $V_1 = -12$ volts, $I_1 = -0.2$ milliamperes, $\lambda = 30$ meters, $V_{rf} = 15$ volts.

In order to obtain a larger plate swing without destroying the virtual cathode, and also to obtain a larger effective negative conductance by reducing the anode conductance, an additional screen grid may be placed in front of the anode. In this way the space-charge conditions in the G_3-G_4 region can be adjusted independently of the output circuit impedance by control of the potential of the screen grids G_3 and G_4. A tube of this type with relative electrode spacings of 0.6:0.6:1.0:8.0:2.0 showed an anode conductance of only 40 μmhos in the negative-transconductance region.

VI. CONCLUSIONS

The effects of space charge in the region between grid and anode are of fundamental importance in determining the behavior of vacuum tubes, particularly when the anode is preceded by a grid operated at a positive potential. The effects of space charge between the grid and anode of a parallel-plane vacuum tube have been determined in this study from the results of a simple analysis. The assumptions which underlie this analysis necessarily introduce modifications of the theory, but as the experimental verification indicates, these do not invalidate the main results, and their effects can be taken into account in a qualitative way.

The principal effects of the space charge in the grid-anode region are: (a) to introduce departures from the linear potential-distribution characteristic of the electrostatic case; (b) to set an upper limit to the current which can be collected at the anode, the limiting current density being

$$(I_a)_{\max.} = 2.33 \times 10^{-6} \times \frac{(V_g^{1/2} + V_a^{1/2})^3}{a^2} \text{ amp per cm}^2$$

where V_g and V_a are the effective grid and anode voltages, respectively, and a is the distance between grid and anode; (c) to introduce instabilities and hysteresis phenomena in the behavior of the tube; and (d) to increase the electron-transit time in this region.

For the four modes of potential distribution which have been treated, expressions have been derived for the distribution of potential and electric intensity throughout the grid-anode region; the time of flight of electrons from grid to anode, and (when a zero-potential plane is formed) also from grid to this plane of zero potential; and the location and magnitude of the minimum potential. A formula has also been derived for the dependence of the anode current on the space current, grid-anode distance, grid voltage and anode voltage. These expressions have been plotted, using dimensionless parameters, in Figures 5-11.

The experimental verification of these theoretical results indicate that the theory can be employed in a qualitative way at least, to predict and explain the behavior of a large variety of vacuum tubes. This has been done for the 6L6 "beam power" tube, and for amplifier and oscillator tubes which make use of the decrease of anode current with increasing space current which the theory predicts.

BIBLIOGRAPHY

[1] G. Holst and B. D. H. Tellegen, U. S. Patent 1,945,040.

[2] J. H. O. Harries, U. S. Patents 2,045,525; 2,045,526; 2,045,527.

[3] J. H. O. Harries, "The Anode to Accelerating Electrode Space in Thermionic Valves", *Wireless Engineer*, 13, pp. 190-199, April, 1936.

[4] O. H. Schade, "Beam Power Tubes", to be published in *Proc. I.R.E.*

[5] E. W. B. Gill, "Distribution of Electric Forces in Spaces Traversed by Electrons", *Phil. Mag.*, 10, pp. 134-139, July, 1930.

[6] E. W. B. Gill, "A Space Charge Effect", *Phil. Mag.*, 49, pp. 993-1005, May, 1925.

[7] L. Tonks, "Space Charge as a Cause of Negative Resistance in a Triode and its Bearing on Short Wave Generation", *Phys. Rev.*, 30, pp. 501-511, October, 1927.

[8] D. C. Prince, "Four-Element Tube Characteristics as Affecting Efficiency", *Proc. I.R.E.*, 7, pp. 805-821, June, 1928.

[9] F. Below, "Zur Theorie der Raumladegitterröhren", *Zeitschrift für Fernmeldetechnik*, 8, pp. 113-143.

[10] D. A. Bell, "Secondary Emission in Valves", *Wireless Engineer*, 13, pp. 311-313, June, 1936.

[11] Discussion by S. Rodda and J. H. O. Harries, *Wireless Engineer*, 13, pp. 315-316, June, 1936.

[12] I. Langmuir, "Fundamental Phenomena in Electron Tubes Having Tungsten Cathodes", *G. E. Review*, 23, pp. 503-513, June, 1920, and pp. 589-596, July, 1920.

[13] G. Plato, W. Kleen, and H. Rothe, "Die Raumladegleichung für Elektronen mit Anfangsgeschwindigkeit", *Zeitschrift für Physik*, 101, No. 5, pp. 509-520.

[14] H. C. Calpine, "Conditions in the Anode Screen Space of Thermionic Valves", *Wireless Engineer*, 13, No. 156, pp. 473-474, September, 1936.

[15] W. Lukoshkow, "Electron Space Charge and the Theory of the Triode", *Technical Physics of the U.S.S.R.*, 3, No. 5, pp. 408-432.

[16] W. Kleen and H. Rothe, "Die Raumladegleichung für Elektronen mit Anfangsgeschwindigkeit. II. Teil", *Zeitschrift für Physik*, 104, Nos. 11 and 12, pp. 711-723.

THE SECONDARY EMISSION PHOTOTUBE*†

By

HARLEY IAMS AND BERNARD SALZBERG

RCA Radiotron Company, Inc.,
Harrison, N. J.

Summary

A type of phototube is described in which the secondary electron emission from an auxiliary cathode (bombarded by the photoelectrons) is utilized to obtain amplification of the primary photocurrent. Phenomena of secondary emission, particularly as applied to the vacuum phototube, are discussed. The operating performance of a typical developmental embodiment is illustrated, and it is shown that its static sensitivity is comparable with that of a corresponding gas phototube; that as regards fidelity, it retains the freedom of the vacuum phototube from the considerable loss in response at the higher audio frequencies which is inherent in the gas phototube; and that on the basis of noise produced by the microscopic fluctuations of its current, it is somewhat superior to the comparable gas tube, and approximately equivalent to a vacuum phototube having the same emission and followed by an amplifier having an over-all gain equivalent to the secondary emission amplification. Life tests indicate that the stability of these tubes is entirely comparable with that of the vacuum phototube, both as regards secondary emitter and photocathode behavior. In addition to the usual applications, various incidental uses of these phototubes are suggested.

(10 pages; 6 figures)

* Decimal Classification: 535.38.
† *Proc. I. R. E.*, January, 1935.

DEVELOPMENT OF CATHODE-RAY TUBES FOR OSCILLOGRAPHIC PURPOSES*†

By

R. T. ORTH, P. A. RICHARDS, AND L. B. HEADRICK

RCA Manufacturing Company, Inc.,
Harrison, N. J.

Summary

Some typical electrical characteristics of a cathode-ray-tube electron gun are shown and the function of the various gun elements described. Light output, luminescent screen efficiency, space distribution of radiation, as well as decay and spectral distribution characteristics of willemite screens, are shown and the relations of the various factors discussed. The

* Decimal Classification: R388.
† *Proc. I. R. E.*, November, 1935.

starting and dynamic characteristics of the tube are discussed. Magnetic and electrostatic deflection are discussed with regard to sensitivity, frequency range of application, and impedance of deflection plates. In conclusion, a few general precautions in the operating of cathode-ray tubes are given.

(16 pages; 14 figures)

THE ELECTRON-IMAGE TUBE, A MEANS FOR MAKING INFRARED IMAGES VISIBLE*†

BY

G. A. MORTON

RCA Manufacturing Company, Inc.,
Camden, N. J.

Summary

The construction and theory of operation are described of the electron-image tube, which consists of a photosensitive cathode, a fluorescent screen, and an electron-optical system which focuses the electron "image" from the cathode upon the viewing screen. Due to the wide spectral response of the cathode, the tube can be used to convert infrared, visible, or ultraviolet images into visible images upon the fluorescent screen.

The electron optical system is discussed and its analogy to the conventional optical system is shown. To reproduce an image faithfully the electron "lens" system must be corrected for various aberrations. Methods of making these corrections are indicated, and applications of the device are described.

(10 pages; 12 figures)

---

* Decimal Classification: R339.
† *Jour. Soc. Mot. Pic. Eng.*, September, 1936.

THEORETICAL LIMITATIONS OF CATHODE-RAY TUBES*†

BY

DAVID B. LANGMUIR

RCA Manufacturing Company, Inc.,
Harrison, N. J.

Summary

The current density in a focused beam of cathode rays is shown to have an upper limit defined by $I = I_o\,(Ee/kT + I)\sin^2\phi$, *where I is the maximum current density obtainable in the focused spot,* I_o *is the current density at*

---

* Decimal Classification: R388.
† *Proc. I. R. E.*, August, 1937.

the cathode, E is the voltage at the focus relative to the cathode, T is the absolute temperature of the cathode, e is the electronic charge, k is Boltzmann's constant, and ø is the half angle subtended by the cone of electrons which converge on the focused spot. The cases in which the focused spot is an image of the cathode, and in which it is a pupil, or "crossover", are considered separately, and the above formula is shown to apply to both. The necessary initial assumptions are (1) that electrons leave the cathode with a Maxwellian distribution of velocities, and (2) that the focusing system is free from aberrations and obeys the law of sines. Aberrations may reduce the current density, but nothing can raise it above the value defined.

In the Appendix the focusing properties of a uniform accelerating field are calculated. The virtual image of a plane cathode formed by such a field suffers from spherical aberration. The diameter of the circle of least confusion formed by electrons from a single point is approximately equal to the distance the electrons can travel against the field by virtue of their initial velocities. This aberration may be the factor which limits the resolving power of some kinds of electron microscopes.

(15 pages; 6 figures; 1 table; 1 appendix)

VACUUM-TUBE ENGINEERING FOR MOTION PICTURES*†

BY

L. C. HOLLANDS AND A. M. GLOVER

RCA Manufacturing Company, Inc.,
Harrison, N. J.

Summary

Manufacturing and developmental technics of vacuum tubes are described with particular reference to their use in motion picture equipment. A brief discussion of how application requirements affect the choice of materials, structural design, and electrical characteristics of phototubes and amplifiers of both power and voltage types is included. How tubes are designed to meet specific needs is illustrated by reference to recent tube developments. Work on producing tubes having low-hum, low-microphonics, and low-noise characteristics is described as of special interest to the motion picture engineer. The paper closes with recommendations as to how to use tubes to best advantage.

(20 pages; 6 figures; 1 table)

---

* Decimal Classification: R331.

† *Jour. Soc. Mot. Pic. Eng.*, January, 1938.

THE ELECTROSTATIC ELECTRON MULTIPLIER*†

By

V. K. Zworykin and J. A. Rajchman

RCA Manufacturing Company, Inc.,
Camden, N. J.

Summary

This paper describes the design of improved types of electron multipliers in which the electrodes are so shaped and positioned as to provide accurate electrostatic focusing and to minimize space-charge limitations. The first section of the paper describes the general methods available for determining electron trajectories in electrostatic fields. The second section describes the details of design of several experimental self-focusing electron-multiplier tubes.

(9 pages; 13 figures)

* Decimal Classification: 535.38.
† *Proc. I. R. E.*, September, 1939.

AN ELECTRICALLY-FOCUSED MULTIPLIER PHOTOTUBE*†

By

J. A. Rajchman and R. L. Snyder

RCA Manufacturing Company, Inc.,
Camden, N. J.

Summary

A compact secondary-emission multiplier structure using curved targets or "dynodes" is described which develops a maximum current gain of over a million and a luminous sensitivity of over ten amperes per lumen, with signal-to-noise ratio considerably better than conventional phototubes. This is a practical tube useful in sound-track reproduction, light-operated relays and the like.

(6 pages; 10 figures)

* Decimal Classification: 535.38.
† *Electronics*, December, 1940.

THE BEHAVIOR OF ELECTROSTATIC ELECTRON MULTIPLIERS AS A FUNCTION OF FREQUENCY*†

BY

L. MALTER

RCA Manufacturing Company, Inc.,
Harrison, N. J.

Summary

This paper consists of a theoretical and experimental study of the frequency variation of transconductance of electrostatic electron multipliers. It is shown that the decrease of transconductance with frequency up to 500 megacycles, the highest frequency studied, can be ascribed to a spread in transit angle resulting from the emission velocities of secondary electrons and the varying paths of electrons through the stages of the multiplier. The spread in transit angle may be represented by an equivalent angle that is linearly related to the total transit angle unless the latter is quite large.

For a given scale and with multipliers of the form herein studied an upper limit can be set upon the frequency at which multipliers may be profitably employed. A brief analysis of the effect of leads within the tube is included.

An upper limit of 2×10^{-9} second was set upon the time taken for the phenomenon of secondary emission to occur.

(12 pages; 16 figures)

* Decimal Classification: R139.
† *Proc. I. R. E.*, November, 1941.

THE ORBITAL-BEAM SECONDARY-ELECTRON MULTIPLIER FOR ULTRA-HIGH-FREQUENCY AMPLIFICATION*†

BY

H. M. WAGNER AND W. R. FERRIS

RCA Manufacturing Company, Inc.,
Harrison, N. J.

Summary

A developmental ultra-high-frequency receiving tube in which secondary-emission electron multiplication has been applied to a conventional high-transconductance tube structure to increase the transconductance without a corresponding increase in interelectrode capacitances and input conductance is described. It was designed primarily for wide-band amplification at a frequency of approximately 500 megacycles, as required for television radio relay systems. The tube uses conventional circuits and requires a power supply of less than 400 volts. The structure adopted permits the most efficient use of the secondary-emission multiplier consistent with satisfactory life and good high-frequency performance. The *structure also permits the use of beam deflection to provide a convenient gain-control method, free from the input capacitance and conductance variations attending the usual grid-bias control. A novel method of measuring interstage gain, involving the use of transmission lines, is discussed.*

(6 pages; 7 figures)

---

* Decimal Classification: R330×R262.4.
† *Proc. I. R. E.*, November, 1941.

VOLTAGE-CONTROLLED ELECTRON MULTIPLIERS*†

By

B. J. THOMPSON

RCA Manufacturing Company, Inc.,
Harrison, N. J.

Summary

The application of secondary-emission multiplication to conventional grid-controlled amplifier tubes is discussed from the viewpoints of practical voltage gain per stage of amplification, signal-to-noise ratio, and ultra-high-frequency applications. It is pointed out that the gain per stage is limited by the practical output current and the quotient of transconductance by current (N) and that electron multiplication increases the gain only as it permits the attaining of higher values of N. If the output current is assumed to be 20 milliamperes and N is taken as 1 milliampere per volt per milliampere, the output transconductance would be 20 milliamperes per volt—little, if any, better than could be achieved without multiplication. If N is assumed to be 11.6 (the theoretical maximum for conventional grid control with a cathode temperature of 1000 degrees Kelvin) the output transconductance could be greater than 200 milliamperes per volt per milliampere. Higher values of N might be attained by some other method of control. In this case, the ultimate limit of transconductance would be set by the difficulty in stabilizing the effective control-electrode bias voltage.

The signal-to-noise ratio of the voltage-controlled multiplier is determined chiefly by the input system of the multiplier, the multiplier being a relatively noiseless amplifier following this input system. The noise level of the input system is determined by the input transconductance. If the use of a multiplier leads to reduced input transconductance, the noise level will be increased as compared with conventional tubes.

The principal advantages to be attained from the use of the multiplier are found in ultra-high-frequency applications where input loading and input capacitance are serious. The reduction in transconductance of the input system for a given over-all gain which is permissible leads to a corresponding reduction of input conductance (whether arising from electron-transit-time or lead effects) and input capacitance.

(5 pages; 6 figures; 1 appendix)

---

* Decimal Classification: R132.
† *Proc. I. R. E.*, November, 1941.

APPENDIX I

ELECTRON TUBES

A Bibliography of Technical Papers by RCA Authors (1919-1941)

This listing includes some 400 technical papers on electron tubes, thermionics, and related subjects, selected from those written by RCA Authors and published during the period 1919-1941.

Papers are listed chronologically except in cases of multiple publication. Papers which have appeared in more than one journal are listed once, with additional publication data appended.

Abbreviations used in listing the various journals are given on the following pages.

Any requests for copies of papers listed herein should be addressed to the publication to which credited. However, *RCA Licensee Bulletins* are not published and are issued only as a service to licensees of the Radio Corporation of America.

ABBREVIATIONS

(Note—Titles of periodicals not listed below, as well as book titles, are not abbreviated.)

Amer. Jour. Phys.	AMERICAN JOURNAL OF PHYSICS
Amer. Rev.	AMERICAN REVIEW
An. Amer. Acad. Polit. Soc. Sci.	ANNALS OF THE AMERICAN ACADEMY OF POLITICAL AND SOCIAL SCIENCES
Broad. Eng. Jour.	BROADCAST ENGINEERS JOURNAL (A.T.E. JOURNAL)
Comm. and Broad. Eng.	COMMUNICATION AND BROADCASTING ENGINEERING
Elec. Eng.	ELECTRICAL ENGINEERING (TRANSACTIONS A.I.E.E.)
Electronic Ind.	ELECTRONIC INDUSTRIES
FM and Tele.	FM AND TELEVISION
G.E. Review	GENERAL ELECTRIC REVIEW
Ind. Eng. Chem.	INDUSTRIAL AND ENGINEERING CHEMISTRY
Ind. Standard.	INDUSTRIAL STANDARDIZATION (AMERICAN STANDARDS ASSOCIATION JOURNAL)
Inter. Project	INTERNATIONAL PROJECTIONIST
Jour. Acous. Soc. Amer.	JOURNAL OF THE ACOUSTICAL SOCIETY OF AMERICA
Jour. A.I.E.E.	JOURNAL OF THE AMERICAN INSTITUTE OF ELECTRICAL ENGINEERS
Jour. Appl. Phys.	JOURNAL OF APPLIED PHYSICS
Jour. Amer. Ceramic Soc.	JOURNAL OF THE AMERICAN CERAMIC SOCIETY
Jour. Bacteriology	JOURNAL OF BACTERIOLOGY
Jour. British Inst. Cine.	JOURNAL OF THE BRITISH INSTITUTE OF CINEMATICS
Jour. Chem. Phys.	JOURNAL OF CHEMICAL PHYSICS
Jour. Eng. Educ.	JOURNAL OF ENGINEERING EDUCATION
Jour. Frank. Inst.	JOURNAL OF THE FRANKLIN INSTITUTE
Jour. Opt. Soc. Amer.	JOURNAL OF THE OPTICAL SOCIETY OF AMERICA
Jour. Sci. Inst. (Brit.)	JOURNAL OF SCIENTIFIC INSTRUMENTS (BRITISH)
Jour. Soc. Mot. Pic. Eng.	JOURNAL OF THE SOCIETY OF MOTION PICTURE ENGINEERS
Jour. Tele. Soc. (Brit.)	JOURNAL OF THE TELEVISION SOCIETY (BRITISH)
Phys. Rev.	PHYSICAL REVIEW
Proc. Amer. Phil. Soc.	PROCEEDINGS OF THE AMERICAN PHILOSOPHICAL SOCIETY
Proc. I.R.E.	PROCEEDINGS OF THE INSTITUTE OF RADIO ENGINEERS
Proc. Nat. Elec. Conf.	PROCEEDINGS OF THE NATIONAL ELECTRONICS CONFERENCE

ABBREVIATIONS (Continued)

Proc. Rad. Club Amer.	PROCEEDINGS OF THE RADIO CLUB OF AMERICA
Project. Jour. (Brit.)	PROJECTIONISTS JOURNAL (BRITISH)
Product Eng.	PRODUCT ENGINEERING
Project. Eng.	PROJECTION ENGINEERING
QST	QST (A.R.R.L.)
Radio and Tele.	RADIO AND TELEVISION
Radio Eng.	RADIO ENGINEERING
Radio Tech. Digest	RADIO TECHNICAL DIGEST
RCA Rad. Serv. News	RCA RADIO SERVICE NEWS
Rev. Mod. Phys.	REVIEWS OF MODERN PHYSICS
Rev. Sci. Instr.	REVIEW OF SCIENTIC INSTRUMENTS
RMA Eng.	RMA ENGINEER
Sci. Monthly	SCIENTIFIC MONTHLY
Sci. News Ltr.	SCIENCE NEWS LETTER
Short Wave and Tele.	SHORT WAVE AND TELEVISION
TBA Annual	ANNUAL OF THE TELEVISION BROADCASTERS ASSOCIATION
Teleg. & Teleph. Age	TELEGRAPH AND TELEPHONE AGE
Tele. News	TELEVISION NEWS
The T & R Bulletin (Brit.)	BULLETIN OF THE RADIO SOCIETY OF GREAT BRITAIN
Trans. Amer. Soc. Mech. Eng.	TRANSACTIONS OF THE AMERICAN SOCIETY OF MECHANICAL ENGINEERS
Trans. Electrochem. Soc.	TRANSACTIONS OF THE ELECTROCHEMICAL SOCIETY

ELECTRON TUBE BIBLIOGRAPHY

Year

"An Oscillation Source for Radio Receiver Investigations", J. Weinberger, *Proc. I.R.E.* (December) 1919

"Note on the Input Impedance of Vacuum Tubes at Radio Frequency", J. Weinberger, *Proc. I.R.E.* (August) 1920

"The Possibility of Pulling Electrons from Metals by Powerful Electric Fields", B. E. Shackelford, *Phys. Rev.* 15 1920

"How to Choose and Use Dry Cell Tubes for Portable Vacation Sets", J. O. Smith, *N. Y. Eve. World* (June 23) 1923

"Practical Master Oscillator Sets", E. A. Laport, *QST* (June) 1924

"Design of Non-Distorting Power Amplifiers", E. W. Kellogg, *Jour. A.I.E.E.* (May) 1925

Additional matter in contributed discussion (June) 1925

"Frequency Multiplication Principles and Practical Application of Ferro Magnetic Methods", N. E. Lindenblad and W. W. Brown, *Jour. A.I.E.E.* 1925

"A Method for Generating and Measuring Very Weak Radio-Frequency Currents", W. van B. Roberts, *Jour. Frank. Inst.* (March) 1926

"Notes on the Testing of Audio Frequency Amplifiers", E. T. Dickey, *Proc. I.R.E.* (August) 1927

"Note on Detection by Grid Condenser and Leak", W. van B. Roberts, *Proc. I.R.E.* (September) 1927

"A Radio-Frequency Oscillator for Receiver Investigations", G. Rodwin and T. A. Smith, *Proc. I.R.E.* (February) 1928

"The Three-Electrode Vacuum Tube as Applied to the Talking Motion Picture", E. W. Kellogg, *Jour. Soc. Mot. Pic. Eng.* (September) 1928

"Vacuum Tube Production Tests", A. F. Van Dyck and F. H. Engel, *Proc. I.R.E.* (November) 1928

"The Screen Grid Tube", A. F. Van Dyck, *N. Y. Times* (May) 1929

"Calculating Detector Output", J. M. Stinchfield, *Radio Broadcast* (August) 1929

"Grid-Leak Versus Bias Detection", J. M. Stinchfield, *Radio Broadcast* (October) 1929

"Television with Cathode-Ray Tube for Receiver", V. K. Zworykin, *Radio Eng.* (December) 1929

"Novel Electrical Controls Developed in Making Radio Tubes", B. E. Shackelford, *Jour. Chem. and Met. Eng.* 36 1929

"Notes on a Method for Measuring the Microphonic Sensitivity of Tubes", F. H. Engel, *RCA Licensee Bulletin LB-102* (May 10) 1930

"A Note on the Mathematical Theory of the Multielectrode Tube", P. Caporale, *Proc. I.R.E.* (September) 1930

"The RCA Photophone System of Sound Recording and Reproduction for Sound Motion Pictures", A. N. Goldsmith and M. C. Batsel, *Proc. I.R.E.* (October) 1930

"Specification for Vacuum Tube Test Equipment Manufactured by RCA Victor", F. H. Engel, *RCA Licensee Bulletin LB-109* (November 5) 1930

"Hot-Cathode Grid-Controlled Arc Tubes", F. H. Engel, *RCA Licensee Bulletin LB-112* (December 31) 1930

"Notes on a Method of Measuring Plate Resistance of Vacuum Tubes", E. B. Boise and F. H. Engel, *RCA Licensee Bulletin LB-114* (January 14) 1931

"Notes on Super-Heterodyne Design", D. Grimes, *RCA Licensee Bulletin LB-115* (January 26) 1931

"Circuit Considerations of the Screen Grid Radiotron RCA 235", D. Grimes and W. S. Barden, *RCA Licensee Bulletin LB-120* (March 2) 1931

"Notes on a Method of Measuring Plate Resistance and Mutual Conductance of Vacuum Tubes", D. Grimes and E. B. Boise, *RCA Licensee Bulletin LB-128* (June 17) 1931

Year

"Maximum Amplification in Capacity-Coupled Circuits", W. van B. Roberts, *Electronics* (July) 1931
"High Audio Power from Relatively Small Tubes", L. E. Barton, *Proc. I.R.E.* (July) 1931
"What Happens Within the Bulb of a Radio Tube?", L. G. Lessig, *Projection Eng.* (August) 1931
"Some Thermionic Properties of Barium Films Adsorbed on Tungsten", H. Nelson, *Physics* (August) 1931
"Composite First Detector-Oscillator Considerations", D. Grimes and W. S. Barden, *RCA Licensee Bulletin LB-132* (September 14) ... 1931
"Notes on the '47 Power Pentode", W. S. Barden, D. Grimes and E. B. Boise, *RCA Licensee Bulletin LB-125* (September 21) 1931
"Radio Tube Yardsticks", L. G. Lessig, *Radio Eng.* (October) 1931
"A Reversed Current Feed-Back Oscillator", W. van B. Roberts, *QST* (February) 1932
"Gm and Rp Test Circuit", E. B. Boise, *RCA Licensee Bulletin LB-146* (March 9) 1932
"Class B Amplification in Radio Receivers", W. S. Barden and C. Travis, *RCA Licensee Bulletin LB-153* (April 29) 1932
"Application of Class B Audio Amplifiers to A-C Operated Receivers", L. E. Barton, *Proc. I.R.E.* (July) 1932
"The New 57 as a High-Gain Amplifier", L. C. Waller, *QST* (July) .. 1932
"Recent Trends in Receiving Tube Design", J. C. Warner, E. W. Ritter and D. F. Schmit, *Proc. I.R.E.* (August) 1932
"Notes on Push-Pull Circuit Considerations", C. Travis, *RCA Licensee Bulletin LB-163* (August 18) 1932
"New Forms of Short Wave Tubes", I. E. Mouromtseff, G. R. Kilgore and H. V. Noble, *Electronics* (September) 1932
"A Theory of Diode Detection", C. Travis, *RCA Licensee Bulletin LB-167* (September 15) 1932
"Notes on Class A Prime Considerations", W. S. Barden, *RCA Licensee Bulletin LB-178* (October 21) 1932
"Magnetostatic Oscillators for Generation of Ultra Short Waves", G. R. Kilgore, *Proc. I.R.E.* (November) 1932
"Some General Principles of Frequency Conversion in Superheterodyne Receivers", D. Grimes and W. S. Barden, *RCA Licensee Bulletin LB-187* (November 11) 1932
"Diode Triode Delayed AVC", C. Travis, *RCA Licensee Bulletin LB-179* (November 14) 1932
"Triple-Grid Power Amplifier Tubes", E. W. Herold, *Radio Eng.* (December) 1932
"Use of The 77 as a Biased Detector With 100 Volts Plate Supply", *RCA Tube Dept. Applic. Note No. 1* (March 10) 1933
"Use of The 57 as a Biased-Detector Resistance-Coupled to a 2A5", *RCA Tube Dept. Applic. Note No. 2* (March 17) 1933
"Use and Operation of the 2A7 and 6A7 as Pentagrid Converters", *RCA Tube Dept. Applic. Note No. 3* (March 29) 1933
"Graphical Determination of Performance of Push-Pull Audio Amplifiers", B. J. Thompson, *Proc. I.R.E.* (April) 1933
"The 2B7, 6B7, 55, 75 and 85 as Resistance Coupled Audio-Frequency Amplifiers", *RCA Tube Dept. Applic. Note No. 4* (April 5) 1933
"The Application of the Type 79 Tube", *RCA Tube Dept. Applic. Note No. 5* (April 12) 1933
"Higher Voltage Ratings for The 36, 37, 38, 39-44, and 89", *RCA Tube Dept. Applic. Note No. 6* (April 12) 1933
"Bulletin on Pentagrid Converter", C. Travis, *RCA Licensee Bulletin LB-226* (April 12) 1933
"250-Volt Rating for the 79", *RCA Tube Dept. Applic. Note No. 7* (April 19) 1933
"The 2A6 as a Resistance-Coupled Audio-Frequency Amplifier", *RCA Tube Dept. Applic. Note No. 8* (April 26) 1933

Year

"Recent Advances in Tube Design", *RCA Tube Dept. Applic. Note No. 9* (April 26) 1933
"Reflex Circuits in Superheterodyne Receivers", J. Yolles, *RCA Licensee Bulletin LB-232* (April 28) 1933
"Notes on the 2A7 and 6A7 Converter Tubes", C. Travis, *RCA Licensee Bulletin LB-233* (April 29) 1933
"On Electron Optics", V. K. Zworykin, *Jour. Frank. Inst.* (May) ... 1933
"Effect of Diode Detection on I-F Driver Stage Design", W. S. Barden, *RCA Licensee Bulletin LB-230* (May 2) 1933
"The Use and Operation of the 25Z5", *RCA Tube Dept. Applic. Note No. 11* (May 10) 1933
"Half-Wave Operation of the 25Z5 with Separate Load Circuits for Each Rectifier Unit", *RCA Tube Dept. Applic. Note No. 12* (May 17) 1933
"Recommended Operating Conditions for the 38, 41, 42, 43, and 89", *RCA Tube Dept. Applic. Note No. 13* (May 24) 1933
"Operating Conditions for the 53 Tube", *RCA Tube Dept. Applic. Note No. 14* (May 31) 1933
"Reflex Circuit Considerations", O. H. Schade and J. M. Stinchfield, *Electronics* (June) 1933
"The Operation of the Type 48 Tube as a Triode", *RCA Tube Dept. Applic. Note No. 15* (June 7) 1933
"Further Notes on Reflex Considerations", D. Grimes and W. S. Barden, *RCA Licensee Bulletin LB-246* (June 23) 1933
"Operation of the 2B7, or 6B7, as a Reflex Amplifier", *RCA Tube Dept. Applic. Note No. 16* (July 7) 1933
"Special Applications of the Type 53 Tube", *RCA Tube Dept. Applic. Note No. 17* (July 13) 1933
"Operation Conditions for the Type 19 Tube", *RCA Tube Dept. Applic. Note No. 18* (July 27) 1933
"The Application for Graphite as an Anode Material to High-Vacuum Transmitting Tubes", E. E. Spitzer, *Proc. I.R.E.* (August) 1933
"Tubes to Fit the Wavelength", B. J. Thompson, *Electronics* (August) 1933
"Operating Conditions for the 1A6 as an Oscillator-Mixer", *RCA Tube Dept. Applic. Note No. 19* (August 23) 1933
"An Increase in the Maximum Allowable Grid Resistor for Types 38, 41, 42, 89 and 2A5", *RCA Tube Dept. Applic. Note No. 20* (August 23) 1933
"Operation Characteristics of the Type 1-v and the type 12Z3 Tube", *RCA Tube Dept. Applic. Note No. 21* (August 30) 1933
"Operation of the 2A6, 2B7, 6B7, 55, 75, 77 and 85 as Resistance-Coupled Audio-Frequency Amplifiers", *RCA Tube Dept. Applic. Note No. 22* (September 6) 1933
"The Operating Characteristics of the Type 84 Tube", *RCA Tube Dept. Applic. Note No. 23* (October 5) 1933
"Use of the 1A6 as a Half-Wave Diode-Tetrode", *RCA Tube Dept. Applic. Note No. 24* (October 12) 1933
"Influence of Circuit Constants on Receiver Output Noise", *RCA Tube Dept. Applic. Note No. 25* (October 19) 1933
"The 37, 56, 57 and 77 Tubes as Resistance-Coupled High-Voltage Amplifiers", *RCA Tube Dept. Applic. Note No. 26* (October 26) 1933
"A Cathode-Ray Modulation Indicator", E. C. Ballentine, *Broadcast News* (November) 1933
"An Analysis of Super-Regeneration", W. van B. Roberts, *RCA Licensee Bulletin LB-266* (November 1) 1933
"Use of Pentagrid Converter Tubes in Multi-Range Receivers", *RCA Tube Dept. Applic. Note No. 27* (November 2) 1933
"Super-Regeneration and Its Application to High-Frequency Reception", D. Grimes and W. S. Barden, *RCA Licensee Bulletin LB-267* (November 8) 1933
"Special Applications of the Type 79 Tube", *RCA Tube Dept. Applic. Note No. 28* (November 9) 1933

Year

"Cathode-Ray Tubes for Oscillograph Purposes", C. W. Taylor, L. B. Headrick and R. T. Orth, *Electronics* (December) 1933
"Vacuum Tubes of Small Dimensions for Use at Extremely High Frequencies", B. J. Thompson and G. M. Rose, Jr., *Proc. I.R.E.* (December) 1933
"Description of an Experimental Television System and the Kinescope", V. K. Zworykin, *Proc. I.R.E.* (December) 1933
"Notes on the Measurement of Inter-Electrode Capacities with a Tentative Standard of Procedure", C. Travis, *RCA Licensee Bulletin LB-270* (December 5) 1933
"Design of Audio Systems Employing Type 2A3 Power Amplifier Triodes", *RCA Tube Dept. Applic. Note No. 29* (December 29) .. 1933
"Vacuum Tubes", J. M. Stinchfield, Section of RADIO ENGINEERING HANDBOOK, Henney, McGraw-Hill Book Co., New York, N. Y. ... 1933
"Problems of Cathode-Ray Television", I. G. Maloff, *Electronics* (January) 1934
"The Iconoscope—A Modern Version of the Electric Eye", V. K. Zworykin, *Proc. I.R.E.* (January) 1934
"Characteristics of The 6F7 Tube", *RCA Tube Dept. Applic. Note No. 30* (January 3) 1934
"Operating Considerations of Cathode Ray Tubes 905 and 906 for Oscillographic Purposes", *RCA Tube Dept. Applic. Note No. 31* (January 11) 1934
"Revision of Characteristics for the Type 48 Tube", *RCA Tube Dept. Applic. Note No. 32* (January 17) 1934
"The RCA-800 in Class B Audio Amplifiers", *RCA Tube Dept. Applic. Note No. 33* (January 31) 1934
"Characteristics of the 868 Phototube", *RCA Tube Dept. Applic. Note No. 34* (February 15) 1934
"Triode Operation of Type 42 and Type 2A5 Pentodes", *RCA Tube Dept. Applic. Note No. 35* (February 26) 1934
"Voltage Multiplying Circuits", C. Travis, *RCA Licensee Bulletin LB-283* (February 26) 1934
"100-Volt Operation of 6C6 and 6D6 Tubes", *RCA Tube Dept. Applic. Note No. 37* (March 27) 1934
"Power Supply and Linear Time Axis for Cathode-Ray Oscillographs", P. A. Richards and W. L. Meier, *Electronics* (April) .. 1934
"A Simple Method for Converting Pentode Characteristics", *RCA Tube Dept. Applic. Note No. 38* (April 25) 1934
"The Input Impedance of Vacuum Tubes", J. Yolles, *RCA Licensee Bulletin LB-290* (April 28) 1934
"Improved Magnetron Oscillator for the Generation of Microwaves", E. G. Linder, *Phys. Rev.* (May 1) 1934
"The Design of a Voltage Supply for the 905 and 906 Cathode Ray Tubes", *RCA Tube Dept. Applic. Note No. 39* (May 11) 1934
"Notes on an Ionized Gas Modulator for Short Radio Waves", E. G. Linder and I. Wolff, *Proc. I.R.E.* (June) 1934
"High Power Output from Type 45 Tubes", *RCA Tube Dept. Applic. Note No. 40* (June 14) 1934
"The 1C6", *RCA Tube Dept. Applic. Note No. 41* (July 6) 1934
"Tube Consideration in Class-B Amplification", L. E. Barton, *Broadcast News* (August) 1934
"Push-Pull vs. Parallel Operation", J. L. Reinartz, *Radio* (September, December) 1934
"Design and Use of 'Acorn' Tubes for Ultra High Frequencies", B. Salzberg, *Electronics* (September) 1934
"Short-cut Method for Determining Operating Conditions of Power Output Triodes", *RCA Tube Dept. Applic. Note No. 42* (September 5) 1934
"Notes on Tests and Ratings of Tubes for Oscillator Service", C. Travis, *RCA Licensee Bulletin LB-307* (October 1) 1934

Year

"Operating Conditions for the 6A6", *RCA Tube Dept. Applic. Note No. 44* (November 14) 1934

"Theory of Electron Gun", I. G. Maloff and D. W. Epstein, *Proc. I.R.E.* (December) 1934

"Cathode-Ray Tubes and Their Applications", J. M. Stinchfield, *Elec. Eng.* (December) 1934

"An Electron Oscillator with Plane Electrodes", B. J. Thompson and P. D. Zottu, *Proc. I.R.E.* (December) 1934

"Vacuum Tube Amplifiers", L. E. Barton, Section of ELECTRICAL ENGINEERS' HANDBOOK, Pender-McIlwain, New York, N. Y. 1934

"The Secondary Emission Phototube", H. Iams and B. Salzberg, *Proc. I.R.E.* (January) 1935

"The Use of the 57 or 6C6 to Obtain Negative Transconductance and Negative Resistance", *RCA Tube Dept. Applic. Note No. 45* (February 7) 1935

"The Application of Superheterodyne Frequency-Conversion System to Multirange Receivers", W. A. Harris, *Proc. I.R.E.* (April) 1935

"Graphical Harmonic Analysis for Determining Modulation Distortion in Amplifier Tubes", W. R. Ferris, *Proc. I.R.E.* (May) 1935

"Automatic Frequency Control", C. Travis, *RCA Licensee Bulletin LB-326* (May) 1935

"Use of the 954 as a Vacuum-Tube Voltmeter", *RCA Tube Dept. Applic. Note No. 47* (May 20) 1935

"Miscellaneous Applications of Vacuum Tubes", E. H. Shepard, *Proc. Rad. Club Amer.* (June) 1935

"The Construction of a Top-Cap Shield for Metal Tubes", *RCA Tube Dept. Applic. Note No. 49* (July 23) 1935

"High-Gain Audio Frequency Amplifiers", E. H. Shepard, *Radio Craft* (August) 1935

"Characteristics of the Photophone Light-Modulating System", L. T. Sachtleben, *Jour. Soc. Mot. Pic. Eng.* (August) 1935

"Operation of the 6L7 as a Mixer Tube", *RCA Tube Dept. Applic. Note No. 50* (August 19) 1935

"The 6F5", *RCA Tube Dept. Applic. Note No. 51* (September 25) 1935

"Recent Developments in Miniature Tubes", B. Salzberg and D. G. Burnside, *Proc. I.R.E.* (October) 1935

"Negative Resistance and Devices for Obtaining It", E. W. Herold, *Proc. I.R.E.* (October) 1935

"Automatic Frequency Control", C. Travis, *Proc. I.R.E.* (October) 1935

"Class AB Operation of Type 6F6 Tubes Connected as Triodes", *RCA Tube Dept. Applic. Note No. 52* (October 31) 1935

"Halation (Interference in Fluorescent Screens)", Berthold Sheffield, *Electronics* (November) 1935

"Development of Cathode-Ray Tubes for Oscillographic Purposes", R. T. Orth, P. A. Richards and L. B. Headrick, *Proc. I.R.E.* (November) 1935

"Luminescent Materials for Cathode-Ray Tubes", T. B. Perkins and H. W. Kaufman, *Proc. I.R.E.* (November) 1935

"Cathode-Ray Tube Terminology", T. B. Perkins, *Proc. I.R.E.* (November) 1935

"Anode Materials and Design for High-Vacuum Transmitting Tubes", E. E. Spitzer, *Elec. Eng.* (November) 1935

"Quantitative Influence of Tube and Circuit Properties on Random Electron Noise", W. S. Barden and S. W. Seeley, *RCA Licensee Bulletin LB-341* (November 7) 1935

"Method for Measurement of Conversion Conductance", S. W. Seeley, *RCA Licensee Bulletin LB-342* (November 16) 1935

"The 6L7 as a Volume Expander for Phonographs", *RCA Tube Dept. Applic. Note No. 53* (November 27) 1935

"Influence of Tube and Circuit Properties in Electron Noise", S. W. Seeley and W. S. Barden, *Electronics* (December) 1935

Year

"Improved and Simplified Methods for Automatic Frequency Control", D. E. Foster and S. W. Seeley, *RCA Licensee Bulletin LB-343* (December 12) 1935
"Class AB Operation of Type 6F6 Tubes Connected as Pentodes", *RCA Tube Dept. Applic. Note No. 54* (December 20) 1935
"Operation of the 6A8", *RCA Tube Dept. Applic. Note No. 55* (December 27) 1935
"Possibilities of the Iconoscope in Television", V. K. Zworykin and G. A. Morton, booklet, Geo. Newnes, Ltd., England 1935
"Input Resistance of Vacuum Tubes as Ultra-High-Frequency Amplifiers", W. R. Ferris, *Proc. I.R.E.* (January) 1936
"Analysis of the Effects of Space Charge on Grid Impedance", D. O. North, *Proc. I.R.E.* (January) 1936
"Receiver Design", *RCA Tube Dept. Applic. Note No. 56* (January 15) 1936
"A New Tube for Use in Superheterodyne Frequency Conversion Systems", C. F. Nesslage, E. W. Herold and W. A. Harris, *Proc. I.R.E.* (February) 1936
"A Detector Circuit for Reducing Noise Interference in Phone Reception", L. E. Thompson, *QST* (February) 1936
"Balanced Amplifiers", A. Preisman, *Comm. and Broad. Eng.* (February, March, September, October, November, December) 1936
(January) 1937
"The 6L7 as an R-F Amplifier", *RCA Tube Dept. Applic. Note No. 57* (February 5) 1936
"The Secondary Emission Multiplier—A New Electronic Device", V. K. Zworykin, G. A. Morton and L. Malter, *Proc. I.R.E.* (March) 1936
"A High Efficiency Crystal Oscillator", J. L. Reinartz, *Radio* (March) 1936
"Intermediate Frequency Considerations", D. E. Foster and E. W. Wilby, *RCA Licensee Bulletin LB-349* (March 2) 1936
"Output Tubes for Radio Receivers", J. F. Dreyer, Jr., *Electronics* (April) 1936
"Description and Characteristics of the End-Plate Magnetron", E. G. Linder, *Proc. I.R.E.* (April) 1936
"Applied Electron Optics", V. K. Zworykin and G. A. Morton, *Jour. Opt. Soc. Amer.* (April) 1936
"The Electron Image Tube", V. K. Zworykin, *Broadcast News* (April) 1936
"Automatic Frequency Control for Single I-F Stage Receivers", D. E. Foster, *RCA Licensee Bulletin LB-355* (April 13) 1936
"Simplified Means for Determination of Converter Tube Performance", C. N. Kimball and C. E. Coon, *RCA Licensee Bulletin LB-356* (April 27) 1936
"A Different Amplifier Tube", Berthold Sheffield, *Electronics* (May) .. 1936
"Operation of the 6Q7", *RCA Tube Dept. Applic. Note No. 59* (May 7) 1936
"Effect of Electron Pressure on Plasma Electron Oscillations", E. G. Linder, *Phys. Rev.* (May 15) 1936
"Notes on the Theory of the Single Stage Amplifier", B. Salzberg, *Proc. I.R.E.* (June) 1936
"A Study of Polarization Capacity and Electrode Condition", I. Wolff, *Jour. Chem. Phys.* (June) 1936
"Power Saving Tubes With Copper Cathodes", Berthold Sheffield, *Electronics* (June) 1936
"Operation of the 6L6", *RCA Tube Dept. Applic. Note No. 60* (June 10) 1936
"The Conversion of a 6L6 Plate Family to New Screen Voltage Conditions", *RCA Tube Dept. Applic. Note No. 61* (June 25) 1936
"Iconoscopes and Kinescopes in Television", V. K. Zworykin, *RCA Review* (July) 1936
Jour. Soc. Mot. Pic. Eng. (May) 1937
"New Developments in Audio Power Tubes", R. S. Burnap, *RCA Review* (July) 1936

Year

"The Cathode-Ray Tube in Television Reception", I. G. Maloff, TELEVISION, Vol. I (July) 1936

"A New Operating Condition for Two Type 6F6 Tubes Connected as Pentodes", *RCA Tube Dept. Applic. Note No. 62* (July 13) 1936

"A High-Gain Single-Tube Phase Inverter", *RCA Tube Dept. Applic. Note No. 63* (July 30) 1936

"Electron Optical System of Two Cylinders as Applied to Cathode-Ray Tubes", D. W. Epstein, *Proc. I.R.E.* (August) 1936

"Magnetron Oscillators for the Generation of Frequencies Between 300 and 600 Megacycles", G. R. Kilgore, *Proc. I.R.E.* (August) .. 1936

"Recent Developments of the Class 'B' Audio and Radio-Frequency Amplifiers", L. E. Barton, *Proc. I.R.E.* (July) 1936

"Study of Cathode Loaded Drivers and Detectors", C. N. Kimball and W. S. Barden, *RCA Licensee Bulletin LB- 371* (August) 1936

"Inverse-Feedback Circuits for A-F Amplifiers", *RCA Tube Dept. Applic. Note No. 64* (August 26) 1936

"The Sommerfeld Formula", W. A. Fitch, *Electronics* (September) .. 1936

"The Electron-Image Tube, a Means for Making Infra-Red Images Visible", G. A. Morton, *Jour, Soc. Mot. Pic. Eng.* (September) .. 1936

"Tuning-Indicator Circuits for the 6E5 and 6G5", *RCA Tube Dept. Applic. Note No. 65* (September 10) 1936

"Equal Plate and Screen Voltage Operation of the 6L6", *RCA Tube Dept. Applic. Note No. 66* (September 29) 1936

"Electron Motion in a Plasma", E. G. Linder, *Science* (October) 1936

"5-Meter Crystal Controlled Push-Pull 800 Output", J. L. Reinartz, *QST* (October) 1936

"Electron Beams and Their Applications in Low-Voltage Devices", H. C. Thompson, *Proc. I.R.E.* (October) 1936

"Multitube Oscillators for the Ultra-High-Frequencies", P. D. Zottu, *QST* (October) 1936

"A Study of the Characteristics of Noise", V. D. Landon, *Proc. I.R.E.* (November) 1936

"Application of Conventional Vacuum Tubes in Unconventional Circuits", E. H. Shepard, Jr., *Proc. I.R.E.* (December) 1936

"Electron Optics of an Image Tube", G. A. Morton and E. G. Ramberg, *Physics* (December) 1936

"An Improved Vacuum Tube Microammeter", A. W. Vance, *Rev. Sci. Instr.* 1936

"Vacuum Tubes", B. J. Thompson, J. M. Stinchfield, B. Salzberg. E. W. Herold, Section of ELECTRICAL ENGINEERS' HANDBOOK, Pender-McIlwain, New York, N. Y. 1936

"Simplified Methods for Computing Performance of Transmitting Tubes", W. G. Wagener, *Proc. I.R.E.* (January) 1937

"Resistance-Coupled Audio-Frequency Amplifiers", *RCA Tube Dept. Applic. Note No. 67* (January 20) 1937

"A 55-Watt Amplifier Using Two Type 6L6 Tubes", *RCA Tube Dept. Applic. Note No. 68* (January 20) 1937

"250-Volt Low-Current Operation of the 6L6", *RCA Tube Dept. Applic. Note No. 69* (February 3) 1937

"UHF Diode with Movable Anode", Berthold Sheffield, *Electronics* (March) 1937

"Low-Current, High-Power Operation of Two 6L6's Connected in Push-Pull", *RCA Tube Dept. Applic. Note No. 71* (March 3) 1937

"A 40-Watt Operating Condition for Two Type 6L6 Tubes", *RCA Tube Dept. Applic. Note No. 72* (March 17) 1937

"Operation of the 25L6 in Typical Circuits", *RCA Tube Dept. Applic. Note No. 73* (March 31) 1937

"A Control System for AFC Receivers with Improved Flexibility", G. Mountjoy, *RCA Licensee Bulletin LB-389* (April 20) 1937

"New High-Voltage Choke-Input Rating for the 5T4", *RCA Tube Dept. Applic. Note No. 74* (April 28) 1937

Year

"Receiver Design", *RCA Tube Dept. Applic. Note No. 75* (May 28) ... 1937
"A Wide-Range, Linear-Scale Photoelectric Cell Densitometer", W. W. Lindsay, Jr., and W. V. Wolfe, *Jour. Soc. Mot. Pic. Eng.* (June) .. 1937
"Mixer Circuits", A. Preisman, *Communications* (June, August) 1937
"Automatic Plotting of Electron Trajectories", D. B. Langmuir, *Nature (Brit.)* (June) 1937
"An Amplifier with No Phase Distortion", O. H. Schade, *Electronics* (June) 1937
"Batalum, a Barium Getter for Metal Tubes", E. A. Lederer and D. H. Wamsley, *RCA Review* (July) 1937
"A Fundamental-Reinforced Harmonic-Generating Circuit", J. L. Reinartz, *QST* (July) 1937
"The New RCA Electronic Sweep Oscillator", O. M. Owsley, *RCA Rad. Serv. News* (July) 1937
"Dimensions of Popular Tube Types", *RCA Tube Dept. Applic. Note No. 77* (July 14) 1937
"Use of the Plate Family in Vacuum-Tube Power-Output Calculations",*RCA Tube Dept. Applic. Note No. 78* (July 28) 1937
"A Circuit for Studying Kinescope Resolutions", C. E. Burnett, *Proc. I.R.E.* (August) 1937
"Development of the Projection Kinescope", V. K. Zworykin and W. H. Painter, *Proc. I.R.E.* (August) 1937
"Theory and Performance of the Iconscope", V. K. Zworykin, G. A. Morton and L. E. Flory, *Proc. I.R.E.* (August) 1937
"Television Pickup Tubes with Cathode-Ray Beam Scanning", H. Iams and A. Rose, *Proc. I.R.E.* (August) 1937
"Theoretical Limitation of Cathode-Ray Tubes", D. B. Langmuir, *Proc. I.R.E.* (August) 1937
"High-Current Electron Gun for Projection Kinescope", R. R. Law, *Proc. I.R.E.* (August) 1937
"The Oscillotrol", D. E. Foster and G. Mountjoy, *RCA Licensee Bulletin LB-404* (August 2) 1937
"Characteristics of Inverse Feed-Back Circuits," L. R. Martin, *Radio Eng.* (May) 1937
"Analysis and Design of Video Amplifiers, Part I", C. N. Kimball and S. W. Seeley, *RCA Licensee Bulletin LB-406* (August 17) ... 1937
RCA Review (October) 1937
"Frequency Changers in All-Wave Receivers", E. W. Herold, *Wireless Eng. (Brit.)* (September) 1937
"Significance of Ratings for Power Output Tubes", *RCA Tube Dept. Applic. Note No. 79* (September 8) 1937
"The Magnetron as a High-Frequency Generator", G. R. Kilgore, *Jour. Appl. Phys.* (October) 1937
"Negative Peak Automatic Modulation Control for Plate-Modulated Phone Transmitters", L. C. Waller, *QST* (October) 1937
"Some Unconventional Vacuum Tube Applications", E. H. Shepard, *RCA Review* (October) 1937
"Problems Concerning the Production of Cathode Ray Tube Screens", H. W. Leverenz, *Television*, Vol. II (October) 1937
"A Transformation for Calculating the Constants of Vacuum Tubes with Cylindrical Elements", W. van B. Roberts, *Proc. I.R.E.* (October) 1937
"The Requirements and Performance of a New Ultra-High-Frequency Power Tube", W. G. Wagener, *RCA Review* (October) 1937
"Operation of the 6V6-G", *RCA Tube Dept. Applic. Note No. 80* (October 20) 1937
"Direct Viewing Type Cathode-Ray Tube for Large Television Images", I. G. Maloff, *Proc. I.R.E.* (November) 1937
"Screens for Television Tubes", I. G. Maloff and D. W. Epstein, *Electronics* (November) 1937

Year

"Class B R-F Amplifier Chart", W. van B. Roberts, *Electronics* (November) ... 1937

"Description of the RCA Type 96A Limiting Amplifier", J. M. Brumbaugh and B. W. Robins, *Broadcast News* (November) ... 1937

"Analysis of Admittance Neutralization by Means of Negative Transconductance Tubes", E. W. Herold, *Proc. I.R.E.* (November) ... 1937

"Recent Developments in German Cathode Ray Tubes", Berthold Sheffield, *Electronics* (November) ... 1937

"A Two-Terminal Oscillator", *RCA Tube Dept. Applic. Note No. 81* (November 17) ... 1937

"Effects of Space Charge in the Grid-Anode Region of Vacuum Tubes", A. V. Haeff and B. Salzberg, *RCA Review* (January) ... 1938

"Television Cathode-Ray Tubes for the Amateur", R. S. Burnap, *RCA Review* (January) ... 1938

"Vacuum-Tube Engineering for Motion Pictures", A. M. Glover and L. C. Hollands, *Jour. Soc. Mot. Pic. Eng.* (January) ... 1938

"Wide-Angle Tuning with the 6E5, 6G5 or 6U5", *RCA Tube Dept. Applic. Note No. 82* (January 5) ... 1938

"Resistance-Coupled Amplifier Data for the 6L6, 6T7-G and 6S7-G", *RCA Tube Dept. Applic. Note No. 83* (January 5) ... 1938

"Video I. F. System Considerations", S. W. Seeley and W. S. Barden, *RCA Licensee Bulletin LB-417* (January 5) ... 1938

"Oscillator Frequency Stability in Relation to Receivers with Spread Short Wave Bands", D. E. Foster, *RCA Licensee Bulletin LB-418* (January 8) ... 1938

"The Operation of Phototubes", *RCA Tube Dept. Applic. Note No. 84* (January 12) ... 1938

"Operation of the 6AC5-G", *RCA Tube Dept. Applic. Note No. 85* (January 26) ... 1938

"Operation of the 6Y6-G", *RCA Tube Dept. Applic. Note No. 86* (January 26) ... 1938

"Beam Power Tubes", O. H. Schade, *Proc. I.R.E.* (February) ... 1938

"The 6K8—A New Converter Tube", *RCA Tube Dpet. Applic. Note No. 87* (February 16) ... 1938

"Excess Energy Electrons and Electron Motion in High Vacuum Tubes", E. G. Linder, *Proc. I.R.E.* (March) ... 1938

"The New RCA-153 Service Oscillator", O. M. Owsley, *RCA Rad. Serv. News* (March) ... 1938

"Hum in Heater-Type Tubes", *RCA Tube Dept. Applic. Note No. 88* (March 9) ... 1938

"Some Notes on Video-Amplifier Design", A. Preisman, *RCA Review* (April) ... 1938

"The Monoscope and Its Uses", C. E. Burnett, *RCA Review* (April) ... 1938

"The Developmental Problems and Operation Characteristics of Two New Ultra-High-Frequency Triodes", W. G. Wagener, *Proc. I.R.E.* (April) ... 1938

"Resistance-Coupled Amplifier Data for the 6C8-G, 6F1-G, 6J5, 6J5-G and 6Z7-G", *RCA Tube Dept. Applic. Note No. 90* (April 13) ... 1938

"Operation of the Gas-Triode OA4-G", *RCA Tube Dept. Applic. Note No. 91* (April 29) ... 1938

"A New Cold-Cathode Gas Triode", W. E. Bahls and C. H. Thomas, *Electronics* (May) ... 1938

"Effect of High-Energy Electron Random Motion Upon the Shape of the Magnetron Cut-off Curve", E. G. Linder, *Jour. Appl. Phys.* (May) ... 1938

"Operation of the Improved Type 906 Cathode-Ray Tube at Low Voltages", *RCA Tube Dept. Applic. Note No. 92* (May 25) ... 1938

"Metal Evaporators", H. B. DeVore, *Rev. of Sci. Instr.* (June) ... 1938

"An Inverse-Feedback Circuit for Resistance-Coupled Amplifiers", *RCA Tube Dept. Applic. Note No. 93* (June 8) ... 1938

Year

"Operation of the 6AF6-G", *RCA Tube Dept. Applic. Note No. 94* (June 22) 1938
"A Discussion on Video Modulation Detection", W. S. Barden, *RCA Licensee Bulletin LB-435* (June 27) 1938
"Teledynamic Control by Selective Ionization With Application to Radio Receivers", H. B. Deal, S. W. Seeley, and C. N. Kimball, *Proc. I.R.E.* (July) 1938
"Linear Rectifier Design Calculations", E. A. Laport, *RCA Review* (July) 1938
"A New Converter Tube for All-Wave Receivers", E. W. Herold, W. A. Harris and T. J. Henry, *RCA Review* (July) 1938
"Inverse Feedback Circuits for Output Tubes", D. E. Foster and J. A. Rankin, *RCA Licensee Bulletin LB-438* (July 19) 1938
"Performance of 6K8 Converter in Short Wave Receivers", A. E. Newlon, *RCA Licensee Bulletin LB-441* (July 19) 1938
"Television I-F Circuits", R. S. Holmes and E. W. Engstrom, *Electronics* (August) 1938
"Wide-Range Beat Frequency Oscillator", E I. Anderson, *RCA Licensee Bulletin LB-444* (August 11) 1938
"Operating Positions of Receiving Tubes", *RCA Tube Dept. Applic. Note No. 95* (August 17) 1938
"A Voltage Regulator For D-C Power Supplies", *RCA Tube Dept. Applic. Note No. 96* (August 24) 1938
"Method of Measuring Luminescent Screen Potential", H. Nelson, *Jour. Appl. Phys.* (September) 1938
"Single-Ended R-F Pentodes", R. L. Kelly and J. F. Miller, *Electronics* (September) 1938
"Improvements in High Frequency Amplifiers", D. E. Foster and A. E. Newlon, *RCA Licensee Bulletin LB-450* (September 22) .. 1938
"A Self-Balancing Phase-Inverter Circuit", *RCA Tube Dept. Applic. Note No. 97* (September 28) 1938
"Review of Ultra-High-Frequency Vacuum-Tube Problems", B. J. Thompson, *RCA Review* (October) 1938
"Application of an Electron Multiplier to the Production of Facsimile Test Wave-Forms", W. H. Bliss, RADIO FACSIMILE, Vol. I (October) 1938
"Analysis and Design of Video Amplifiers, Part II", C. N. Kimball and S. W. Seeley, *Jour. Tele. Soc.* (October) 1938
"A Video Mixing Amplifier", A. A. Barco, *RCA Licensee Bulletin LB-453* (October 11) 1938
"The Operation of Single-Ended Tubes", *RCA Tube Dept. Applic. Note No. 98* (October 19) 1938
"Revision of 6K8 Ratings", *RCA Tube Dept. Applic. Note No. 99* (October 19) 1938
"Photoelectric Cells and Circuits", W. S. Thompson, *International Photographer* (November) 1938
"Operation of the 6SA7", *RCA Tube Dept. Applic. Note No. 100* (December 2) 1938
CATHODE-RAY TUBE IN TELEVISION, I. G. Maloff and D. W. Epstein, McGraw-Hill Book Co., New York, N. Y. 1938
"Amplifiers and Power Supplies", W. S. Thompson, *International Photographer* (January) 1939
"A Bridge Type Set for Measuring Vacuum Tube Parameters", J. R. Pernice, *Communications* (January) 1939
"Analysis and Design of Video Amplifiers—Part II", S. W. Seeley and C. N. Kimball, *RCA Review* (January) 1939
"New Television Amplifier Receiving Tubes", A. P. Kauzmann, *RCA Review* (January) 1939
"Sweep Frequency Signal Generator", J. A. Rankin, *RCA Licensee Bulletin LB-466* (January) 1939

Year

"Input Loading of Receiving Tubes at Radio Frequencies", *RCA Tube Dept. Applic. Note No. 101* (January 25) 1939
"A Fixed-Focus Electron Gun for Cathode-Ray Tubes", H. Iams, *Proc. I.R.E.* (February) 1939
"An Ultra-High-Frequency Power Amplifier of Novel Design", A. V. Haeff, *Electronics* (February) 1939
"Light Output and Secondary Emission Characteristics of Luminescent Materials", S. T. Martin and L. B. Headrick, *Jour. Appl. Phys.* (February) 1939
"Simplified Derivation of the General Properties of an Electron-Optical Image", E. G. Ramberg, *Jour. Opt. Soc. Amer.* (February) 1939
"Using Electromagnetic-Deflection Cathode-Ray Tubes in the Television Receiver", J. B. Sherman, *QST* (February) 1939
"Variation of Light Output with Current Density and Classification of Willemite Phosphors", E. G. Ramberg and G. A. Morton, *Phys. Rev.* (February) 1939
"Circuit Design and Its Relation to Tube Performance", L. C. Hollands, *Electronics* (March) 1939
"Electrostatic Deflection Kinescope Unit for the Television Receiver", J. B. Sherman, *QST* (March) 1939
"Transmitter Circuit Design for Frequencies Above 100 Mc", O. E. Dow, *Proc. Rad. Club Amer.* (March) 1939
"The 6SK7 As An I-F Amplifier", *RCA Tube Dept. Applic. Note No. 102* (March 15) 1939
"Tubes at Work", D. Pollack, *Electronics* (April) 1939
"A Wide-Range Video-Amplifier for a Cathode-Ray Oscilloscope", A Preisman, *RCA Review* (April) 1939
"Kinescopes for Television Receivers", L. C. Waller, *Communications* (April) 1939
"Measurements of Admittances at Ultra-High Frequencies", J. M. Miller and B. Salzberg, *RCA Review* (April) 1939
"Transient Response of Multistage Video-Frequency Amplifiers", A. V. Bedford and G. L. Fredendall, *Proc. I.R.E.* (April) 1939
"Rate of Evaporation of Tantalum", L. Malter and D. B. Langmuir, *Phys. Rev.* (April 15) 1939
"Resistance, Emissivities, and Melting Point of Tantalum", L. Malter and D. B. Langmuir, *Phys. Rev.* (April 15) 1939
"Operation of the 35L6-GT" *RCA Tube Dept. Applic. Note No. 103* (April 26) 1939
"Phenomenon of Secondary Electron Emission", H. Nelson, *Phys. Rev.* (May 15) 1939
"An Iconoscope Pre-Amplifier", Allen A. Barco, *RCA Review* (July) 1939
"A Push-Pull Ultra-High-Frequency Beam Tetrode", A. K. Wing, *RCA Review* (July) 1939
"Effect of Electron Transit Time on Efficiency of a Power Amplifier", A. V. Haeff, *RCA Review* (July) 1939
"Electron Optics", E. G. Ramberg and G. A. Morton, *Jour. Appl. Phys.* (July) 1939
"Luminescent Materials", H. W. Leverenz (Coauthor), *Jour. Appl.* Phys. (July) 1939
"Survey of Radio Tube Sales for 1938", E. W. Wilby, *RCA Licensee Bulletin LB-491* (August) 1939
"Contrast in Kinescopes", R. R. Law, *Proc. I.R.E.* (August) 1939
"Recent Improvements in the Design and Characteristics of Iconoscopes", R. B. Janes and W. H. Hickok, *Proc. I.R.E.* (September) 1939
"Space Charge Effects in Electron Beams", A. V. Haeff, *Proc. I.R.E.* (September) 1939
"Television Pickup Tubes Using Low-Velocity Beam Scanning", A. Rose and H. Iams, *Proc. I.R.E.* (September) 1939
"The Class A-B Push-Pull Recording Systems", C. Hawley Cartwright and W. S. Thompson, *Jour. Soc. Mot. Pic. Eng.* (September) 1939

Year

"The Electrostatic Electron Multiplier", V. K. Zworykin and J. A. Rajchman, *Proc. I.R.E.* (September) 1939
"The Image Iconoscope", H. Iams, G. A. Morton, and V. K. Zworykin, *Proc. I.R.E.* (September) 1939
"Point Projector Electron Microscope", G. A. Morton and E. G. Ramberg, *Phys. Rev.* (October) 1939
"Television Signal-Frequency Circuit Considerations", Garrard Mountjoy, *RCA Review* (October) 1939
"The Orthicon, a Television Pickup Tube", A Rose and H. Iams, *RCA Review* (October) 1939
"Miniature Battery Tubes", K. G. Bucklin, *Electronics* (November) 1939
"The Anode-Tank-Circuit Magnetron", Ernest G. Linder, *Proc. I.R.E.* (November) 1939
"A Direct Reading Vacuum Tube Mille-Voltmeter for Bio-Electric Studies", Walter Lyons and R. E. Heller, *Electronics* (November) 1939
"A Change in Maximum Ratings of Receiver Tubes", *RCA Tube Dept. Applic. Note No. 105* (November 15) 1939
"Performance of 6AC7 Tube as a Television Converter", A. E. Newlon, *RCA Licensee Bulletin LB-501* (December) 1939
"Electron Optics of Cylindrical Electrical and Magnetic Fields", Albert Rose, *Proc. I.R.E.* (January) 1940
"Fluctuations in Space-Charge-Limited Currents at Moderately High Frequencies—Part I", B. J. Thompson, D. O. North and W. A. Harris, *RCA Review* (January) 1940
"Recent Advances in Barium Getter Technique", E. A. Lederer, *RCA Review* (January) 1940
"Simplified Television I-F Systems", Garrard Mountjoy, *RCA Review* (January) 1940
"Superheterodyne Converter System Considerations in Television Receivers", E. W. Herold, *RCA Review* (January) 1940
"A Cathode Ray Frequency Modulation Generator", Robert E. Shelby, *Electronics* (February) 1940
"A Behavior of Willemite Under Electron Bombardment", G. A. Morton and E. R. Piore, *Jour. Appl. Phys.* (February) 1940
"Untuned Radio-Frequency Amplifiers", C. W. Finnigan, *RCA Licensee Bulletin LB-508* (February 2) 1940
"Wide-Band Inductive Output Amplifier", A .V. Haeff and L. S. Nergaard, *Proc. I.R.E.* (March) 1940
"The Formation and Maintenance of Electron and Ion Beams", L. P. Smith and P. L. Hartman, *Jour. Appl. Phys.* (March) 1940
"Signal Generators for Frequency Modulated Waves", J. A. Rankin and D. E. Foster, *RCA Licensee Bulletin LB-514* (March 5) 1940
"Design of Superheterodyne Intermediate-Frequency Circuits", F. E. Spaulding, Jr., *RCA Review* (April) 1940
"Development and Production of the New Miniature Battery Tubes", N. R. Smith and A. H. Schooley, *RCA Review* (April) 1940
"Fluctuations in Space-Charge-Limited Currents at Moderately High Frequencies—Part II", B. J. Thompson, D. O. North, and W. A. Harris, *RCA Review* (April and July) 1940
"Simple Methods for Checking R-F Distortion or Cross-Modulation of Pentode Amplifier Tubes", E. W. Herold, *Electronics* (April) 1940
"U.H.F. Oscillator Frequency Stability Considerations", S. W. Seeley and E. I. Anderson, *RCA Licensee Bulletin LB-524* (May 6) 1940
"A V-T Voltmeter for Coaxial Line Measurements", G. L. Usselman, *Electronics* (July) 1940
"Flash-Arc Currents in Transmitter Tubes", J. C. Walter, *Broadcast News* (July) 1940
"Optimum Efficiency Conditions for White Luminescent Screens in Kinescopes", H. W. Leverenz, *Jour. Opt. Soc. Amer.* (July) 1940
"Reactance Tube Frequency Modulators", M. G. Crosby, *QST* (June) 1940
RCA Review (July) 1940

Year

"U-H-F Oscillator Stability Considerations", E. I. Anderson, S. W. Seeley, and W. Stuart, *RCA Review* (July) 1940

"Space Charge Limitations on the Focus of Electron Beams", B. J. Thompson and L. B. Headrick, *Proc. I.R.E.* (July) 1940

"A New High Sensitivity Photosurface", A. M. Glover and R. B. Janes, *Electronics* (August) 1940

"Materials Used in Vacuum Tube Manufacture", A. J. Monack, *Jour. Ind. Eng. Chem.* (August) 1940

"Fluctuations in Space-Charge-Limited Currents at Moderately High Frequencies—Part III", B. J. Thompson, D. O. North, and W. A. Harris, *RCA Review* (October) 1940

"Cathodoluminescence as Applied in Television", H. W. Leverenz, *RCA Review* (October) 1940
Jour. Tele. Soc. (Brit.) (June) 1941

"A New Electron Microscope", L. Morton, M. C. Banca, and J. F. Bender, *RCA Review* (October) 1940

"Survey of Radio Tube Sales for 1939", E. W. Wilby, *RCA Licensee Bulletin LB-536* (October 2) 1940

"A Mechanical Model for the Motion of Electrons in a Magnetic Field", Albert Rose, *Jour. Appl. Phys.* (November) 1940

"Fresnel Diffraction of Electrons as a Contour Phenomenon in Electron Supermicroscope Images", J. Hillier, *Phys. Rev.* (November) 1940

"Effect of Temperature on Frequency of 6J5 Oscillator", *RCA Tube Dept. Applic. Note No. 108* (November 13).................... 1940

"Operation of Fifty Milliampere Tubes by the 117N7-GT", *RCA Tube Dept. Applic. Note No. 109* (November 13).................... 1940

"An Improved Inter-Electrode Capacitance Meter", A. A. Barco, *RCA Licensee Bulletin LB-541* (November 19) 1940

"An Electrical-Focused Multiplier Phototube", J. A. Rajchman and R. L. Snyder, *Electronics* (December) 1940

"The RCA Miniature Tubes", *RCA Tube Dept. Applic. Note No. 106* 1940

"A Miniature-Tube Hearing-Aid Amplifier for Use With an Air-Conduction Earpiece", *RCA Tube Dept. Applic. Note No. 107*........ 1940

"A New Ultra-High Frequency Tetrode and Its Use in a One Kilowatt Television Sound Transmitter", A. K. Wing and F. E. Young, *Proc. I.R.E.* (January) 1941

"A Transmitter for Frequency Modulated Broadcast Service Using a New Ultra-High-Frequency Tetrode", A. K. Wing and J. E. Young, *RCA Review* (January) 1941

"Cascade Amplifiers with Maximal Flatness", V. D. Landon, *RCA Review* (January, April) 1941

"Fluctuations in Space-Charged-Limited Currents at Moderately High Frequencies—Part IV", B. J. Thompson, D. O. North and W. A. Harris, *RCA Review* (January) 1941

"Generation and Detection of Frequency Modulated Waves", S. W. Seeley, C. N. Kimball and A. A. Barco, *RCA Licensee Bulletin LB-546* (January 7) 1941

"I-F Amplifier Design for Battery Receivers", D. E. Foster and G. Mountjoy, *RCA Licensee Bulletin LB-544* (January 7).......... 1941

"Fluctuations Induced in Vacuum-Tube Grids at High Frequencies", W. R. Ferris and D. O. North, *Proc. I.R.E.* (February).......... 1941

"The Electron Optics of the Electron Microscope", J. Hillier, *Jour. Bacteriology* (February) 1941

"Instantaneous Plate-Voltage Capability of RCA-6L6, *RCA Tube Dept. Applic. Note No. 110* (March 4) 1941

"The New High-Transconductance R-F Pentode RCA 63G7", *RCA Tube Dept. Applic. Note No. 111* (March 4) 1941

"A New Series of Insulators for Ultra-High Frequency Tubes", L. R. Shardlow, *RCA Review* (April) 1941

Year

"An Electron Microscope for Practical Laboratory Service", V. K. Zworykin, J. Hillier and A. W. Vance, *Elec. Eng.* (April) 1941
"Deflection and Impedance of Electron Beams at High Frequencies in The Presence of a Magnetic Field", L. Malter, *RCA Review* (April) 1941
"Fluctuations in Space-Charge-Limited Currents at Moderately High Frequencies—Part V", B. J. Thompson, D. O. North and W. A. Harris, *RCA Review* (April and July) 1941
"Recent Developments in the Electron Microscope", J. Hillier and A. W. Vance, *Proc. I.R.E.* (April) 1941
"Use of the RCA 6SF7", *RCA Tube Dept. Applic. Note No. 112* (April 8) 1941
"Characteristics of Converters for Broadcast Receivers", C. W. Finnigan, *RCA Licensee Bulletin LB-563* (June 20) 1941
"Recent Developments in Phototubes", R. B. Janes and A. M. Glover, *RCA Review* (July) 1941
"The Equivalent Characteristics of Vacuum Tubes Operating in Feedback Circuits", J. H. Pratt, *RCA Review* (July) 1941
"Properties of Untuned R-F Amplifier Stages", *RCA Tube Dept. Applic. Note No. 116* (July 2) 1941
"A Review of the Development of Sensitive Phototubes", A. M. Glover, *Proc. I.R.E.* (August) 1941
"Applications of the Inductive Output Tube", O. E. Dow, *Proc. Rad. Club Amer.* (August) 1941
"New Sensitive and Inexpensive Gas-Control Tubes", W. E. Bahls, *Electronics* (September) 1941
"Silver-Magnesium Alloy as a Secondary Electron Emitting Material", V. K. Zworykin, J. E. Ruedy and E. W. Pike, *Jour. Appl. Phys.* (September) 1941
"Low Capacitance A-C Power Supplies", G. Mountjoy and C. W. Finnigan, *RCA Licensee Bulletin LB-575* (September 3) 1941
"A Preliminary Report on the Development of a 300-kilovolt Magnetic Electron Microscope", V. K. Zworykin, J. Hillier, and A. W. Vance, *Jour. Appl. Phys.* (October) 1941
"A Discussion of the Fundamental Limit of Performance of an Electron Microscope", J. Hillier, *Phys. Rev.* (November) 1941
"Behavior of Electron Multipliers as a Function of Frequency", L. Malter, *Proc. I.R.E.* (November) 1941
"The Orbital-Beam Secondary-Electron Multiplier for Ultra-High Frequency Amplification", H. M. Wagner and W. R. Ferris, *Proc. I.R.E.* (November) 1941
"Voltage-Controlled Electron Multipliers", B. J. Thompson, *Proc. I.R.E.* (November) 1941
"Design Precaution for Oscillators Employing Filament-Type Tubes", *RCA Tube Dept. Applic. Note No. 117* (December 22) 1941
"Electron Optics", G. A. Morton, Section of PROGRESS OF SCIENCE, Grolier Society, Chicago, Ill. 1941

APPENDIX II

LIST OF APPLICATION NOTES

(1933-1941)

While the RCA Application Notes published by the RCA Tube Department before World War II are out of print and extra copies are no longer available, the list below is included to provide a convenient additional reference source for the many organizations and engineers who have maintained files of the notes.

APPLICATION NOTES

NUMBER	YEAR	TITLE
AN-1	1933	Use of the 77 as a Biased Detector with 100 Volts Plate Supply
AN-2	1933	Use of the 57 as a Biased Detector Resistance-Coupled to a 2A5
AN-3	1933	Use and Operation of the 2A7 and 6A7 as Pentagrid Converters
AN-4	1933	The 2B7, 6B7, 55, 75, 77 & 85 as Resistance-Coupled Audio-Frequency Amplifiers
AN-5	1933	Application of the Type 79 Tube
AN-6	1933	Higher Voltage Ratings for the 36, 37, 38, 39/44, and 89
AN-7	1933	250-Volt Rating for the 79
AN-8	1933	2A6 as a Resistance-Coupled Audio-Frequency Amplifier
AN-9	1933	Recent Advances in Tube Design
AN-10	1933	Hum Elimination in Universal Receivers
AN-11	1933	The Use and Operation of the 25Z5
AN-12	1933	Half-Wave Operation of the 25Z5 with Separate Load Circuits for each Rectifier Unit
AN-13	1933	Recommended Operating Conditions for the 38, 41, 42, 43, and 89
AN-14	1933	Operating Conditions for the Type 53 Tube
AN-15	1933	The Operation of the Type 48 Tube as a Triode
AN-16	1933	The Operation of the 2B7, or 6B7, as a Reflex Amplifier
AN-17	1933	Special Applications of the Type 53 Tube
AN-18	1933	Operation Conditions for the Type 19 Tube
AN-19	1933	Operating Conditions for the 1A6 as an Oscillator-Mixer
AN-20	1933	An Increase in the Maximum Allowable Grid Resistor for Types 38, 41, 42, 89, and 2A5
AN-21	1933	Operation Characteristics of the Type 1-v and the Type 12Z3 Tube
AN-22	1933	The Operation of the 2A6, 2B7, 6B7, 55, 75, 77, and 85 as Resistance-Coupled Audio-Frequency Amplifiers

Number	Year	Title
AN-23	1933	The Operating Characteristics of the Type 84 Tube
AN-24	1933	Use of the 1A6 as a Half-Wave Diode-Tetrode
AN-25	1933	Influence of Circuit Constants on Receiver Output Noise
AN-26	1933	The 37, 56, 57, and 77 Tubes as Resistance-Coupled High-Voltage Amplifiers
AN-27	1933	Use of Pentagrid Converter Tubes in Multi-Range Receivers
AN-28	1933	Special Applications of the Type 79 Tube
AN-29	1933	Design of Audio Systems Employing Type 2A3 Power Amplifier Triodes
AN-30	1934	Characteristics of the 6F7 Tube
AN-31	1934	Operating Considerations of Cathode-Ray Tubes 905 and 906 for Oscillographic Purposes
AN-32	1934	Revision of Characteristics for the Type 48 Tube
AN-33	1934	RCA-800 in Class B Audio Amplifiers
AN-34	1934	Characteristics of the 868 Phototube
AN-35	1934	Triode Operation of Type 42 and Type 2A5 Pentodes
AN-36	1934	Lissajou's Figures
AN-37	1934	100-Volt Operation of 6C6 and 6D6 Tubes
AN-38	1934	A Simple Method for Converting Pentode Characteristics
AN-39	1934	The Design of a Voltage Supply for the 905 and 906 Cathode-Ray Tubes
AN-40	1934	High Power Output from Type 45 Tubes
AN-41	1934	The 1C6
AN-42	1934	Short-Cut Method for Determining Operating Conditions of Power Output Triodes
AN-43	1934	Cathode-Ray Curve-Tracing Apparatus for Aligning Tuned Circuits
AN-44	1934	Operating Conditions for the 6A6
AN-45	1935	Use of the 57 or 6C6 to Obtain Negative Transconductance and Negative Resistance
AN-46	1935	The Design of Six-Volt Battery-Operated Receivers
AN-47	1935	The Use of the 954 as a Vacuum-Tube Voltmeter
AN-48	1935	Graphical Determination of the Decrease in Inductance Produced by a Coil Shield
AN-49	1935	Construction of a Top-Cap Shield for Metal Tubes
AN-50	1935	Operation of the 6L7 as a Mixer Tube
AN-51	1935	The 6F5
AN-52	1935	Class AB Operation of Type 6F6 Tubes Connected as Triodes
AN-53	1935	The 6L7 as a Volume Expander for Phonographs
AN-54	1935	Class AB Operation of Type 6F6 Tubes Connected as Pentodes
AN-55	1935	Operation of the 6A8

NUMBER	YEAR	TITLE
AN-56	1936	Receiver Design
AN-57	1936	The 6L7 as an R-F Amplier
AN-58	1936	Receiver Design
AN-59	1936	Operation of the 6Q7
AN-60	1936	Operation of the 6L6
AN-61	1936	The Conversion of a 6L6 Plate Family to New Screen Voltage Conditions
AN-62	1936	A New Operating Condition for Two Type 6F6 Tubes Connected as Pentodes
AN-63	1936	A High-Gain Single-Tube Phase Inverter
AN-64	1936	Inverse-Feedback Circuits for A-F Amplifiers
AN-65	1936	Tuning-Indicator Circuits for the 6E5 and 6G5
AN-66	1936	Equal Plate and Screen Voltage Operation of the 6L6
AN-67	1937	Resistance-Coupled Audio-Frequency Amplifiers
AN-68	1937	A 55-Watt Amplifier Using Two Type 6L6 Tubes
AN-69	1937	250-Volt, Low-Current Operation of the 6L6
AN-70	1937	An Exposure Meter for Cathode-Ray Oscillographs
AN-71	1937	Low-Current, High-Power Operation of Two 6L6's Connected in Push-Pull
AN-72	1937	A 40-Watt Operating Condition for Two Type 6L6 Tubes
AN-73	1937	Operation of the 25L6 in Typical Circuits
AN-74	1937	A New High-Voltage Choke-Input Rating for the 5T4
AN-75	1937	Receiver Design
AN-76	1937	An Audio-Frequency Curve Tracer Using a Cathode-Ray Tube
AN-77	1937	Dimensions of Popular Tube Types
AN-78	1937	Use of the Plate Family in Vacuum-Tube Power-Output Calculations
AN-79	1937	Significance of Ratings for Power Output Tubes
AN-80	1937	Operation of the 6V6-G
AN-81	1937	A Two-Terminal Oscillator
AN-82	1938	Wide-Angle Tuning with the 6E5, 6G5, or 6U5
AN-83	1938	Resistance-Coupled Amplifier Data for the 6L5-G, 6T7-G, and 6S7-G
AN-84	1938	The Operation of Phototubes
AN-85	1938	Operation of the 6AC5-G
AN-86	1938	Operation of the 6Y6-G
AN-87	1938	The 6K8 — A New Converter Tube
AN-88	1938	Hum in Heater-Type Tubes
AN-89	1938	Receiver Design
AN-90	1938	Resistance-Coupled Amplifier Data for the 6C8-G, 6F8-G, 6J5, 6J5-G, and 6Z7-G
AN-91	1938	Operation of the Gas-Triode 0A4-G
AN-92	1938	Operation of the Improved Type 906 Cathode-Ray Tube at Low Voltages
AN-93	1938	An Inverse-Feedback Circuit for Resistance-Coupled Amplifiers

Number	Year	Title
AN-94	1938	Operation of the 6AF6-G
AN-95	1938	Operating Positions of Receiving Tubes
AN-96	1938	A Voltage Regulator for D-C Power Supplies
AN-97	1938	A Self-Balancing Phase-Inverter Circuit
AN-98	1938	The Operation of Single-Ended Tubes
AN-99	1938	Revision of 6K8 Ratings
AN-100	1938	Operation of the 6SA7
AN-101	1939	Input Loading of Receiving Tubes at Radio Frequencies
AN-102	1939	The 6SK7 as an I-F Amplifier
AN-103	1939	Operation of the 35L6-GT
AN-104	1939	A Television Bibliography and RMA Television Standards
AN-105	1939	A Change in Maximum Ratings of Receiver Tubes
AN-106	1940	The RCA Miniature Tubes
AN-107	1940	A Miniature-Tube Hearing-Aid Amplifier for use with an Air-Conduction Earpiece
AN-108	1940	Effect of Temperature on Frequency of 6J5 Oscillator
AN-109	1940	Operation of Fifty Milliampere Tubes by the 117N7-GT
AN-110	1941	Instantaneous Plate-Voltage Capability of RCA-6L6
AN-111	1941	The New High-Transconductance R-F Pentode RCA-6SG7
AN-112	1941	Use of the RCA-6SF7
AN-113	1941	Precaution in Assembly of Receivers Employing Button-Base Tubes
AN-114	1941	Use of Cushioned Sockets in Small Receivers
AN-115	1941	A Discussion of Noise in Portable Receivers
AN-116	1941	Properties of Untuned R-F Amplifier Stages
AN-117	1941	Design Precaution for Oscillators Employing Filament-Type Tubes